New Fluorene Based Materials for Organic Electronics

Dissertation

For the award of the academic degree of
Doctor of Natural Science (Dr. rer. nat.)
From the faculty of Biology, Chemistry and Geosciences
University of Bayreuth

submitted by
Heiko Thiem
born in Pegnitz

Bayreuth, 2005

Die vorliegende Arbeit wurde in der Zeit von Oktober 2001 bis Juni 2005 am Lehrstuhl für Makromolekulare Chemie I der Universität Bayreuth unter der Leitung von Prof. Dr. Peter Strohriegl angefertigt.

Vollständiger Abdruck der von der Fakultät für Biologie, Chemie und Geowissenschaften der Universität Bayreuth genehmigten Dissertation zur Erlangung des akademischen Grades Doktor der Naturwissenschaften (Dr. rer. nat.)

Datum der Einreichung der Arbeit: 29.06.2005

Datum des wissenschaftlichen Kolloquiums: 18.10.2005

Prüfungsausschuß:

Prof. Dr. G. Krausch	(Vorsitzender)
Prof. Dr. P. Strohriegl	(Erstgutachter)
Prof. Dr. R. Schobert	(Zweitgutachter)
Prof. Dr. H.G. Alt	

Für Simone

Danksagung

Herrn Prof. Dr. Peter Strohriegl danke ich, neben der Möglichkeit auf diesem interessanten Themengebiet zu arbeiten, für die stetige Motivation, Diskussionsbereitschaft, Freiheit im wissenschaftlichen Arbeiten und die Möglichkeit im Laufe der Zeit mit sehr vielen Leuten aus Forschung und Industrie zu kooperieren.

Herrn Prof. Dr. Hans-Werner Schmidt danke ich für die Überlassung eines sehr gut ausgestatteten Laborplatzes an seinem Lehrstuhl.

Dr. Iain McCulloch, Dr. Maxim Shkunov und Dr. Martin Heeney von der Firma Merck KGaA in Southampton danke ich für die Bereitstellung von Reaktivmesogenen für die PhotoDSC Experimente und die Unterstützung und Hilfe bei kleineren Syntheseproblemen.

Dr. Dago deLeeuw, Dr. Sepas Setayesh und Dr. Bart-Hendrik Huisman von den Philips Research Laboratories in Eindhoven danke ich für die freundliche Aufnahme bei zahlreichen Aufenthalten in Eindhoven und die vielen Erklärungen, die ein Chemiker braucht um OFETs annähernd zu verstehen.

Dr. Martin Schadt und Dr. Mohammed Ibn-Elhaj von der Firma Rolic in Basel danke ich für die freundliche Aufnahme während meines Aufenthalts im Jahre 2002 und die gemeinsame Durchführung der Orientierungsexperimente auf Photoorientierungsschichten.

Mein Dank gilt auch allen Mitarbeitern am Lehrstuhl für das sehr motivierende Arbeitsklima und viele, viele private Unternehmungen, die wichtig sind, damit man nicht das Gefühl hat als Fremder auf die Arbeit zu kommen. Herauszuheben sind hierbei Markus Bäte, Oscar Lafuente, Stefan Lindner, Katja Peter und Martin Sonntag.

Mindestens genauso wichtig ist ein gutes Arbeitsklima im Labor. Hier möchte ich mich speziell bei Doris Hanft bedanken, die als technische Angestellte sehr großen Ehrgeiz bei der Ausarbeitung und Verbesserung von Synthesen zeigte. Während meiner Promotion haben Frank Abraham, Anja Goldmann, Michael Rothmann und Esther Scheler als

Studenten an den verschiedensten Projekten mitgearbeitet und mehr oder weniger zu dieser Arbeit beigetragen. Bei Martin Sonntag möchte ich mich für unendlich viele Diskussionen, das gemeinsame Umsetzen von etlichen Vorhaben und die gegenseitige Motivation bedanken. Bei Dr. Klaus Kreger, Dr. Jörg Schröder, Dr. Thomas Pfeuffer und Dr. Markus Jandke bedanke ich mich für viele Diskussionen und ihren Beitrag zu einem sehr guten Laborklima. Meinen Nachfolgern auf den Forschungsgebieten Esther Scheler und Michael Rothmann wünsche ich gutes Gelingen und viele neue Ideen.

Für die finanzielle Unterstützung danke ich dem Bundesministerium für Bildung und Forschung (BMBF), der Philips GmbH und der Merck KGaA im Rahmen des POLITAG Programms, sowie der Europäischen Union im Rahmen des EUROFET/TMR-Projekts.

Meiner Familie möchte ich für das stetige Interesse an meiner Arbeit und die zahlreichen Aufmunterungen danken.

Meiner Frau Simone danke ich für das große Verständnis bei etlichen Problemen und die sehr große Unterstützung und Geduld während der nicht immer einfachen Zeit einer Promotion.

Table of Content

1. Introduction

1.1. Organic electronics

In the last years technologies like flat panel displays or radio frequency identification tags (RFID) from organic materials received a lot interest in academic and industrial research. Organic electronics became an important keystone of such modern technologies because the fabrication gets cheaper by the use of organic materials compared to established semiconductor techniques. A sign for the importance and a mark of recognition was the Nobel prize for A. Heeger, A. Mac Diarmind and H. Shirakawa in the year 2000[1,2,3,4] for the discovery and development of semiconducting polymers. Up to now the first commercially available products with semiconducting organic materials are on the market. In 1999 Pioneer sold a car radio with a display made of organic light emitting diodes (OLEDs)[5]. In the following years a lot of companys came up with OLED displays in low resolution applications like mobile phones[6] and mp3 players[7]. In the year 2004 31 million OLED panels were sold mainly for mobile phone displays, which is twice the amount of 2003 and forecasts estimate another doubling in the next year[8]. For the year 2010 experts estimate a market of three billion US Dollars. So small OLED displays are on the way to establish themselves in the market and the technology has a good chance to expand in the near future even for larger and high resolution displays.

Another potential market for organic electronics are RFID tags, which are simple chips, in which information can be stored and read out by a contactless technique[9]. There the silicon circuits can be replaced by integrated circuits from transistors made of organic semiconducting materials. Such tags may be the next generation price labels in supermarkets, where up to now barcode tags are used. The main advantage is that such new tags must not have direct contact with the laser system like a usual barcode. RFID tags based on silicon are in use in several areas. For example modern skiing areas use them as

skiing tickets, where the information about validity is stored on the chips. The permission for taking the lift will be read out from the chip by crossing an antenna without direct contact. So this process gets much faster and it is nearly impossible to cheat the system. The main problem of the silicon based tags is the price of 50 Cent per tag. This makes it inefficient to use such tags in supermarkets, where the whole price of some products is significantly lower than 50 Cent. The solution can be RFID tags based on organic electronics. By the use of semiconducting organic materials the price for such a tag will be in the range of one Cent, due to the cheaper and easier production of the organic electronic materials compared to silicon. Additionally the use of organic materials ensures a higher flexibility and with this the chance of producing flexible chips. Due to the fact that some materials are solution processable, it will be possible to print the chips for example with ink-jet printing technique. Companys like PolyIC try hard to realise the production of so called printed chips[10]. Up to now they are able to present a preproduction line for the printing step on flexible foils. In Figure 1 this production line is shown.

Figure 1: Pre production line for printable chips from PolyIC[10].

My work focussed on two areas of organic electronics. First I have developed new synthetic routes towards photocrosslinkable reactive mesogens based on fluorene units for the use as blue emitting materials in OLEDs. These fluorene based compounds can be aligned on different orientation layers and used as emitters for linear polarized light in OLEDs. Due to the fact that the photocrosslinking process is a crucial step in the treatment of reactive mesogens this issue was examined in detail by PhotoDSC measurements. There I managed photocrosslinking in different liquid crystalline phases and showed the dependence of the total conversion and the reaction kinetics from the temperature and the initiator concentration. The second part of my work is focussed on materials for the use in OFETs. Due to the fact that molecules containing only fluorene units do not fit perfectly in OFETs because of their low lying HOMO levels, I investigated molecules which contain additional bithiophene units. First I made oligomers with different molecular weight to detect differences in thermal behaviour and to examine the orientation behaviour of such oligomers on orientation layers. Trimers with fluorene and bithiophene units were taken to measure the performance of this class of materials in OFETs. Important points are here the mobility and stability of the material in the device which was demonstrated by long term measurements.

1.2. Organic light emitting diodes

1.2.1. Principle of an OLED

Fluorescence of a material is one possible mechanism of the relaxation of an exited state into the ground state. In Figure 2 this principle is shown[11].

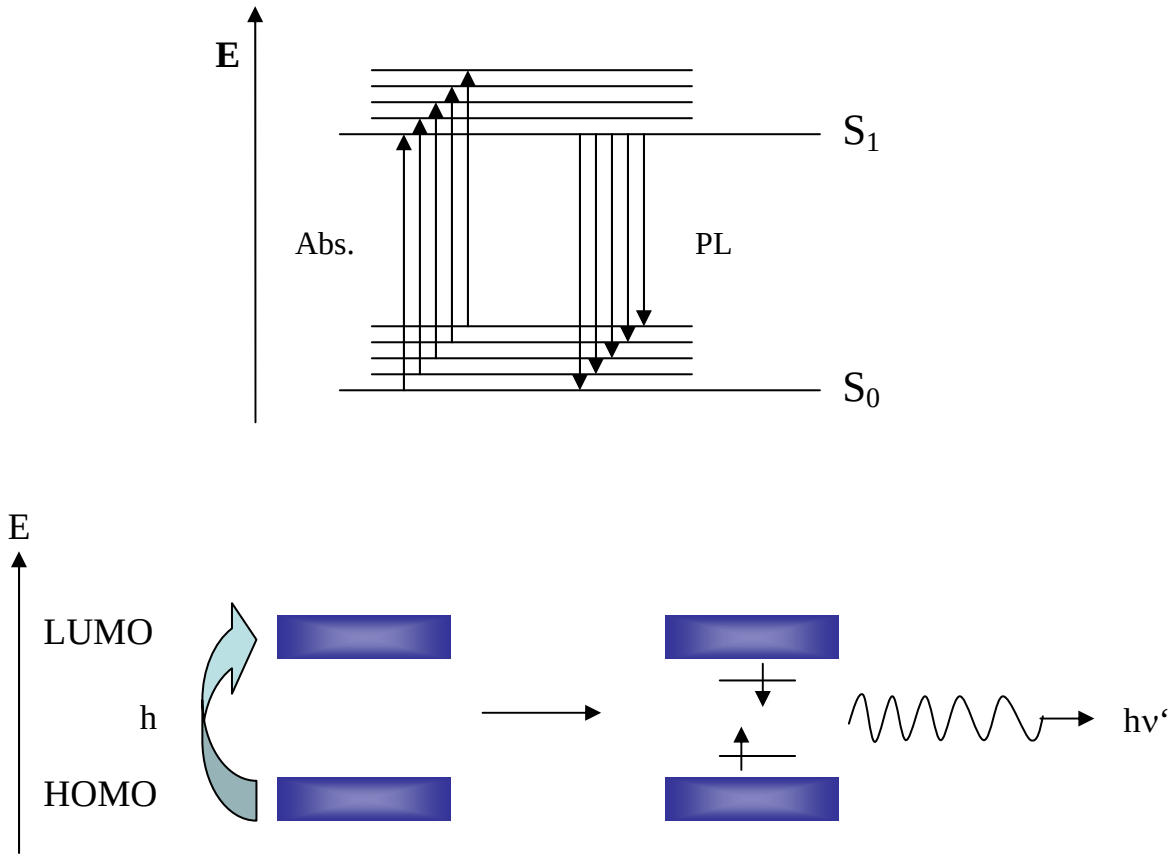

Figure 2: Irradiation and relaxation of a fluorescent material. Above: Jablonski diagrams; Below: conduction band model.

By the excitation of an electron from the HOMO level to the LUMO level, two new energy states are generated upon relaxation within the original HOMO-LUMO energy gap. Each energetic state is filled with one electron of opposite sign. This excited state may then relax to the ground state with emission of light at a longer wavelength than the absorbed light. This process is called photoluminescence. These principles are equivalent with the Jablonski diagrams (Figure 2 up). The procedures in an OLED are shown in Figure 3.

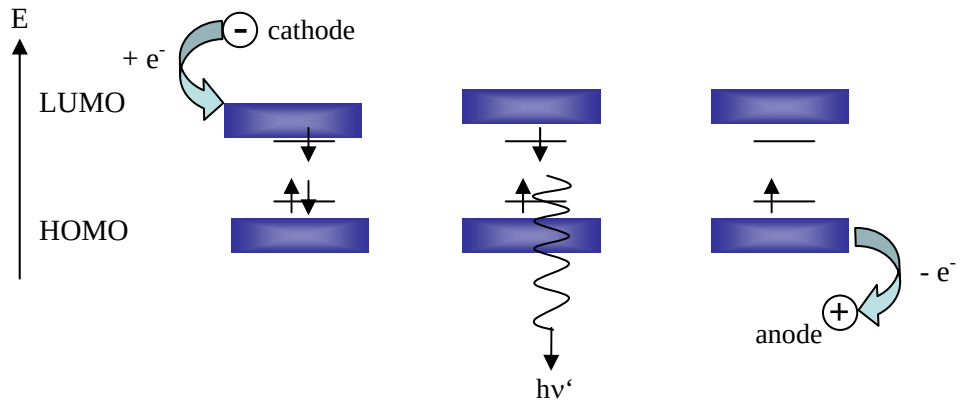

Figure 3: Energetic procedures in a single layer OLED.

In a single layer OLED electrons are injected in the LUMO and holes in the HOMO of the electroluminescent material. The resulting charges migrate from molecule to molecule under the influence of the applied electric field. When these two different charge carriers combine on a single conjugated segment, exited states are formed, which can emit light upon relaxation.

A single layer OLED consists of a thin film of the light emitting material which is sandwiched between two electrodes. One of these electrodes has to be semitransparent to get the light out of the device. Such an OLED is shown in Figure 4.

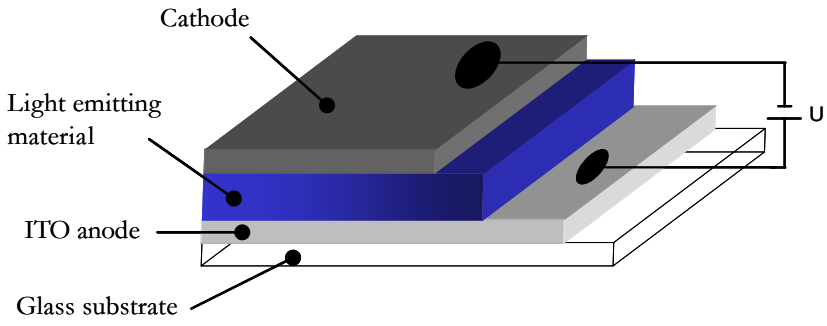

Figure 4: Schematic drawing of a single layer OLED.

As anode indium-tin-oxide (ITO) is mainly used which ensures conductivity and is transparent. Electropositive metals with low work functions like Al, Ca or Mg are used as

cathodes in order to guarantee efficient electron injection. J. Tang and S. van Slyke reported in the year 1987 the first time about the electroluminescence of evaporated tris(8-hydroxyquinoline)aluminium (Alq_3) in an organic light emitting diode [12]. Additionally they used a bis(triarylamines) layer to ensure hole injection in the emitting layer. In Figure 5 the chemical structures of these compounds are shown.

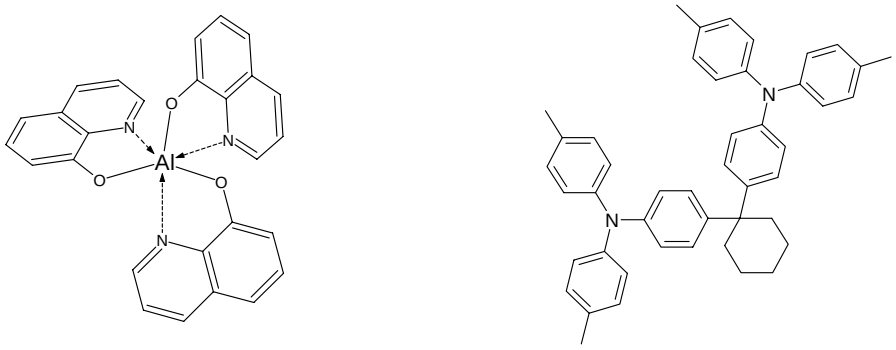

Figure 5: Structure of Alq_3 (left) and bis(triarylamines) (right).

As cathode they used a stable Mg/Al alloy and reached a brightness of over 1000 Cd/m^2 at voltages lower then 10 V. In the following years many groups developed new small molecules for the use in OLEDs. But a significant drawback of all these materials is that they are not solution processable and so industrial production is based on expensive evaporation procedures.

1.2.2. Polymeric materials for OLEDs

In the year 1990 the electroluminescence of polymers was first described by the groups of D.D.C. Bradley, R.H. Friend and A.B. Holmes in Cambridge[13]. They overcame the drawback of expensive and technologically inconvenient vapour deposition of fluorescent

dyes by using the highly fluorescent conjugated polymer poly(p-phenylene-vinylene) (PPV) as active material in a single layer OLED.[13]. The structure can be seen in Figure 6.

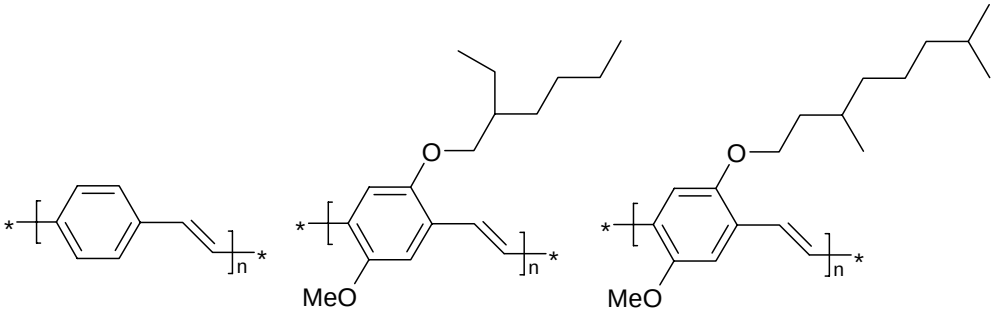

Figure 6: Structures of poly(p-phenylenevinylene) (PPV) (left), poly[2-methoxy-5-(2-ethylhexyloxy)-p-phenylenevinylene] (MEH-PPV) (middle), poly[2-(3,7-dimethyl-octyloxy)-5-methoxy-1,4-phenlenevinylene] (OC_1C_{10}-PPV) (right).

Apart from the PPV, which can be obtained from a precursor polymer by thermal treatment[13], in the following years solution processable derivates like poly[2-methoxy-5-(2-ethylhexyloxy)-p-phenylenevinylene] (MEH-PPV, see Figure 6) were developed[14]. By the use of alloy groups the emission colour changes from green for PPV to red-orange for MEH-PPV. Pure red emission and a better stability than with MEH-PPV can be obtained by OC_1C_{10}-PPV (see Figure 6), which was mostly investigated by Philips and Hoechst[15]. Multicolour display applications require at least three basic colours: red, green and blue. The first two can be realised by the mentioned groups of materials. For blue colour emission the highest energy gap between HOMO and LUMO level is needed. This makes it difficult to get a stable, highly efficient bright blue emitting polymer. In Figure 7 the so called ladder-type polymer, which was first described by U. Scherf et al. is shown[16].

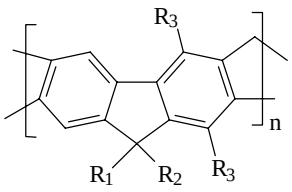

Figure 7: Structure of the ladder-type polymer (R_1: methyl; R_2: phenyl; R_3: n-hexyl).

Due to the formation of aggregates in the solid state, the emission gets yellowish parts and so the use as blue emitter in OLEDs is hindered. One of the most promising polymers for blue emission in OLEDs is the dialkylated polyfluorene, which is shown in Figure 8.

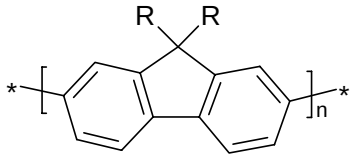

R = n-octyl, 2-ethylhexyl

Figure 8: Structure of dialkylated poly(2,7-fluorene).

A detailed description of the synthesis, properties and applications of polyfluorenes will be given in chapter 1.2.4.

1.2.3. Displays

The accessibility of all three basic colours for OLEDs makes it possible to design full colour displays. Up to now the competition between the two different techniques (evaporation of small molecules or solution processing of polymers) is very close. The first prototypes of full colour displays were developed in 2000 by Sanyo/Kodak[17]. They used an evaporation process to realize 5 inch displays. In the last years many companys showed prototypes of OLED displays. The two largest with a display size of 40 inch were announced in the last months by Epson[18] and Samsung[6]. For the production of such large area displays the evaporation technique is not efficient. These displays were all made from solution processed polymers by ink jet printing. One of these prototypes from Sony[19] is shown in Figure 9.

Figure 9: above: 13 inch prototype OLED display from Sony[19], below: OLED display of a Samsung E700A mobile phone with 64 x 96 pixels (right)[6], white OLED from Philips/Novaled for lightning application (left)[20].

Here the realisation of full colour displays can be seen. In the right part of the picture the independence of the colours from the viewing angle can be seen nicely, which is one of the big advantages towards LC displays. Due to the fact, that the active layers of such a display are in the nanometer scale, the thickness is much smaller than in comparable LCDs. Additionally the power consumption is lower than in any other display type.

So full colour displays are possible to realise, but need a little bit more time to become a competitive display technology on the market. The first small and monochrome OLED products are on the market for a few years. So Samsung forced the use of OLED displays in mobile phones and is now the leading supplier for these displays (see Figure 9)[6].

Another application for OLEDs is the lightning sector. A combination of all three basic colours delivers white light as we now it from usual bulbs. On this sector Philips and Novaled together designed white emitting OLEDs with a maximum efficiency of 25 lm/W at a brightness of 1000 cd/m^2 which are shown in Figure 9[20].

In a common light bulb and in inorganic LEDs the light is produced in a very small area. The use of OLEDs in this field would increase the active area and lead to a new type of light sources.

So OLED displays are on their way to be established on the market. Many companys believe that OLEDs maybe the future of display technology, due to the advantages of low power consumption, cheap production by printing techniques and the possibility of making flexible displays. The near future will show, if they can compete with the established technologies.

1.3. Polyfluorenes

1.3.1. Synthesis

One of the most investigated class of polymers for blue emission in OLEDs are polyfluorenes. First attempts to synthesise soluble, processable dialkylated poly(2,7-fluorene) were published in 1989 by Yoshino et al.[21]. They coupled 9,9-dihexylfluorene oxidatively with $FeCl_3$ and obtained a polymer with a M_n of 5000 g/mol.

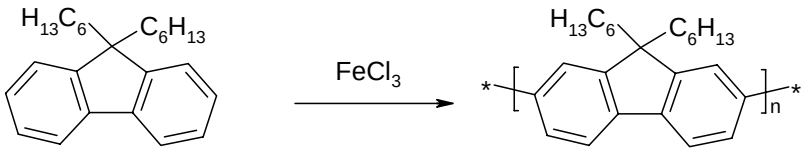

Figure 10: Oxidative synthesis of poly[(9,9'-dihexyl)-2,7-fluorene].

The main disadvantage of this reaction is the not perfect regioselectivity which leads to defects in the desired 2,7-linkage. An enormous progress in the synthesis was made by the use of transition metal catalysed aryl-aryl couplings. High molecular weights of up to 200000 g/mol can be achieved by the Yamamoto coupling[22,23]. The synthesis is outlined in Figure 11.

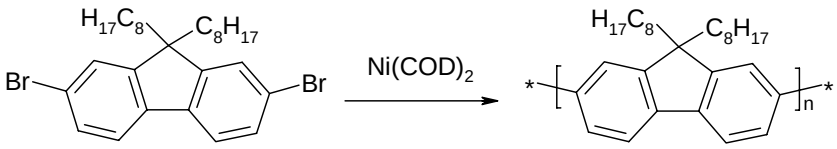

Figure 11: Synthesis of 9,9'-dialkylated polyfluorene via Yamamoto coupling.

One disadvantage of this system is, that the $Ni(COD)_2$ has to be added equimolar to the reaction. Apart from the coupling reaction by a Grignard reagent with $PdCl_2$(dppb) as catalyst[24] the Suzuki cross coupling reaction[25] of 9,9'-dialkylfluorene-2,7-bisboronic esters with 2,7-dibromo-9,9'-dialkylfluorenes is one of the most investigated reaction for the synthesis of polyfluorenes[26]. In Figure 12 the synthesis is outlined.

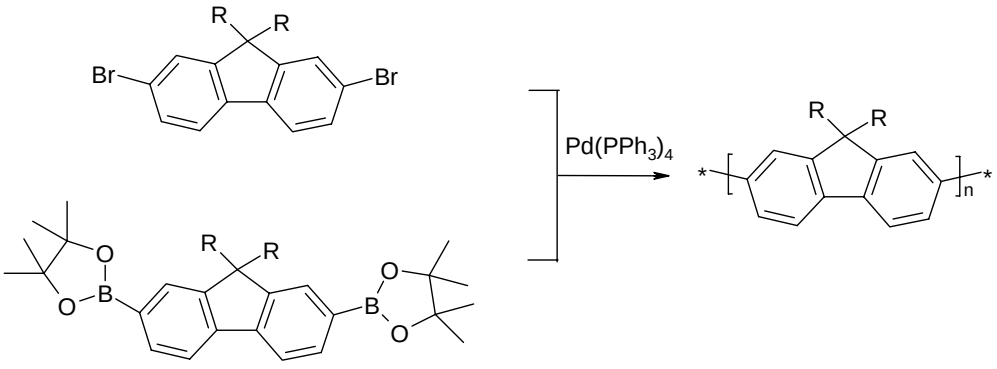

Figure 12: Synthesis of 9,9'-dialkylated polyfluorene via Suzuki cross coupling.

The difference to the other described coupling reactions is the use of two functionalised monomers with different functional groups. If the reaction is carried out with two different alkylated fluorenes or other conjugated systems like carbazoles or thiophenes the synthesis of alternating copolymers is possible, which cannot be realised by the other coupling reactions[26]. The detailed catalytical circuit is shown in Figure 13.

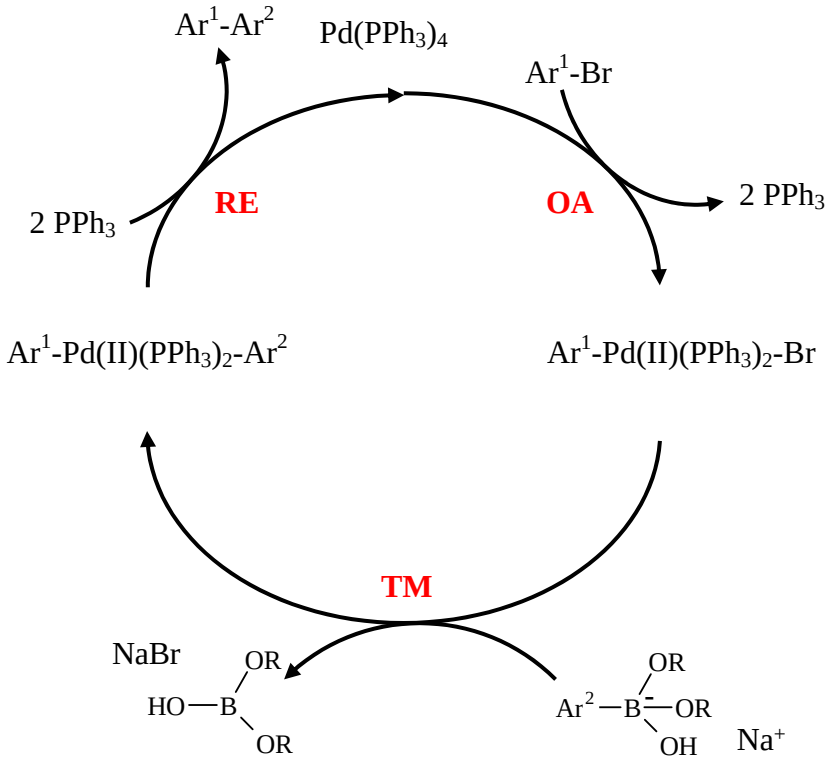

Figure 13: Catalytical cycle of the Suzuki cross coupling.

By oxidative addition (OA) of an arylbromide to the $Pd(0)(PPh_3)_4$ catalyst a stable palladium(II) complex is formed. By the transmetallisation (TM) the second aromatic system is coupled to the palladium catalyst. The reductive elimination of the palladium species leads to the formation of a new aryl-aryl bond and the regeneration of the active catalyst[27].

1.3.2. Properties and applications

Many polyfluorenes show broad nematic liquid crystalline phases[28], which were first shown by M. Grell et al.[29]. The transition to the liquid crystalline state can be found in the temperature range from 100-180 °C depending on the alkyl side chains in 9 position of the fluorene and the molecular weight of the polymers. So 9,9-di- n-octyl polyfluorene shows a phase transition at 160 °C. This temperature can be reduced by the introduction of branched side chains like 2-ethylhexyl or 3,7-dimethyloctyl, where this phase transition can be detected at 100 °C[30]. More information about the thermal properties of polyfluorene comes from a series of low molar mass model compounds. The group of G. Wegner succeed in the synthesis of fluorene oligomers up to the heptamer[31], which are shown in Figure 14.

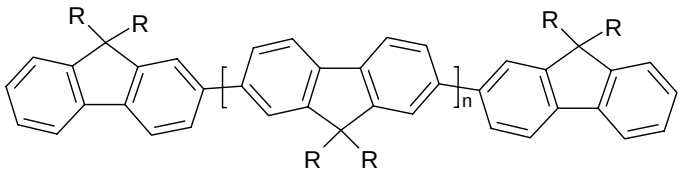

Figure 14: Structure of fluorene oligomers (R = 2-ethylhexyl; n = 0 - 5)[31].

There the transition from the nematic to the isotropic phase changes from 64 °C (tetramer, n = 2) to 246 °C (heptamer, n = 5). Another very interesting result was the synthesis of

fluorene trimers with lateral octyl chains which form a smectic mesophase[32]. The chemical structure is shown Figure 15.

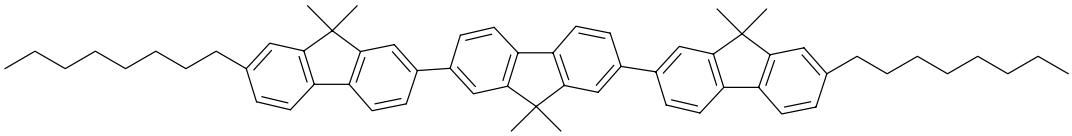

Figure 15: Structure of a fluorene trimer with smectic mesophase[32].

This molecule has a transition from the crystalline state to a smectic mesophase at 108 °C. At 140 °C a transition to a nematic phase can be detected, before the isotropic phase is reached at 168 °C. This very interesting result can be explained by the high ratio of length to diameter in this molecule compared to the other described fluorene derivates. With methyl groups in the 9 position of the fluorene the minimum diameter of substituted fluorenes is reached and by the introduction of the n-octyl groups the length is increased. So it is possible to reach a higher ordered smectic mesophase.

Many groups took benefit from the nematic phases by alignment of fluorene compounds on orientation layers. Such an alignment can be reached by heating a thin film on top of an orientation layer into the isotropic phase, followed by a slow cooling in the nematic phase. There the film is anealed for a certain time, before a fast quenching to room temperature follows. In Figure 16 this principle is shown.

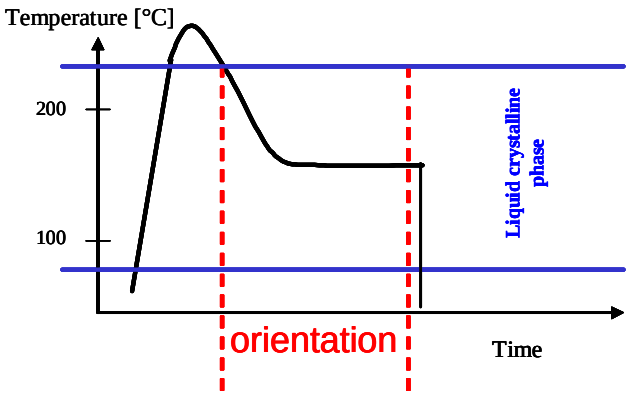

Figure 16: Temperature program for the alignment of fluorenes on orientation layers.

Different orientation layers are used for this process. In our group we used a rubbed segmented PPV layer as orientation layer for the design of an OLED, which emits linear polarized light due to the orientation of the polyfluorene[33]. The production of the orientation layer is illustrated in Figure 17.

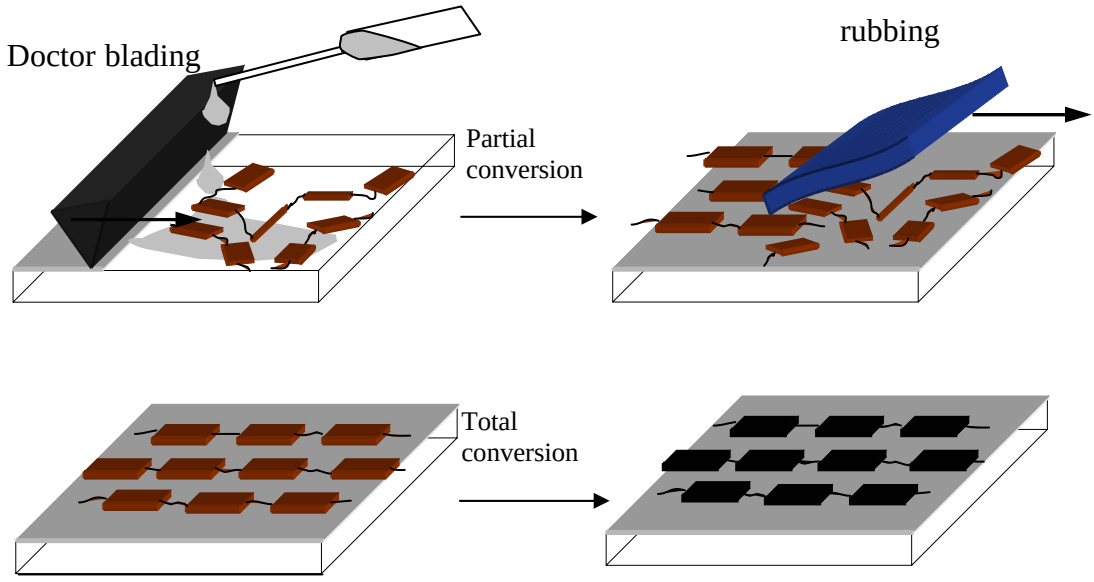

Figure 17: Production of a rubbed PPV orientation layer[34].

After the doctor blading process the seg-PPV was partial converted by heating for a certain time at 180 °C. Then the layer was rubbed with a piece of lint free paper followed by the total conversion at 180 °C for 2 hours. On top of this orientation layer poly(9,9'-di-n-octylfluorene) was spin coated. With the temperature program (see Figure 16) the polymer was aligned, before the OLED was completed by the evaporation of a calcium electrode. The schematic view and the polarized electroluminescence spectra are shown in Figure 18.

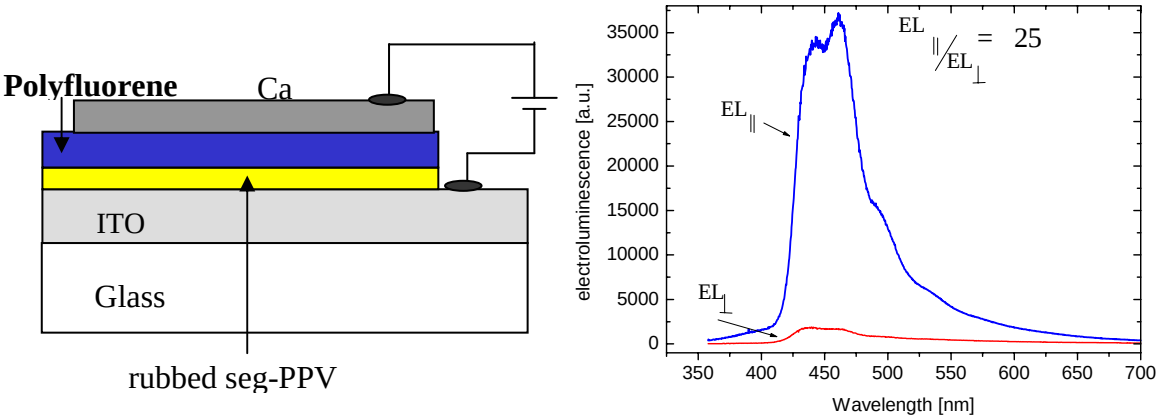

Figure 18: Design of a polarized OLED with seg-PPV as orientation layer and the polarized electroluminescence spectra[33].

By the integration of the two electroluminescence spectra an orientation ratio of 25 was obtained. The big advantage of this polarized OLED is the fact, that the PPV layer works as a hole transport layer and so no additional doping with hole conducting materials is necessary. Such doping is a must when rubbed polyimide is used as orientation layer[35]. In such an OLED with rubbed polyimide an orientation ratio of 15 can be obtained. Apart from the orientation of polymers the alignment of oligomeric systems has received increasing interest in the last years. So the groups of S.H. Chen and C.W. Tang published the synthesis of fluorene oligomers with up to ten fluorene units and their orientation on rubbed PEDOT / PSS layers[36,37]. They reached orientation ratios up to 24 in electroluminescence. These papers are one proof that low molecular mass chromophores show better orientation ratios than polymers. This can be explained by entropic effects in a polymer which hinders a perfect orientation. One disadvantage of the oligomers is their lower glass transition temperatures compared to the polymers. So a freezing in of the orientation is not so easy to achieve and the orientation can decrease with time due to relaxation processes.

1.3.3. Synthesis and orientation of fluorene containing reactive mesogens (Paper I)

One solution of this problem is the use of a crosslinking reaction to fix the orientation of low molecular mass chromophores by the formation of a densely crosslinked network[38]. For this purpose the molecules must have photocrosslinkable groups. One example of such a reactive mesogen is given in Figure 19.

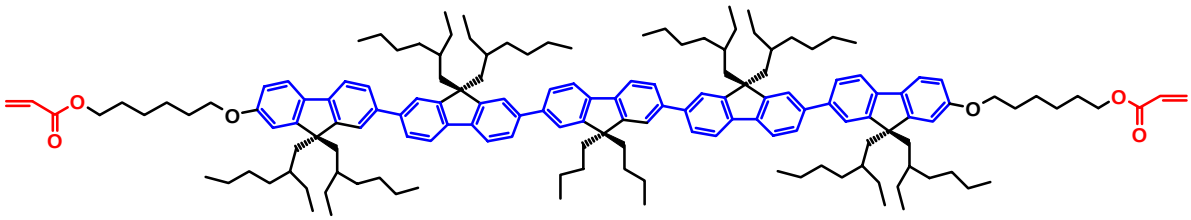

Figure 19: Structure of a reactive mesogen containing five fluorene units and photopolymeriseable acrylate end groups[39].

This molecule has a backbone of five fluorene units, which ensures nematic mesophase between -10 °C and 123 °C. By the use of branched alky side chains the solubility and film forming properties were optimised. At the α,ω positions acrylate end groups for the polymerisation are separated from the core by a C6-spacer. The orientation process is summarised in Figure 20.

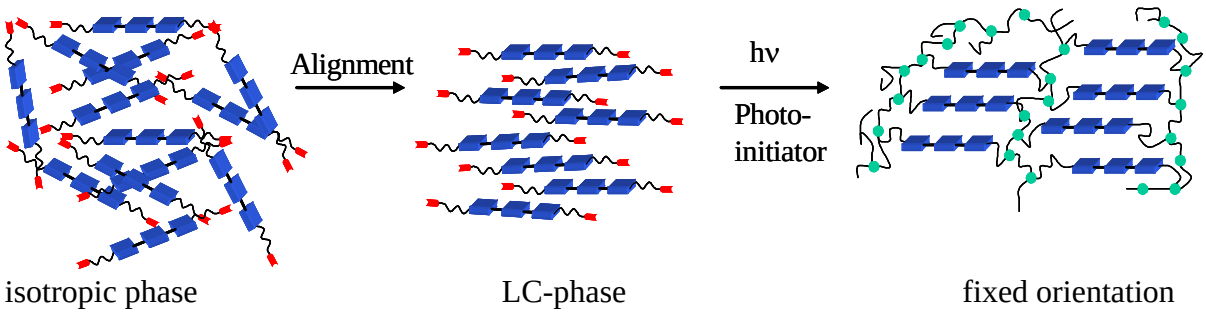

Figure 20: Orientation and photocrosslinking of reactive mesogens.

The crosslinking process takes place with a photoinitiator, which gives rise to the formation of free radicals. These radicals initiate the polymerization (crosslinking) of the acrylate endgroups in the fluorene bisacrylates.

In the paper I describe the synthesis of such reactive mesogens containing fluorene units in detail. On the next pages a short summary of the most important results is given. After that some additional experiments concerning orientation of reactive mesogens are summarised which have not yet been published.

The synthesis of such reactive mesogens containing three or five fluorene units is described in detail. Additionally we report on the synthesis of oligomeric mixtures containing fluorene units in order to produce such materials in gram scale, which is not possible with pentameric structures. In Figure 21 the oligomer synthesis is summarised. All synthetic details are given in paper I. The key step towards the mesogens is the Suzuki cross coupling. There a monofunctionalised endcapper is used for the control of the molecular weight of the oligomers. The higher the amount of the endcapper, the lower is the resulting molecular weight. Due to the formation of side products during the reaction when free hydroxy groups are present a THP protecting group was introduced in the molecule to prevent undesired side reactions.

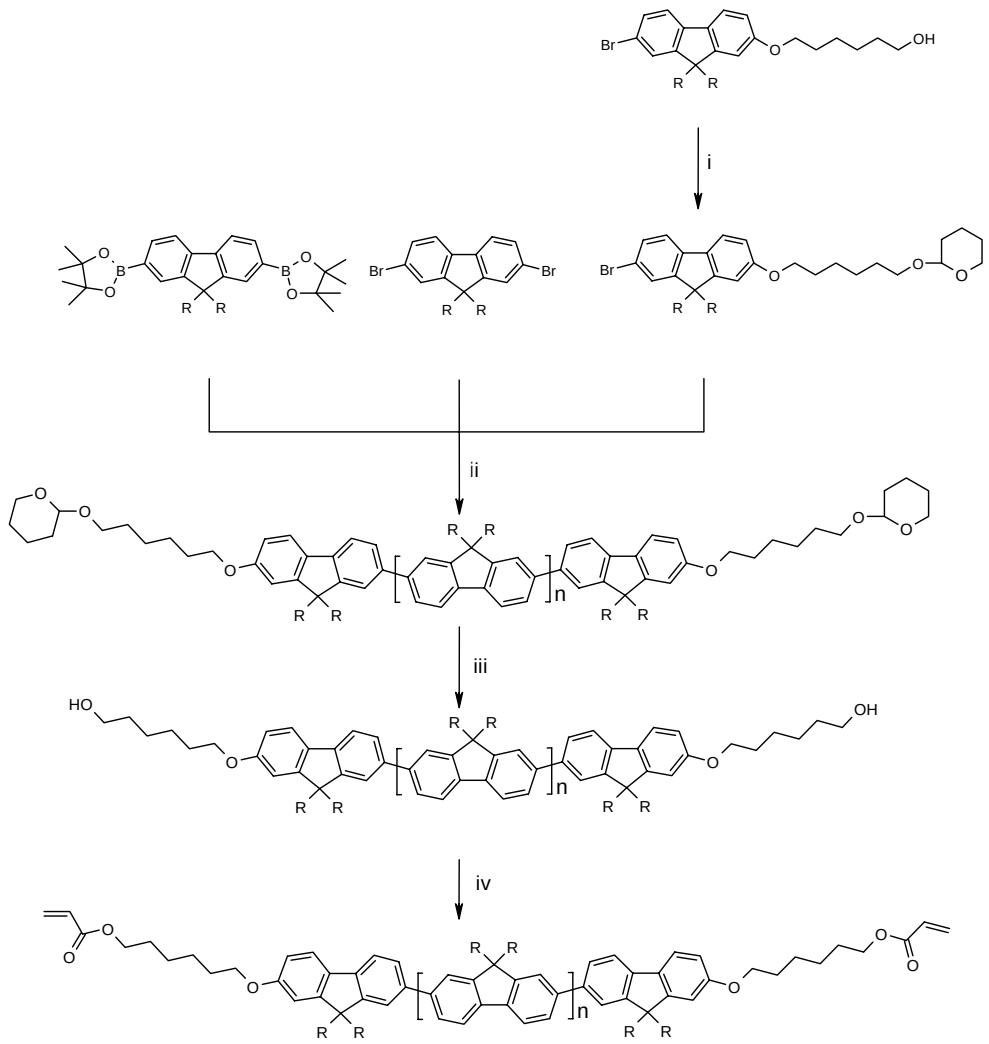

R = 2-ethylhexyl

i) Et_2O, DHP, 0 °C; ii) $Pd(PPh_3)_4$, K_2CO_3 (2 M aq.), toluene, 50 °C; iii) ether, HCl, 50 °C; iv) acryloyl chloride, DMA, toluene, 40 °C.

Figure 21: Synthesis of fluorene containing, photocrosslinkable reactive mesogens.

The characterisation was made by GPC and MALDI-TOF analysis. There the different oligomers can be determined. In Figure 22 these spectra are shown.

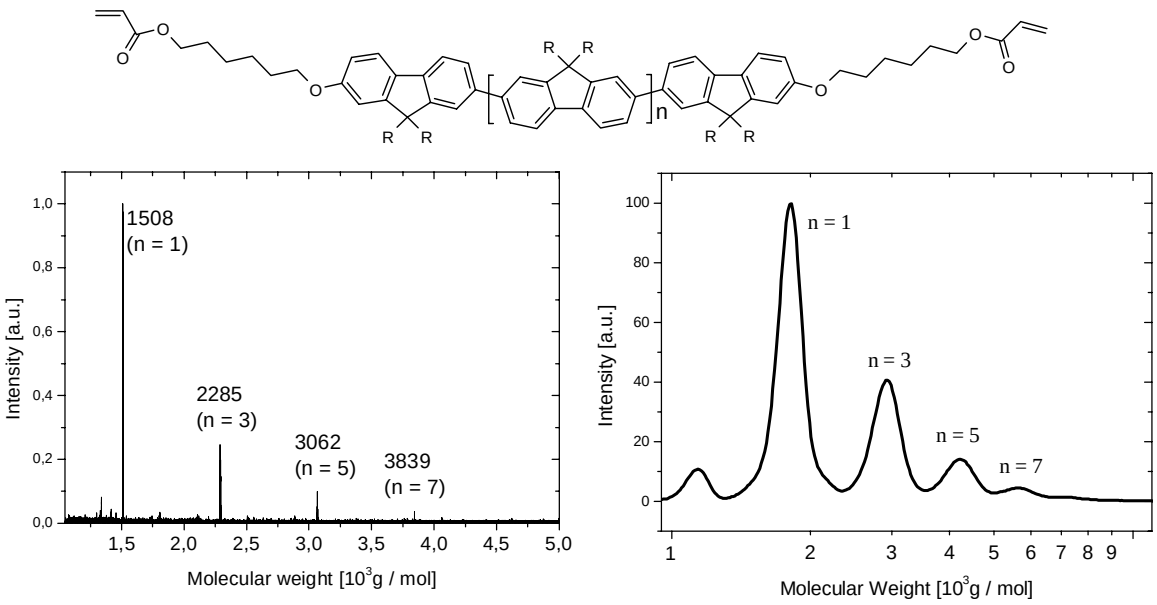

Figure 22: Structure, MALDI-TOF measured without matrix (left) and GPC scan (right) of **14g** from paper I.

As expected from the synthesis only one homologous series can be detected. This analysis ensures that every oligomer is endcapped and has two photopolymerisable end groups.

The orientation of the crosslinked reactive mesogens on top of rubbed polyimide layers is also described in paper I (see chapter 2). There a maximum orientation of 15/1 can be obtained. So in summary a new class of reactive mesogens containing fluorene units was synthesised and well analysed. The materials show broad nematic mesophases. The liquid crystalline properties and particularly the clearing temperatures can be shifted from 100 °C to 310 °C by changing the molecular weight of the oligomers.

1.3.4. Additional results

In addition to the results on the orientation on rubbed polyimide layers in paper I we made orientation experiments on photoorientation layers. It is not necessary to rubb these layers as it is described before for other orientation layers. They were pioneered by the group of M. Schadt (Rolic) who started to commercialise them in the last years. The principle is shown in Figure 23.

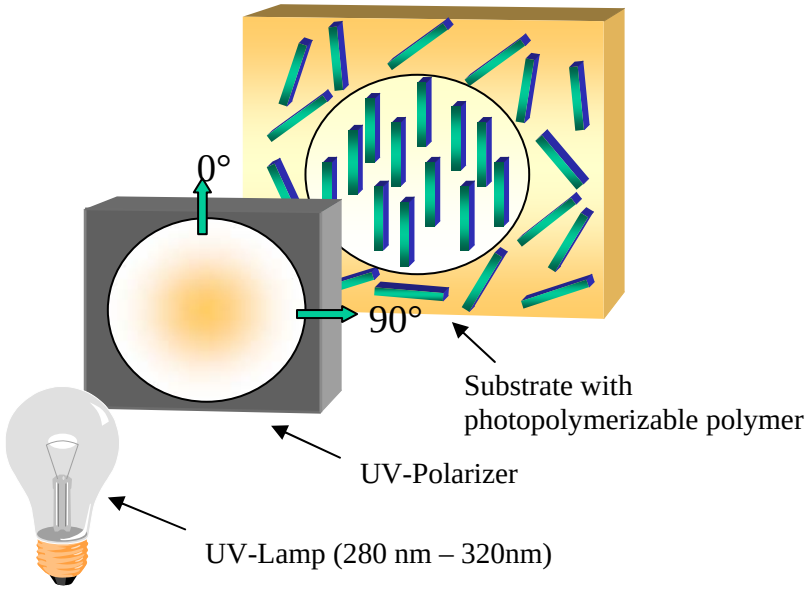

Figure 23: Principle of a photoorientation layer.

The orientation layer is formed by irradiation of a film with linear polarized light. This light leads to a photochemical 2 + 2 cycloaddition in the molecules of the layer[40]. The active species of such a photoorientation layer are polymers which contain cinnamic acid side groups as shown in Figure 24.

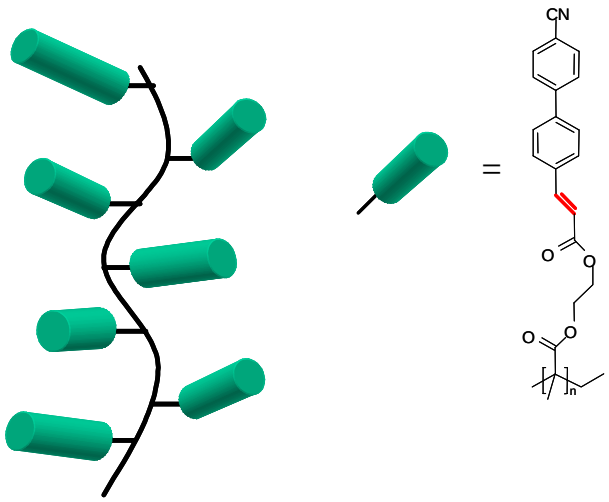

Figure 24: Structure of a photoorientation layer.

By the irradiation with polarized light the active double bond can make a 2+2 cycloaddition as shown in Figure 25.

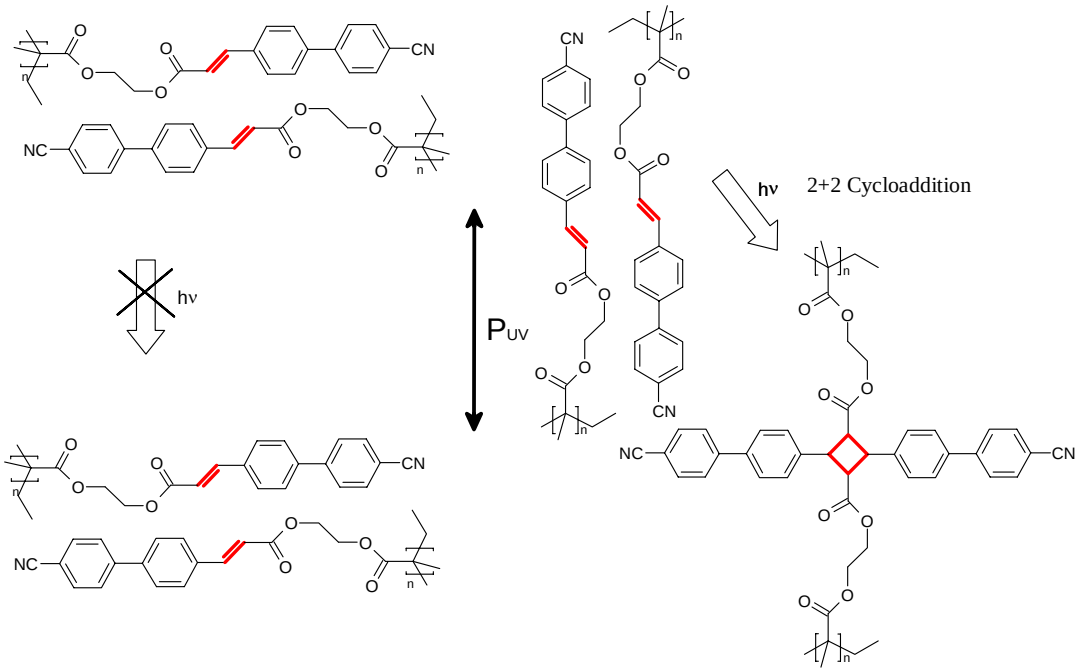

Figure 25: Chemical reaction in a photoorientation layer.

The reaction is only possible, when the dipole moment of the molecule is parallel to the polarization direction of the light[41]. The advantage of such an orientation layer is that it is

formed without any mechanical treatment. Smooth surfaces are guarantied and the use in OLEDs becomes possible. This was first described by the group of S. Kelly, who designed a polarized OLED with a photoorientation layer[42]. To ensure a hole injection through the layer they doped it with a hole conductor. Recent papers show that it is possible to synthesise a photoorientation layer, which contains additionally hole conducting segments. With such a material the doping with hole conductors can be avoided, which always leads to a decrease of the performance of the layer[43]. They achieved orientation ratios of 13/1 in electroluminescence.

To proof the ability of the orientation of the synthesised oligomers (Figure 23) we tested them on a photoorientation layers and obtained ratios of up to 19.5 in the photoluminescence which is shown in Figure 26.

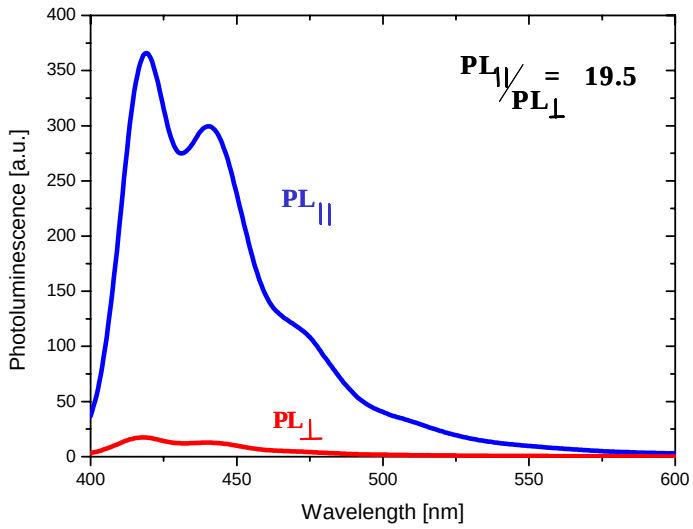

Figure 26. Polarized photoluminescence spectra of a crosslinked fluorene oligomer on photoorientation layer.

These measurements were made in collaboration with Rolic in Basel and show that the fluorene reactive mesogens can be oriented with very high orientation ratios on top of photoorientation layers. In the near future we plan to design a polarized OLED with a photoorientation layer to take benefit from these very promising results.

1.4. PhotoDSC

1.4.1. Principle

One crucial step in the preparation of long term stable oriented films from reactive mesogens is the crosslinking process. To get more information about time and conversion numbers of this kind of photopolymerisation, PhotoDSC measurements are a suitable technique. The principle setup of a PhotoDSC is shown in Figure 27.

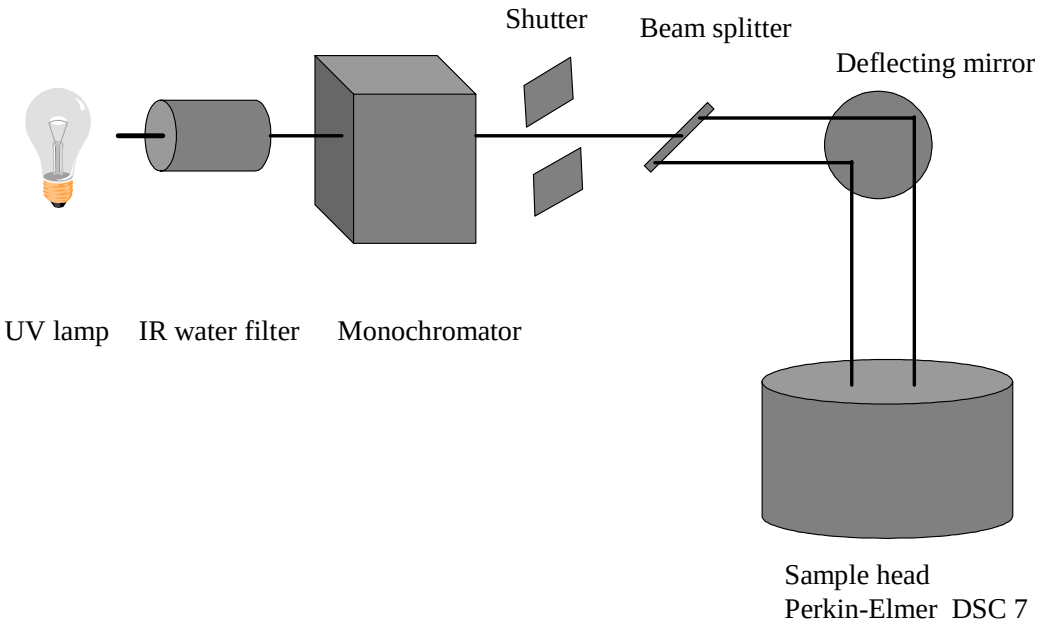

Figure 27: Design of a PhotoDSC set up.

The light from a 450 W xenon short arc lamp is passed through an IR absorbing water filter and a monochromator and split into a sample and a reference beam which are focussed to the polymerizable sample and an empty reference pan in a Perkin-Elmer DSC 7 which monitors the heat of polymerisation. The light intensity is ca. 1 mW/cm^2. This method was pioneered by D. Broer[44,45] and delivers many details about kinetics and total conversion of the crosslinking process.

1.4.2. Photopolymerization of reactive mesogens (Paper II)

In paper II PhotoDSC measurements on two different reactive mesogens are described. One nematic and one smectic reactive mesogen were used for the experiments. Their structures and phase behaviour are shown in Figure 28.

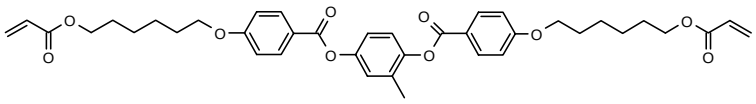

Reactive mesogen **1**

K 82 N 118 I (heating)

I 117 K 35 (cooling)

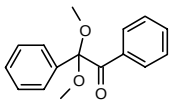

Irgacure 651

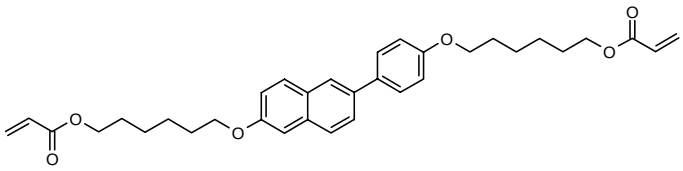

Reactive mesogen **2**

K 85 S_a 111 I (heating)

I 109 S_a 66 S_c 50 K (cooling)

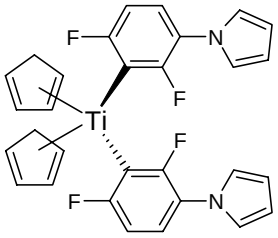

Irgacure 784

Figure 28: Structures and phase behaviour of the two reactive mesogens and the photoinitiators Irgacure 651, 784 (Ciba Geigy).

In paper II the kinetics of the photopolymerisation reactions and the total conversion in dependence from the polymerisation temperature and initiator concentration of the reactive mesogen **1** are shown. It becomes clear that the reaction rate and the total conversion decrease with the amount of photoinitiator. Nevertheless a conversion of 75 % can be realised with only 0.01 weight % of initiator, which is much less than the amount which is usually used in photopolymerisations[46]. A time conversion plot of the polymerisations with different amount of photoinitiator is shown in Figure 29.

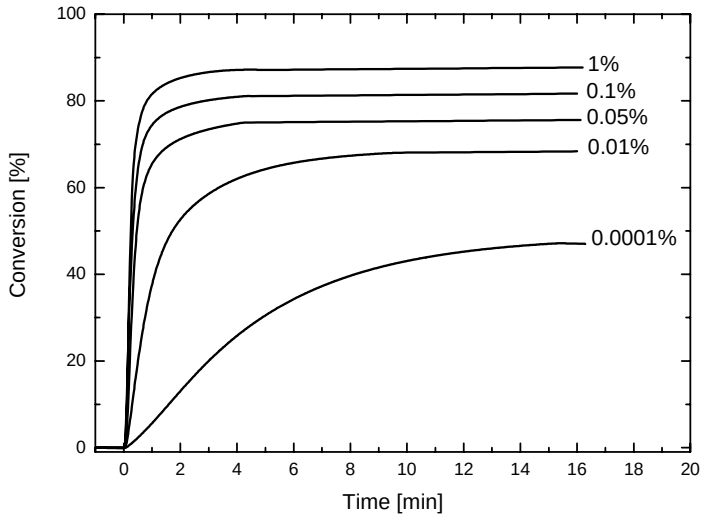

Figure 29: Time conversion plot of the photopolymerisation at 100 °C of the reactive mesogen 1 with different amounts of photoinitiator (Irgacure 651), irradiation wavelength 365 nm.

Reactive mesogen **2** has a smectic A mesophase. It was possible to polymerise within this phase. Although this phase is at lower temperatures compared to the isotropic phase, the total conversion and the polymerisation kinetics are faster. A time conversion plot of these measurements is shown in Figure 30.

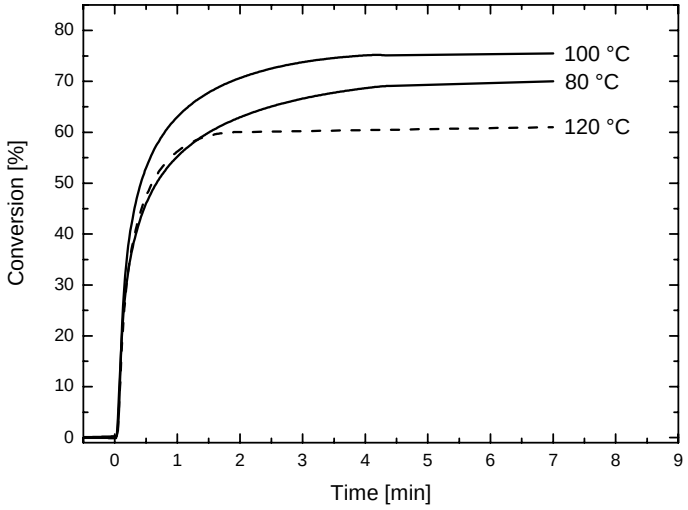

Figure 30: Time conversion plots of the photopolymerisation of reactive mesogen **2** at different temperatures, 1 weight % photoinitiator (Irgacure 651), irradiation wavelength 365 nm.

These results are very important for the use of such reactive mesogens in optoelectronic devices. The use of very low amounts of photoinitiator is above all very important for the development of OFETs from reactive mesogens. There the decomposition products of the photoinitiator may act as traps and lower the carrier mobility in OFETs[47]. So the lowest concentration of initiator is desired to minimize these "impurities" in the material in order to get the best performance. The measurements on the reactive mesogen **2** showed that the photopolymerisation in the smectic mesophase proceeds faster than in the isotropic phase although the experiment was carried out at lower temperatures.

1.4.3. Additional results

In addition to the two reactive mesogens described in paper II we have successfully polymerised one of the fluorene containing reactive mesogens **14c** from paper I. The PhotoDSC scan can be seen in Figure 31.

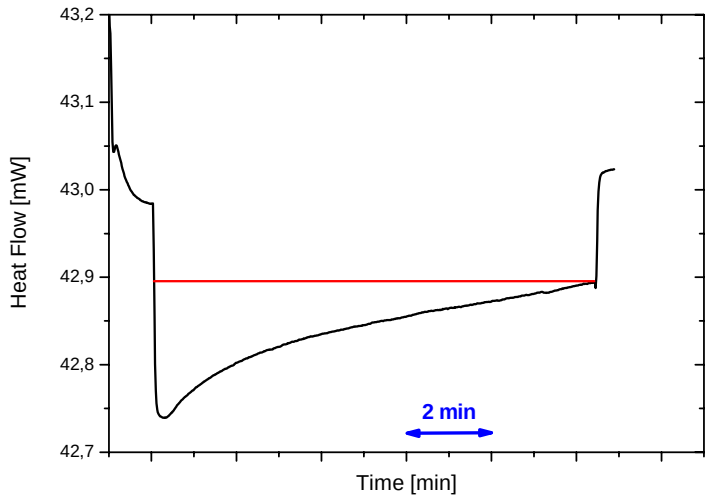

Figure 31: Photopolymerisation of fluorene oligomer **14c** at 100 °C with 1weight % photoinitiator (Irgacure 784), irradiation wavelength 450 nm.

In this case Irgacure 784 was used instead of 651, which was used in all other experiments, because Irgacure 784 absorbs light of a longer wavelength. With Irgacure 651 we were not able to perform a photopolymerisation due to the absorption of the reactive mesogen at the irradiation wavelength of the initiator (detailed description see paper II). We succeeded in getting 45 % of all acrylate end groups converted. The slower polymerisation can be explained by the higher viscosity of the oligomeric mixture compared to the low molecular mass reactive mesogens.

1.5. Organic field effect transistors

1.5.1. Principle

Since J. Bardeen, W. Shockley and W. Brattain invented the world's first transistor in 1947, silicon transistors dominate the electronic industry. The first organic field effect transistor (OFET) was reported in 1986[48]. The motivation came from their easy processibility and flexibility of the devices[49,50,51]. Different designs of OFETs are shown in Figure 32.

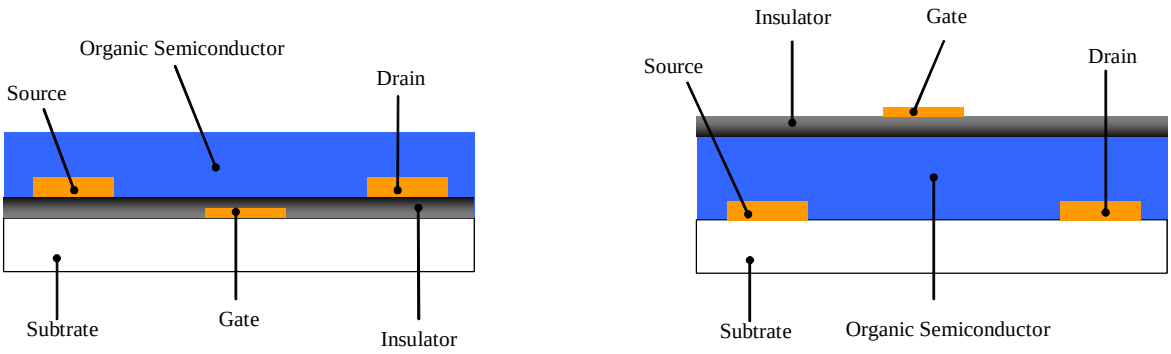

Figure 32: Schematic view on different OFET designs. Left: bottom gate; Right: Top gate structure.

An OFET consists of a three electrode design. These three electrodes (source, drain, gate) are put on top of a substrate and the gate electrode is separated from the other ones by an insulator layer. The source electrode is grounded and different voltages can be applied to the gate and drain electrodes. The organic semiconductor is deposited between source and drain by different techniques (evaporation, spin-coating). The principle operations in an OFET will be explained in Figure 33. In the following the processes will be explained for a p-type material, where holes are the charge carriers. The same principles can be translated to n-type materials with electrons as charge carriers.

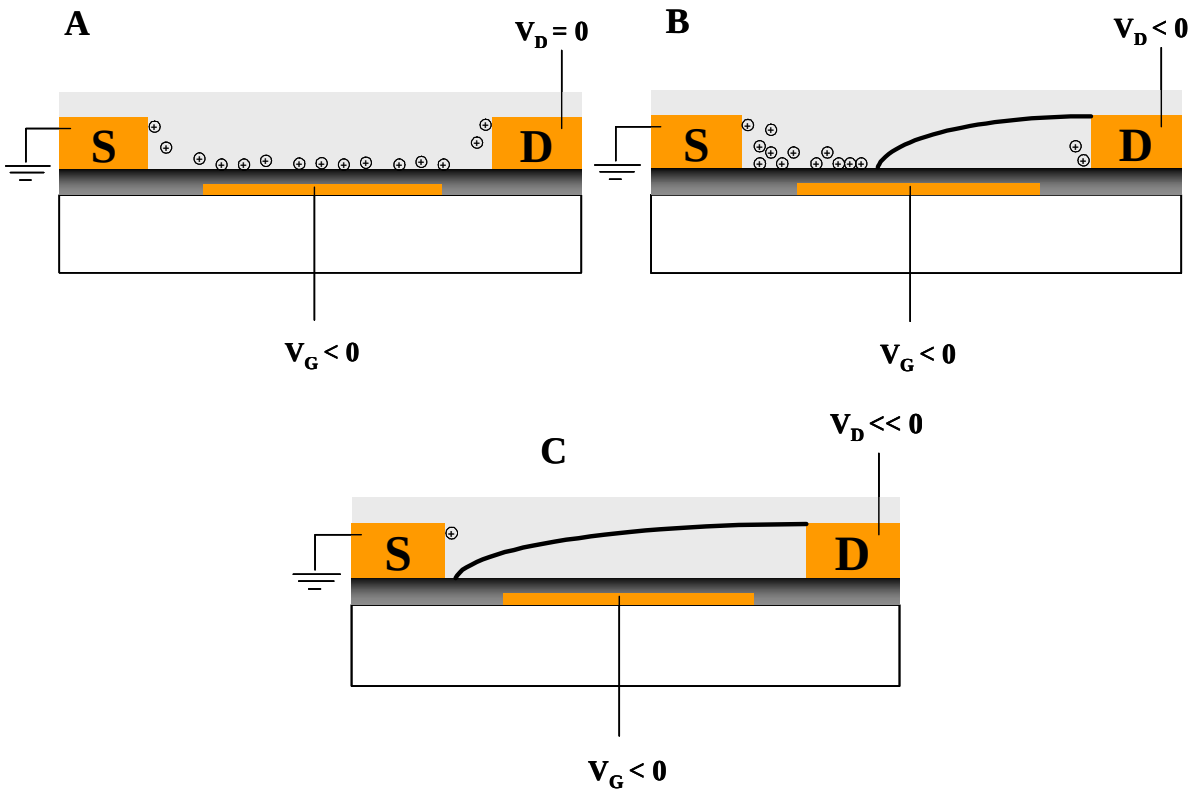

Figure 33: Typical operations in a p-type OFET[52].

If there is a negative voltage applied at the gate electrode (see scheme A), a higher concentration of positive charge carriers at the interface of insulator and semiconducting material is the consequence[52], providing a conducting channel between the source and the drain[53]. The additional induced charges are supplied by the source and drain electrodes.

For a good injection of those charge carriers these electrodes should form an ohmic contact to the semiconductor. When there is a negative voltage applied at the drain electrode (see scheme B) the charge carriers move forward to the drain electrode due to the applied electric field and a source drain current can be measured. This effect increases with the drain voltage and a depletion zone is developed at the drain electrode. If the drain voltage is high enough that the depletion zone reaches the source electrode the saturation current is the result (see scheme C). One typical plot is illustrated in Figure 34 to visualise these effects.

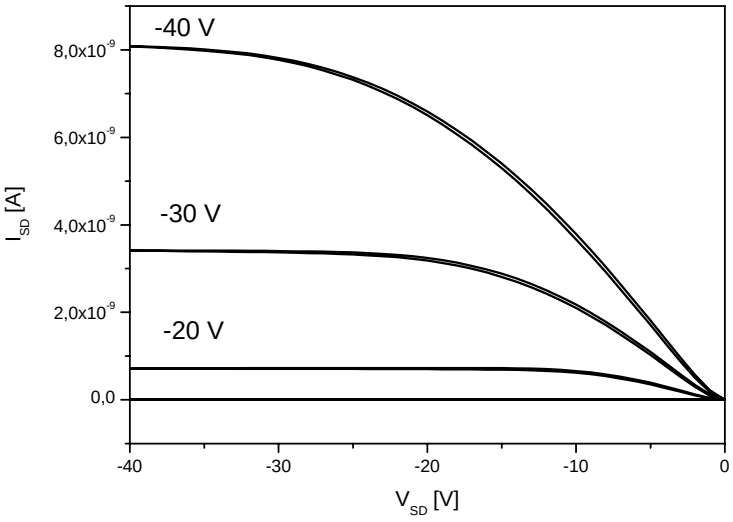

Figure 34: Typical output characteristics of an OFET (see paper IV).

Here the source drain voltage (V_{SD}) is plotted versus the source drain current (I_{SD}). In Figure 34 the experiments for different gate bias are shown (-20 V, -30 V, -40 V). As it can be seen the current rises with larger voltages, before saturation can be detected at higher voltages. So the characteristic can be divided in two regimes. A linear regime at lower voltages and a saturation regime at higher voltages. There a linear increase of the curve is desired. Otherwise the material has a contact resistance to the electrodes. The transition from one into the other regime depends on the applied gate voltage. The higher the gate

voltage the more source drain voltage is necessary to achieve saturation. Another important plot is the drain current as a function of the gate bias which can be seen in Figure 35.

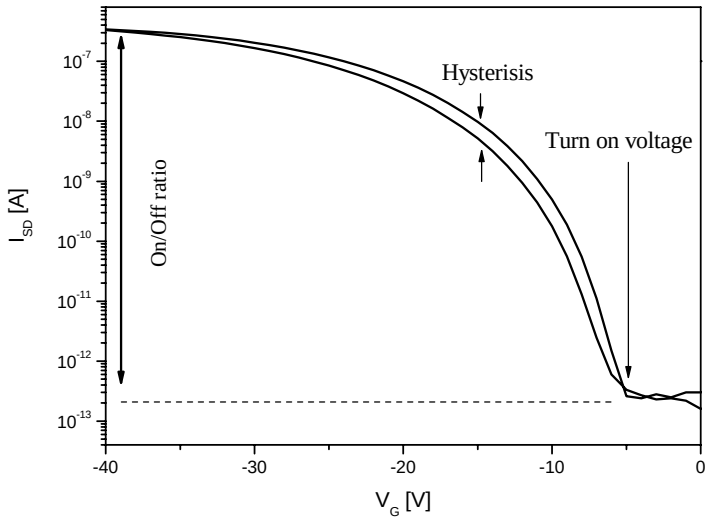

Figure 35: Typical transfer characteristics of an OFET (see paper IV).

At this characteristics the source drain voltage is kept constant. An important factor here is the so called on/off ratio which is the ratio of the current when the transistor is on and off. For applications in integrated circuits an on/off ratio of 10^6 is needed otherwise it gets too complicated to differentiate between the on and off status of the OFET in large integrated circuits. Additionally the turn on voltage can be detected at this OFET at -5 V. A turn on voltage of -1 V would be perfect for application, because then no high voltages are required. In these characteristics the forward and backward sweeps are plotted. The difference of the source drain currents is called hysteresis. A big hysteresis is a hint for impurities or instability of the material. So a small hysteresis is always desired like it is shown in Figure 37. The field effect mobility (μ_{FET}) can be calculated from these characteristics by equation 1,

$$\mu_{FET} = (L/W\ C_i\ V_D)\ (\partial I_D/\partial V_G) \qquad (1)$$

where L is the channel length, W is the channel width, C_i the capacitance of the insulator per unit area, V_D is the drain voltage, I_D is the drain current and V_G is the gate voltage.

1.5.2. Materials for OFETs

The charge carrier mobility in an OFET is closely related to the molecular order in the material. So the highest mobilities are obtained from single crystals like pentacene and rubrene, which are shown in Figure 36.

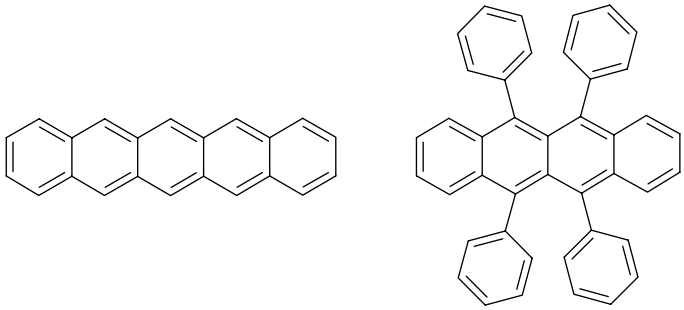

Figure 36: Structures of pentacene (left) and rubrene (right).

One of the most investigated materials in OFET is pentacene. Groups around the world try hard to get perfect single crystals of the material. The best mobilities are in the range of 5 cm^2/Vs[54]. The highest mobilities up to now measured on organic materials are obtained from rubrene single crystals where field effect mobilities of 15.4 cm^2/Vs were recently reported[55]. Apart from these single crystalline materials, where the preparation of OFETs is very complicated and which are not suitable for technical applications many other classes of materials are attractive candidates for OFET applications. So small molecules which can

be evaporated receive great interest. In this field thiophene containing materials show the best performance. Some of them are shown in Figure 37.

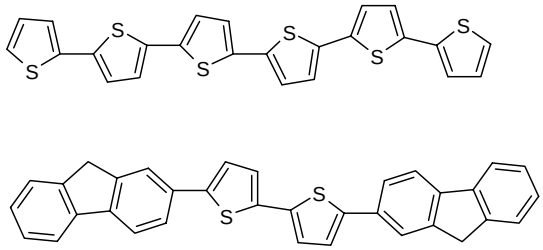

Figure 37: Structure of thiophene containing materials for OFET applications (above: sexithiophene; below: 5,5'-bis-(9H-fluoren-2-yl)-2,2'-bithiophene).

With sexithiophene[56] mobilities of $2 \cdot 10^{-2}$ cm^2/Vs can be reached[57]. The introduction of two hexyl side chains leads to α,ω-dihexylsexithiophene and an improvement of the mobility to 0.13 cm^2/Vs[58]. Another interesting class of materials is the mixed trimer with one bithiophene unit and two fluorene units (see Figure 37)[59,60]. With such materials the group of Z. Bao reached mobilities of 0.1 cm^2/Vs when using heated substrates for the evaporation step and with this getting a much higher performance due to a better film formation on the OFET.

All the described oligomers have the disadvantage, that they are not solution processable. For applications in low cost electronics the deposition of the material should be made from solution. So materials which can be spin coated are of great interest in this field. Some important structures of such polymeric systems are shown in Figure 38.

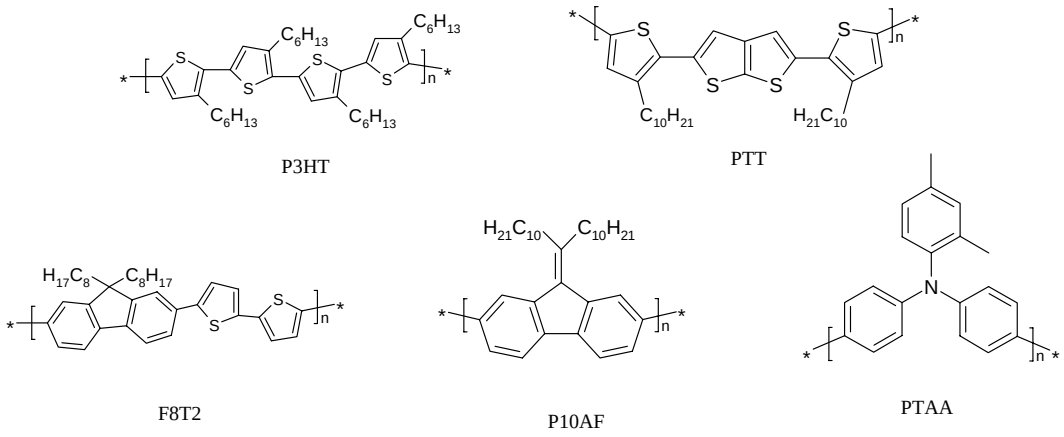

Figure 38: Polymeric materials for OFET applications.

One of the most investigated polymers is regioregular poly(3-hexylthiophene) (P3HT). There a lamella structure with two-dimensional conjugated sheets is formed by interchain stacking. The field effect mobility of $2 \cdot 10^{-4}$ cm^2/Vs for 81 % regioregular P3HT can be increased to 0.1 cm^2/Vs by the use of P3HT with a regioregularity of 96 %. This mobility is in the same range as the mobility of amorphous silicon[61]. McCulloch et al. showed the synthesis of other polythiophenes with different substitution patterns and end up with mobilities up to $3 \cdot 10^{-2}$ cm^2/Vs[62]. The same group showed the synthesis of poly(2,5-bis(3-decylthiophen-2-yl)thieno[2,3-b]thiophene) (PTT) which has mobilities of 0.15 cm^2/Vs[63]. One significant drawback of purely thiophene based structures is their poor stability and high sensitivity towards oxidation especially in the solid state[64]. One approach to a more stable semiconductor is the use of triarylamines (PTAA). This class of material shows perfect film forming properties due to their amorphous morphology and nevertheless a field effect mobility of $5 \cdot 10^{-3}$ cm^2/Vs is achieved in a top gate transistor (see Figure 32) with polyisobutylene as insulator[65]. The mobility can be shifted by two orders of magnitude by the use of different gate insulators. Apart from the different triphenylamines the introduction of fluorene units is another trend towards stable materials for OFETs. Due to the fact that pure fluorenes are not suitable for the use in OFETs because of their too low

HOMO level of -5.8 eV[66], the use of alkylidene fluorenes (C10PAF, see Figure 38) is one of the possible solutions of this problem[67]. With a HOMO level of - 5.5 eV this material is stable to oxidation in air, ensures an injection of charges from the Au-electrodes and shows a nematic liquid crystalline phase from 230 °C to 380 °C. When the material is tempered in the phase a mobility of $2 \cdot 10^{-3}$ cm^2/Vs is reached, which is one order of magnitude higher than in a non tempered sample. This increase of the mobility is attributed to the better alignment in a liquid crystalline film. This effect increases by the use of orientation layers in an OFET. There the poly[(9,9-dioctylfluorene-2,7-diyl)-*co*-bithiophene] (F8T2, see Figure 38) is one of the most interesting materials. Due to the fact that this polymer possesses a nematic liquid crystalline phase, it can be oriented on orientation layers. With this procedure higher order in the material can be achieved, what leads to an increase of the performance in an OFET. The best results were given by H. Sirringhaus et al. with an increase of the field effect mobility from 10^{-3} cm^2/Vs in a non oriented sample to $2 \cdot 10^{-2}$ cm^2/Vs if the polymer is oriented on a rubbed polyimide layer[68]. Recent work showed that F8T2 has a remarkable high electron mobility of $6 \cdot 10^{-3}$ cm^2/Vs[69], what makes the material also attractive for applications where both p- and n-type transistors are needed (CMOS).

1.5.3. New fluorene – bithiophene based oligomers for the use in OFETs (Paper III)

One crucial point during the processing and orientation of F8T2 are the high transition temperatures of the polymer. L. Kinder et al. reported a transition temperature from the nematic to the isotropic phase of 311 °C from a F8T2 sample with a M_w of 31000 g/mol[70]. This temperature makes it difficult to anneal the substance in the isotropic phase in order to get the best orientation without degradation of the organic material.

To overcome this problem, we present in paper III the synthesis of oligomers based on the F8T2 structure but with a lower molecular weight, to obtain a new class of stable and

solution processable materials for OFET applications. The synthesis was carried out with the Suzuki cross coupling as shown in Figure 39.

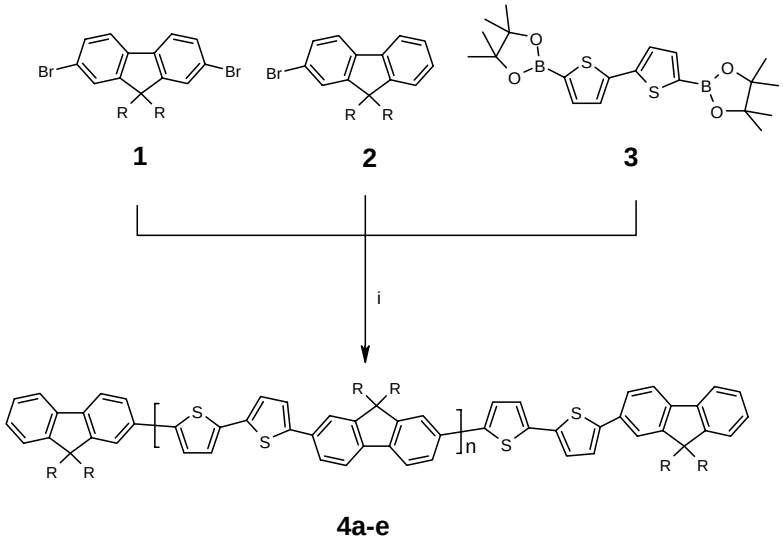

R: n-octyl; i) $Pd(OAc)_2$, tris-o-tolylphosphine, K_2CO_3 (2 M aq.), toluene, PTC, 40 °C.

Figure 39: Synthesis of fluorene – bithiophene based oligomers **4a-e** (paper III).

As described in chapter 1.3.3. the molecular weight can be tuned by the amount of an endcapper, here the monofunctionalised 2-bromofluorene compound. Like F8T2 all oligomers show broad nematic phases. The clearing temperature can be tailored by varying the molecular weight of the oligomers.

The transition temperatures are summarised in table 1. As it can be seen the molecular weight decreases with an increasing amount of endcapper. The transition temperatures can be shifted from 80 °C to 288 °C by different amounts of endcapper.

Table 1: GPC data, calculated degree of polymerisation and clearing temperature of oligomers **4a-e**.

	molar ratio 1 / 2	**M_n [g/mol]***	**M_w [g/mol]***	**P_n**	**$T_{n\text{-}iso}$ [°C]****
4a	0.5	1500	2200	5.1	80
4b	1.0	2000	3350	6.8	155
4c	2.0	2900	5800	10.1	220
4d	3.0	3540	7050	12.4	245
4e	10	5030	12800	17.8	288

*From GPC measurements (polystyrene standards) and corrected by the factor 0.84.
**Determined by polarized microscopy.

The plot of $1/P_n$ against the clearing temperature results in a linear fit of the oligomers as it can be seen in Figure 40.

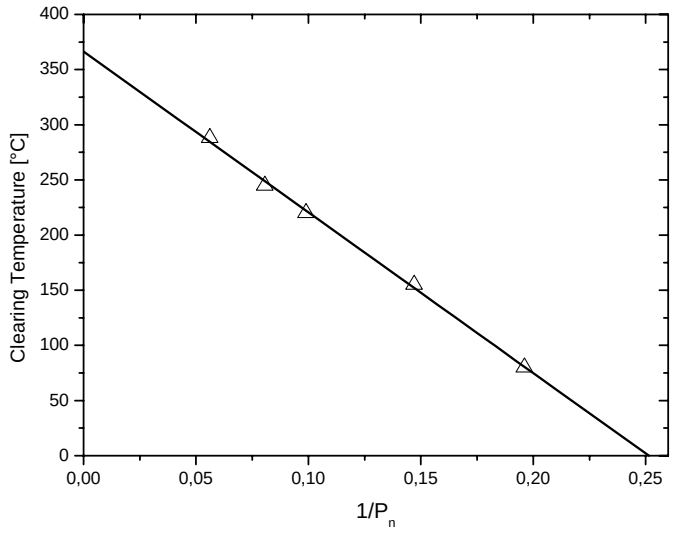

Figure 40: Plot $1/P_n$ versus clearing temperature of the oligomers **4a-e** and the linear fit.

An extrapolation to $1/P_n = 0$ (polymer) yields a clearing temperature of 366 °C. In summary we found an efficient way to synthesise fluorene – bithiophene oligomers with tailored nematic phases within a few synthetic steps. The clearing temperatures can be varied from 80 °C to 288 °C by changing the molecular weight. Additionally the

upscaling of such reactions is possible due to the low number of steps and high yields of each of them. All synthetic details and orientation experiments are given in the paper III.

1.5.4. New fluorene – bithiophene based trimers as p-channel materials in OFETs (Paper IV)

The better control of purity compared with polymers or oligomers and the well defined structure renders small molecules attractive candidates for the use in OFETs. The group of Z. Bao first reported about mixed trimers containing fluorene and bithiophene units (see Figure 37)[59,60]. The morphology of thin films of these materials can be tuned by the substrate temperature during the evaporation process from 180 °C to 25 °C. There the mobility can be shifted by one order of magnitude from 0.02 cm^2/Vs (25 °C) to 0.1 cm^2/Vs (180 °C). These measurements show how important the morphology of the evaporated film is, and how dramatically it can influence the performance of an OFET.

One disadvantage of these trimeric compounds is the unsubstitued 9 position in the fluorenes. As shown in literature this might lead to a degradation of the material and formation of fluorenone compounds[71]. So we synthesised mixed fluorene-bithiophene based trimers with different alkyl side chains in the 9 position as shown in Figure 41.

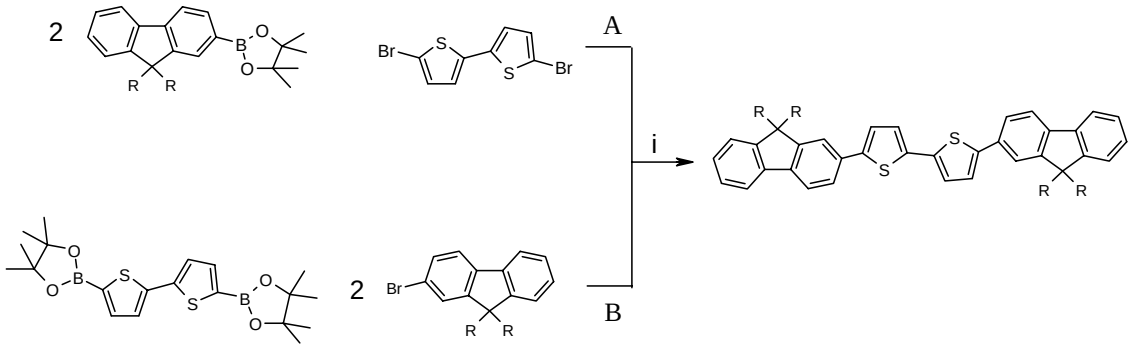

R = ethyl, n-butyl, sec-butyl, 2-ethylhexyl, n-octyl.
i) $Pd(OAc)_2$, tri-o-tolylphosphine, K_2CO_3 (2 M aq.), toluene, PTC, 40 °C.

Figure 41: Different synthetic routes towards 5,5'-bis(9,9'-dialkylfluorene-2-yl)-2,2'-bithiophene.

All synthetic details are given in paper IV. The route B turned out to be the better way to synthesise the trimers. The electrochemical characterisation by cyclic voltammetry results in a HOMO level of – 5.3 eV. This is exactly the desired level to get a good charge carrier injection from the Au-electrodes in an OFET. The thermal characterisation is summarised in table 2.

Table 2: Thermal properties of the mixed trimers from Figure 41 measured by DSC.

R	**M [g/mol]**	**T_g [°C]***	**T_m [°C]***	**$T_{recryst}$ [°C]***
ethyl	607	-	260	226
n-butyl	718	-	207	136
sec-butyl	718	95	-	-
2-ethylhexyl	943	20	90	-
n-octyl	943	-	120	40

As it can be seen it is possible to get amorphous and crystalline materials from the basic structure. To measure the performance in an OFET we have made evaporated films on top of bottom gate OFETs. In Figure 44 the different film morphologies are shown.

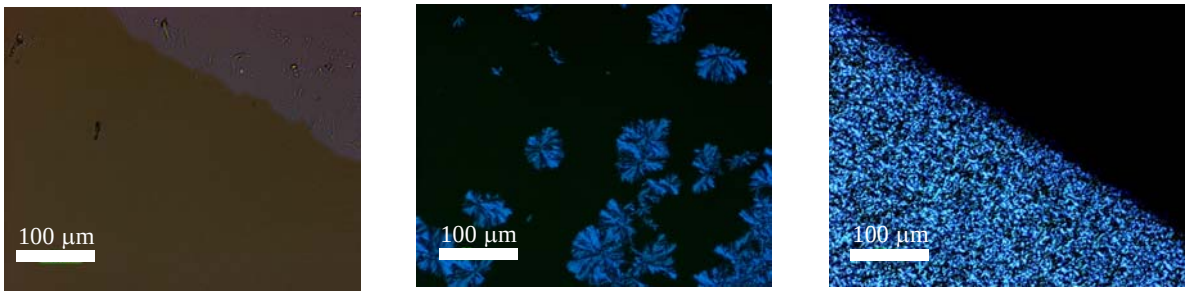

Figure 42: Polarized microscopy with crossed polarizers from 80 nm thick films of trimers with sec-butyl (left), n-butyl (middle) and ethyl (right) side chains.

OFET measurements show how the film morphology influences the performance. In an amorphous film with sec-butyl side chains a mobility of 10^{-5} cm^2/Vs is obtained. The semicrystalline material with n-butyl side chains gives mobilities of up to $2 \cdot 10^{-4}$ cm^2/Vs.

The best performance is given by the trimer with ethyl side chains which shows a mobility of $3 \cdot 10^{-3}$ cm^2/Vs and an on/off ratio of 10^6. To show the stability of this material, measurements were performed after three months storage under ambient conditions. The mobility was the same as in the freshly prepared device. The characteristics are shown in Figure 45. As it can be seen almost no hysteresis can be detected even after a few month at ambient conditions. The high mobility after this time is another hint, that the molecules are much more stable than pure thiophene materials.

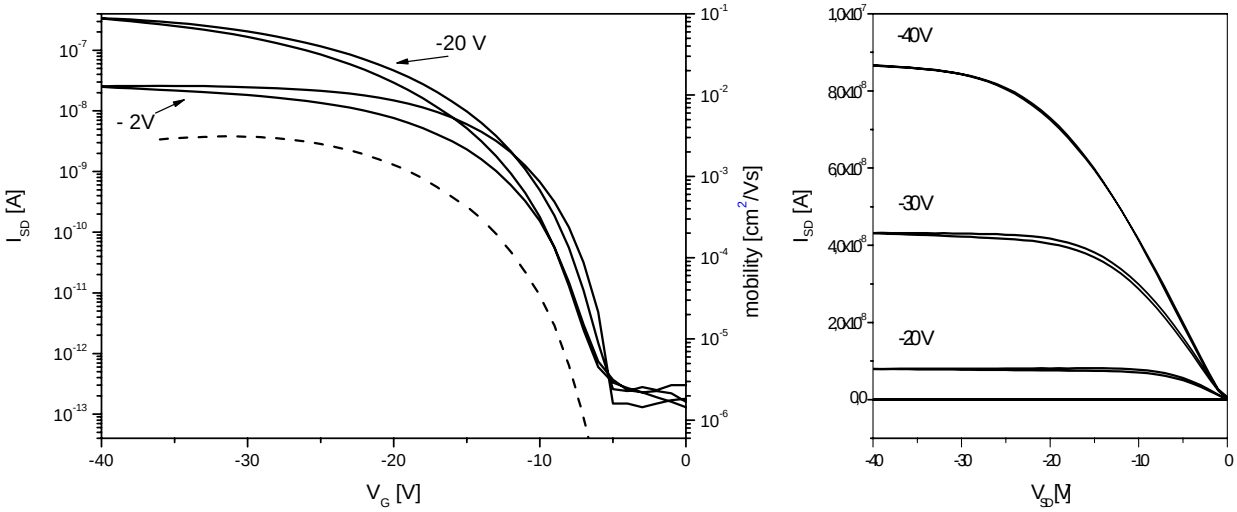

Figure 43: OFET characteristics of the trimer with ethyl side chains after three month (see Figure 41). Left: Transfer characteristics (solid lines, V_D = -2 V, -20 V). The dashed curve shows the mobility values (for V_D = -2 V). Right: Output characteristics at different gate voltages.

So a new class of active materials was synthesised by Suzuki cross coupling. It can be shown very nicely how the film morphology influences the performance in an OFET. The mobility can be shifted by more than two orders of magnitude from an amorphous film to a microcrystalline one.

1.6. Statement

In this short statement I will describe my own role and the role of the co-authors in the scientific work presented in the papers I to IV which are part of this PhD thesis.

Paper I:

The synthesis of fluorene trimers and pentamers was first carried out by Dr. M. Jandke during his PhD work in our group. D. Hanft which works as a technical assistant in our labs helped M. Jandke and me in repeating some synthetic steps. During my PhD thesis I improved the synthesis of all building blocks for the fluorene reactive trimers and pentamers so that they are available now in quantities of a few hundred milligrams. The synthesis of the oligomeric mixtures which allows preparing fluorene reactive mesogens in a gram scale was developed and carried out by myself.

Paper II:

This was one result of a collaboration with the Merck Research Center in Southampton/UK in the framework of the BMBF program POLITAG. I have installed the PhotoDSC equipment and made all measurements and interpretations given in the paper. The two investigated reactive mesogens have been provided to us by the group of Dr. Iain McCulloch and Dr. Maxim Shkunov.

Paper III:

I have carried out all the synthetic work and the orientation experiments described in paper III with the support of M. Rothmann who worked on this topic during his advanced lab course in our group.

Paper IV:

All synthetic work and the detailed characterisation of the compounds was done by myself. The OFET measurements were carried out by myself during several visits to Philips Research in Eindhoven in the labs of Dr. D. deLeeuw and Dr. S. Setayesh, who also helped me with the interpretation of the transistor data.

1.7. Literature

[1] www.nobel.se/chemistry/laureates/2000/public.html.

[2] H. Shirakawa, *Angew.Chem.Int.Ed.* **2001**, *40*, 2574 - 2580.

[3] A.G. MacDiarmind, *Angew.Chem.Int.Ed.* **2001**, *40*, 2581 – 2590.

[4] A.J. Heeger, *Angew.Chem.Int.Ed.* **2001**, *40*, 2591 - 2611.

[5] www.pioneerelectronics.com

[6] www.samsung.com/ PressCenter/PressRelease

[7] www.research.philips.com

[8] www.electronicsweekly.com

[9] R. Butscher, *Bild der Wissenschaft* **2005**, *6*, 100 - 110.

[10] www.polyic.com

[11] A. Kraft, A.C. Grimsdale, A.B. Holmes, *Angew. Chem. Int. Ed.* **1998**, *37*, 402 - .

[12] C.W. Tang, S.A. van Slyke, *Appl. Phys. Lett.* **1987**, *51*, 913 - 915.

[13] J.H. Burroughes, D.D.C Bradley, A.R. Brown, R.N. Marks, K. MacKay, R.H. Friend, P.L. Burn, A.B. Holmes, *Nature* **1990**, *347*, 539 - 541.

[14] A.J. Heeger, D. Braun, *Chem. Abstr*. **1993**, *118*, 157401j.

[15] J. Salbeck, *Ber. Bunsenges. Phys. Chem.* **1996**, 100, 1666 - 16774.

[16] J. Huber, K. Müllen, J. Salbeck, H. Schenk, U. Scherf, T. Stehlin, R. Stern, *Acta Polym.* **1994,** *45*, 244 - 249.

[17] www.kodak.com/eknec/PageQuerier

[18] www.epson.co.jp/e/newsroom

[19] www.sony. net/SonyInfo/News/Press/200409/04-048E/

[20] www.olla-project.org

[21] M. Fukuda, K. Sawada, K. Yoshino, *J. Polym. Sci. A: Polym. Chem.* **1993**, **31**, 2465 - 2469.

[22] T. Yamamoto, Z.-H. Zhou, K. Takaki, M. Shimura, K. Kizu, T. Maruyama, Y. Nakamura, T. Fukuda, B.L. Lee, N. Ooba, S. Tomaru, T. Kurihara, T. Kaino, K. Kubota, S.J. Sasaki, *J. Am. Chem. Soc*. **1996**, *118*, 10389 - 10391.

[23] H.-G. Nothofer, A. Meisel, T. Miteva, D. Neher, M. Forster, M. Oda, G. Lieser, D. Sainova, A. Yasuda, D. Lupo, W. Knoll, U. Scherf, *Macromol. Symp.* **2000**, *154*, 139 - 143.

[24] T. Yamamoto, *Prog. Polym. Sci*. **1992**, 17 1153 - 1205.

[25] A. Suzuki, *Pure Appl. Chem*. **1991**, *63*, 419 - 430.

[26] M.T. Bernius, M. Inbasekaran, J. O'Brien, W. Wu, *Adv. Mater.* **2000**, *12*, 1737 - 1750.

[27] N. Miyaura, A. Suzuki, *Chem. Rev*. **1995**, *95*, 2457 - 1483.

[28] J.Teetsov, M.A. Fox, *J. Mater. Chem.* **1999**, *9*, 2117 - 2123.

[29] M. Grell, D.D.C. Bradley, M.Inbasekaran, E. Woo, *Adv. Mater.* **1997**, *9*, 798 - 802.

[30] U. Scherf, E.J.W. List, *Adv. Mater.* **2002**, *14*, 477 - 487.

[31] J Jo, C. Chi, S. Höger, G. Wegner, D.Y. Yoon, *Chem. Eur. J.* **2004**, *10*, 2681 - 2688.

[32] R. Güntner, T. Farrell, U. Scherf, T. Miteva, A. Yasuda, G. Nelles, *J. Mater. Chem*. **2004**, *14*, 2622 - 2626.

[33] K.S.Whitehead, M. Grell, D.D.C.Bradley, M. Jandke, P. Strohriegl, *Appl. Phys. Letters* **2000**, *76*, 2946 - 2948.

[34] M. Jandke, PhD thesis, University Bayreuth, **2000**, 119.

[35] M. Grell, W. Knoll, D. Lupo, A. Meisel, T. Miteva, D. Neher, H.-G. Nothofer, U. Scherf, A. Yasuda, *Adv. Mater.* **1999**, *11*, 671 - 675.

[36] Y. Geng, A.C.A. Chen, J.J. Ou, S.H. Chen, K. Klubek, K.M. Vaeth, C.W. Tang, *Chem. Mater.* **2003**, *15*, 4352 - 4360.

[37] S.W. Culligan, Y. Geng, S.H. Chen, K. Klubek, K.M. Vaeth, C.W. Tang, *Adv. Mater.* **2003**, *15*, 1176 - 1181.

[38] J. Lub, D.J.Broer, R.A.M. Hikmet, K.G.J. Nierop, *Liquid Crystals* **1996**, *20*, 277 - 282.

[39] M. Jandke, D. Hanft, P. Strohriegl, K. Whitehead,; M. Grell, D.D.C. Bradley, *Proc. SPIE* **2001**, *4105*, 338 - 349.

[40] M.Schadt, H. Seiberle, A. Schuster, *Nature* **1996**, *381*, 212 - 215.

[41] M. Schadt, H. Seiberle, A. Schuster, S.M. Kelly, *Jpn. J. Appl. Phys*. **1995**, *34*, 3240 - 3249.

[42] A.E.A. Contoret, S.R. Farrar, P.O. Jackson, S.M. Kahn, L. May, M. O´Neill, J.E. Nicholls, S.M. Kelly, G.J. Richards, *Adv. Mater*. **2000**, *12*, 971 – 974.

[43] M.P. Aldred, A.E.A. Contoret, S.R. Farrar, S.M. Kelly, D. Mathieson, M. O'Neill, W.C. Tsoi, P. Vlachos, *Adv. Mater.* **2005**, *17*, 1368 - 1372.

[44] D.J. Broer, J. Boven, G.N. Mol, G. Challa *Makromol. Chem.* **1989,** *190*, 2255 - 2268.

[45] D.J. Broer, G.N. Mol, G. Challa *Makromol. Chem*. **1989,** *190*, 19 - 30.

[46] H.F. Mark, N.M. Bikales, C.C. Overberger, *Encyclopedia of Polymer Science and Engineering* , 2nd ed. J.Wiley&Sons, New York, **1988**, *11*, 186.

[47] B.-H. Huisman, J.J.P. Valeton, W.Nijssen, J.Lub, W. ten Hoeve, *Adv. Mater.* **2003**, *15*, 2002 - 2005.

[48] A. Tsumura, H. Koezuka,, T. Ando, *Appl. Phys. Lett.* **1986**, *49*, 1210 - 1212.

[49] C.D. Dimitrakopoloulos, P.R.L. Malenfant, *Adv. Mater.* **2002**, *14*, 99 - 117.

[50] J. Veres, S. Ogier, G. Lloyd, D. deLeeuw, *Chem. Mater.* **2004**, *16*, 4543 - 4556.

[51] M.M. Ling, Z. Bao, *Chem. Mater.* **2004**, *16*, 4824 - 4840.

[52] A.R. Brown, C.P. Jarret, D.M. deLeeuw, M. Matters, *Synth. Met.* **1997**, *88*, 37 - 55.

[53] G. Horowitz, *Adv. Mater.* **1998**, *5*, 365 - 377.

[54] T.W. Kelley, D.V. Muyres, P.F. Baude, T.P. Smith, T.D. Jones, *Mat. Res.Soc. Proc.* **2003**, *771*, L6.5.1.

[55] V.C.Sundar, J. Zaumseil, V. Podzorov, E. Menard, R.L. Willett, T. Someya, M.E. Gershenson, J.A. Rogers, *Science* **2004**, *303*, 1644 - 1646.

[56] F. Garnier, A. Yassar, R. Hajlaoui, G. Horowitz, F. Deloffre, B. Servet, S. Ries, P. Alnot, *J. Am. Chem. Soc.* **1993**, *115* 8716 - 8720.

[57] A. Dodabalapur, L. Torsi, H.E. Katz, Sience **1995**, *268*, 270 - 272.

[58] C.D. Dimitrakopoulos, B.K. Furman, T. Graham, S. Hegde, S. Purushothaman, *Synth. Met.* **1998**, *92*, 47 - 52.

[59] H. Meng, Z. Bao, A.J. Lovinger, B.C. Wang, A.M. Mujsce, *J. Am. Chem. Soc.* **2001**, *123*, 9214 - 9215.

[60] H.Meng, J. Zheng, A.J. Lovinger, B.C. Wang, P. G. van Patten, Z. Bao, *Chem. Mater.* **2003**, *15*, 1778 - 1787.

[61] H. Sirringhaus, P.J. Brown, R.H. Friend, M.M. Nielsen, K. Beechgard, B.M.W. Langeveld-Voss, A.J.H. Spiering, R.A.J. Jannsen, E.W. Meijer, D. deLeeuw, *Nature* **1999**, *401*, 685 - 688.

[62] I. McCulloch, C. Bailey, M. Giles, M. Heeney, I. Love, M. Shkunov, D. Sparrowe, S. Tierney, *Chem. Mater.* **2005**, *17*, 1381 – 1386.

[63] M. Heeney, C. Bailey, K. Genevicius, M. Shkunov, D. Sparrowe, S. Tierney, I. McCulloch, *J. Am. Chem. Soc.* **2005**, *127*, 1078 – 1079.

[64] W. Yu, H. Meng, J. Pei, W. Huang, *J. Am. Chem. Soc.* **1998**, *120*, 11808 - 11809.

[65] J. Veres, S. Ogier, G. Lloyd, D. deLeeuw, *Chem. Mater*. **2004**, *16*, 4543 - 4555.

[66] S. Janietz, D.D.C. Bradley, M. Grell, C. Giebeler, M. Inbasekaran, E.P. Woo, *Appl. Phys. Lett.* **1998**, *73*, 2453 – 2455.

[67] M. Heeney, C. Bailey, M. Giles, M. Shkunov, D. Sparrowe, S. Tierney, W. Zhang, I. McCulloch, *Macromolecules* **2004**, *37*, 5250 – 5256.

[68] H. Sirringhaus, R.J. Wilson, R.H. Friend, M. Inbasekaran, W. Wu, E.P. Woo, M. Grell, D.D.C. Bradley, *Appl. Phys. Lett.*, **2000**, *77*, 406 - 410.

[69] L.-L. Chua, J. Zaumseil, J.-F. Chang, E.C.-W. Ou, P.K.-H. Ho, H. Sirringhaus, R.H. Friend, *Nature* **2005**, *434*, 194 - 199.

[70] L. Kinder, J. Kanicki, P.Petroff, *Synthetic Metals* **2004**, *146*, 181 - 185.

[71] E.J.W. List, R. Guentner, P. Scanducci de Freitas, U. Scherf, *Adv. Mater.* **2002**, *14*, 374 - 378.

Synthesis and orientation of fluorene containing reactive mesogens

Submitted to Macromolecular Chemistry and Physics: 12.10.2005

*Heiko Thiem, Markus Jandke, Doris Hanft and Peter Strohriegl**

Makromolekulare Chemie I and Bayreuther Institut für Makromolekülforschung (BIMF), Universität Bayreuth, D-95440 Bayreuth, Germany

Email: heiko.thiem@uni-bayreuth.de

Email: peter.strohriegl@uni-bayreuth.de

Abstract

The synthesis of new fluorene containing, photocrosslinkable reactive mesogens is described. Both monodisperse trimers or pentamers and oligomeric mixtures containing two photocrosslinkable acrylate end groups were obtained by suzuki cross coupling reactions. The pentamer **12a** shows an ideal phase behaviour for orientation experiments with a broad nematic phase between the glass transition at –10 °C and 123 °C. In the oligomeric mixtures **14a-g** the transition temperature from the nematic to the isotropic phase can be tailored from 100 °C to 310 °C by adjusting the molecular weight of the oligomers by endcapping. This process can be easily characterized by MALDI-TOF spectroscopy. The pentamer **12a** and the oligomeric mixture **14c** were oriented on rubbed polyimide layers and orientation ratios of 15/1 in photoluminescence were obtained. Experiments with different film thicknesses show that the orientation is not homogeneous throughout the film but decreases with increasing distance from the orientation layer.

Introduction

Reactive mesogens are liquid crystalline molecules with polymerizable end groups. By photopolymerization of monomers with two or more end groups a liquid crystalline phase can be stabilized as a densely crosslinked, oriented polymeric network[1]. The principle of orientation and subsequent photocrosslinking is shown in scheme 1.

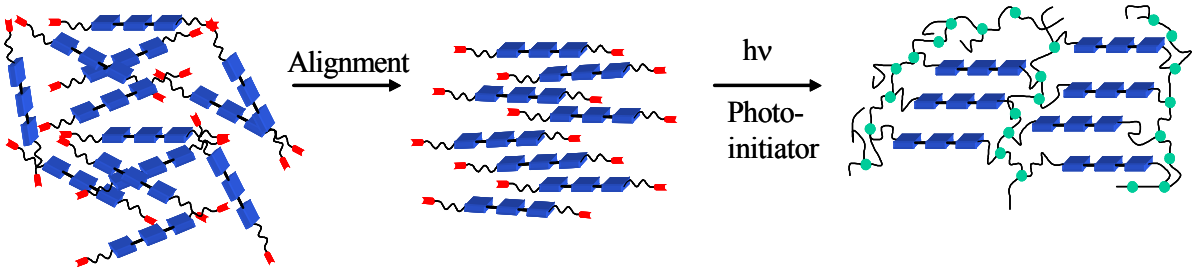

isotropic phase LC-phase LC-network

Scheme 1: Orientation and photopolymerization of reactive mesogens.

Oriented polymer networks from reactive mesogens are used in several applications. Colour flop pigments with a distinct viewing angle dependence of the colour are made by photopolymerization of cholesteric mesophases[2]. A second application of crosslinked cholesteric mesophases are broad band reflective polarizers with transmissions up to 82% in the visible region[3]. In the last years liquid crystals in general and reactive mesogens in particular received a lot of interest as active materials in optoelectronic applications[4]. Two applications are of special interest, organic light emitting diodes (OLEDs) and organic field effect transistors (OFETs). For OFETs materials with high charge carrier mobilities are essential. It is known, that the carrier mobility in organic materials is related to the degree of order in the material. The highest mobilities are obtained in single crystals like rubrene[5] or pentacene, but single crystals of these materials are not well suited for applications. It has been shown that high carrier mobilities can be obtained in ordered, liquid crystalline fluorene-bithiophene copolymers[6]. The field effect mobility increases

from 10^{-3} cm^2/Vs in a nonoriented sample to $2 \cdot 10^{-2}$ cm^2/Vs if the polymer is oriented on a rubbed polyimide layer. Huisman et al. reported on reactive quarterthiophene mesogens with two polymerizable acrylate end groups and their use in OFETs[7]. They achieved field effect mobilities up to $6 \cdot 10^{-4}$ cm^2/Vs in the crosslinked liquid crystalline network. McCulloch et al. prepared reactive mesogens with a quarterthiophene core and photocrosslinkable diene endgroups and achieved mobilities up to $2 \cdot 10^{-4}$ cm^2/Vs after crosslinking[8,9].

The second application for reactive mesogens with π-conjugated systems is their use in OLEDs. Here fluorene containing materials with their strong blue electroluminescence are of special interest[10]. Dialkylated polyfluorenes like 9,9-di(2-ethylhexyl)fluorene exhibit nematic liquid crystalline phases. M. Grell et al. showed that the parallel orientation of the liquid crystalline polyfluorenes in an OLED directly leads to the emission of linear polarized light[11]. As orientation layer they used rubbed polyimide, which was doped with an aromatic amine to ensure hole transport through the orientation layer. They achieved polarization ratios of 14:1 if electroluminescence is measured parallel and perpendicular to the rubbing direction. Neher et al. used a doped photoorientation layer containing azo-groups in polyfluorene OLEDs and reached orientation ratios up to 14:1[12]. We have described the orientation of 9,9-dioctylfluorene with a rubbed poly(1,4-phenylenevinylene) (PPV) layer and obtained an orientation ratio of 25:1 in electroluminescence[13]. Based on these stimulating results on polyfluorene a number of groups synthesized low molar mass model compounds with a different number of fluorene units. The first paper about defined fluorene oligomers is from Klaerner et al., who described the synthesis of a mixture of oligomers and their separation via HPLC[14]. The synthesis of monodisperse oligofluorenes with up to seven fluorene units by repetitive Suzuki and Yamamoto coupling reactions was described recently[15]. Fluorene oligomers with up to twelve units were synthesized by Geng

et al.[16]. Cullingan et al.[17] succeeded in making linear polarized OLEDs from these oligomers with polarization ratios up to 25:1 for an oligomer with twelve fluorene units.

All fluorene oligomers described above have no reactive end groups. Recent work of S. Kelly et al. showed the use of acrylate and diene photopolymerizeable end groups in the α,ω positions of mesogens containing fluorene and thiophene units[18]. They were able to orient them on photoorientation layers and achieve a full colour OLED which emits linear polarized light by the use of different mesogens [19].

We reported a number of reactive mesogens with three and five fluorene units and two photopolymerizable acrylate groups and their use as emitters in polarized OLEDs with rubbed PPV as orientation layer[20]. In this paper we describe the synthesis of a number of fluorene containing reactive mesogens with acrylate end groups in detail. Two groups of materials will be discussed. First the synthesis of monodisperse mesogens with three or five fluorene units, which we have used in polarized OLEDs, will be described. The second part of the synthetic work is about oligomeric mixtures containing fluorene units with two acrylate end groups obtained by end capping. This synthetic strategy allows us to make reactive mesogens in a gram scale within one synthetic step. In the third part of this paper the LC-phase behaviour and the orientation of the reactive mesogens on rubbed polyimide orientation layers are discussed.

Results and Discussion

Synthesis and Characterisation.

The synthesis of the fluorene reactive mesogens described in this paper involves a number of steps which are shown in schemes 2 – 5. The preparation of the three basic building blocks, the dialkylated 2,7–dibromofluorenes **1a-c**, the diboronic esters **2a-c** and the monobromofluorenes **6a-c** with the OH-functionalized side group is outlined in scheme 2.

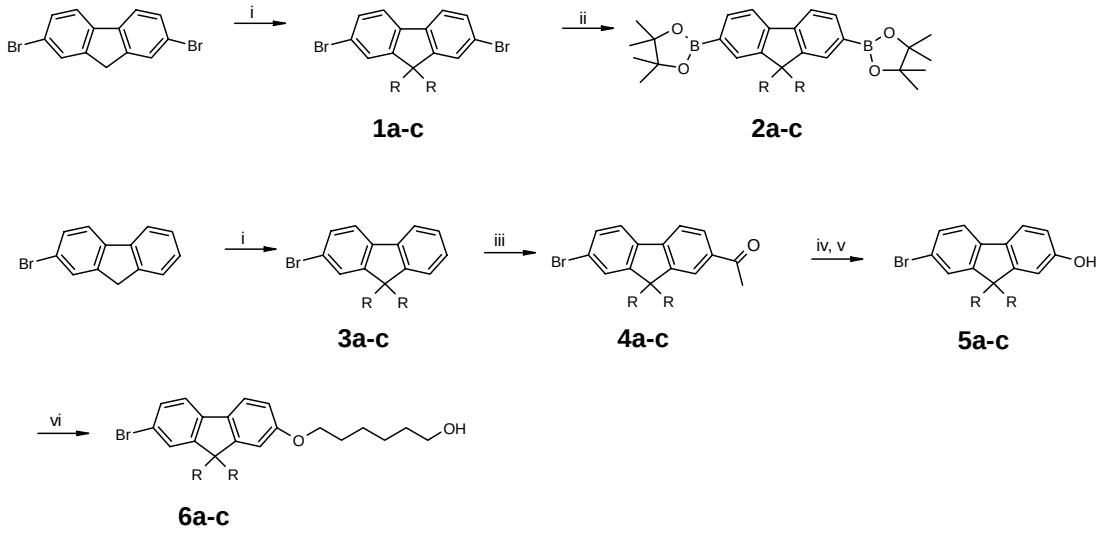

i)R-Br, DMSO, NaOH, 90 °C; ii) n-BuLi, 2-isopropoxy-4,4,5,5-tetramethyl-1,3,2-dioxaborolane, THF; -78 °C; iii) $AlCl_3$, AcCl, CH_2Cl_2, 0 °C; iv) HCOOH, TFAc, H_2O_2, ethyl acetate, 0 °C; v) KOH, MeOH; 70 °C; vi) 6-chlorhexanole, K_2CO_3, KI, cyclohexanone,
160 °C.

	1a, 2a, 3a, 4a, 5a, 6a	**1b, 2b, 3b, 4b, 5b, 6b**	**1c, 2c, 3c, 4c, 5c, 6c**
R	2-ethylhexyl	n-octyl	n-butyl

Scheme 2: Synthesis of the fluorene building blocks.

1a-c and **2a-c** were synthesized using 2,7-dibromofluorene as the starting material following a literature method[21,22]. The first step is the alkylation of 2,7-dibromofluorene with different alkyl bromides in a phase transfer reaction using aqueous NaOH and DMSO as solvents. The dialkylated 2,7-dibromofluorenes **1a-c** are reacted with n-BuLi in THF at -

78 °C, followed by the addition of 2-isopropoxy-4,4,5,5-tetramethyl-1,3,2-dioxaborolane, which leads to the formation of the diboronic esters **2a-c**.

The synthesis of the functionalized monobromofluorenes **6a-c**, with two different substituents in the 2- and 7– position, takes a few more steps. The introduction of a phenolic OH–group into the 7–position of the fluorene involves two steps. First the alkylated 2–bromofluorenes **3a-c**, which were synthesized analogous to **1a-c**, are reacted with acetyl chloride in a Friedel – Crafts reaction with yields of 85 % of the acylated fluorene derivatives **4a-c**. The acetyl function is oxidized by in situ prepared performic acid in a Baeyer-Villiger reaction. The resulting methyl ester is cleaved with KOH to yield the phenols **5a-c**. When we started our synthetic work on fluorene reactive mesogens we used commercially available m–chloroperbenzoic acid in this reaction. Since the reactivity of this reagent is quite low and a number of byproducts are formed the final yield was only 20 – 30 %. If freshly prepared performic acid[23] in a 1:1 mixture of formic acid and ethyl acetate is used, the reaction is finished within one hour and almost no byproducts are formed. Using that procedure **5a** is obtained in 77 % yield from **4a**, which is very important at that early step of the synthesis. In the last step a C6-spacer is introduced by etherfication of the phenolic OH-group with 6-chlorohexanole.

The key steps in the synthesis of the fluorene containing reactive mesogens are Suzuki cross coupling reactions. The simplest reactive mesogens which are accessible from the building blocks in scheme 2 are trimers. For the synthesis of the trimers **10a-d** (scheme 3), diborolanes **2** are reacted with two equivalents of the monobromfluorenes **6a-c** in a 2/1 mixture of toluene and aqueous 2M K_2CO_3 with a crown ether as phase transfer catalyst. The photopolymerizable acrylate groups are introduced in the last step by etherification with acryloyl chloride.

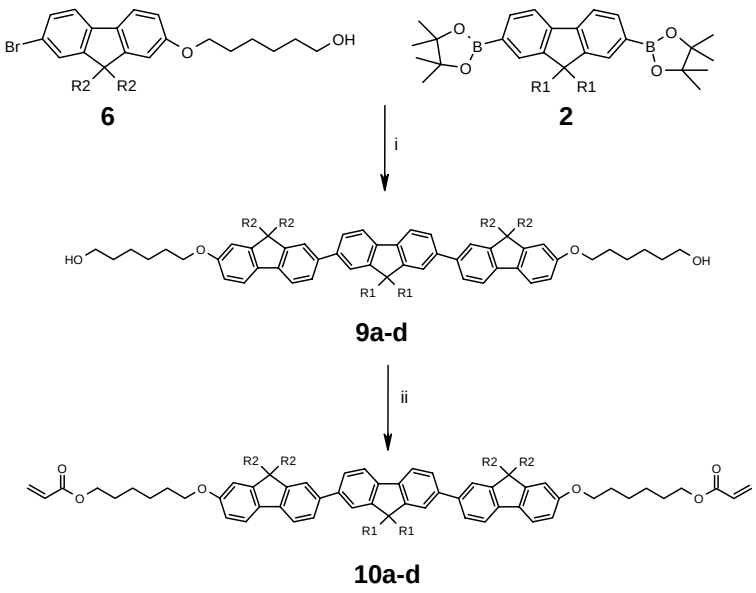

i) $Pd(PPh_3)_4$, K_2CO_3 (2 M aq.), toluene, PTC, 50 °C; ii) DMA, acryloyl chloride, toluene, 40 °C.

	9a, 10a	**9b, 10b**	**9c, 10c**	**9d, 10d**
R1	2-ethylhexyl	n-octyl	n-butyl	n-butyl
R2	2-ethylhexyl	n-octyl	n-butyl	2-ethylhexyl

Scheme 3: Synthesis of photocrosslinkable fluorene containing trimers.

With the same starting molecules, but an equimolar amount of **2** and **6** the dimeric intermediates **8a-c** are obtained in the Suzuki cross coupling reaction (scheme 4). The yield of this step is only in the range of 20 %. Careful analysis of the byproducts shows, that the main product is a dimer with a proton at the 7-position instead of the boronic ester group, which was split off during the reaction. From the intermediates **8a-c** the pentamers **11a-c** are obtained via another suzuki reaction with an alkylated 2,7-dibromofluorene **1**, which is shown in scheme 4. After esterfication with acryloyl chloride the target molecules **12a-c** are obtained.

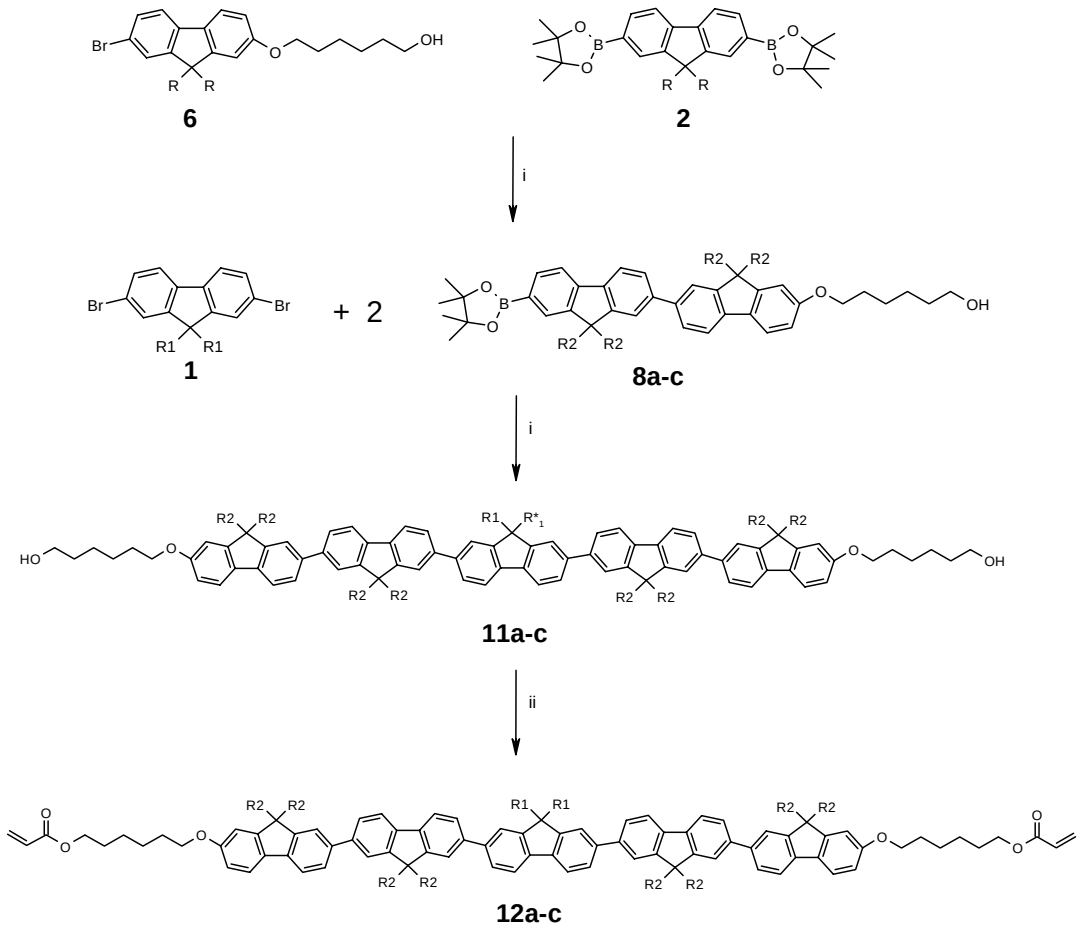

i) $Pd(PPh_3)_4$, K_2CO_3 (2 M aq.), toluene, PTC, 50 °C; ii) DMA, acryloyl chloride, DMA, toluene, 40 °C.

	8a	**8b**	**8c**	**11a, 12a**	**11b, 12b**	**11c, 12c**
R1	-	-	-	n-butyl	n-octyl	n-butyl
R2	2-ethylhexyl	n-octyl	n-butyl	2-ethylhexyl	n-octyl	n-butyl

Scheme 4: Synthesis of photocrosslinkable fluorene pentamers.

The synthetic route to the photopolymerizable fluorene trimers **10a-d** and especially to the pentamers **12a-c** involves a large number of synthetic steps. Some of these steps, e.g. the suzuki cross coupling leading to the intermediates **8a-c**, give only moderate yields. This makes it difficult to synthesize such reactive mesogens with broad nematic phases in a larger scale. To make the synthesis of fluorene reactive mesogens more efficient, a new

synthetic route with a reduced number of steps was developed (scheme 5). Following this procedure a mixture of well defined fluorene oligomers with reactive acrylate endgroups is obtained.

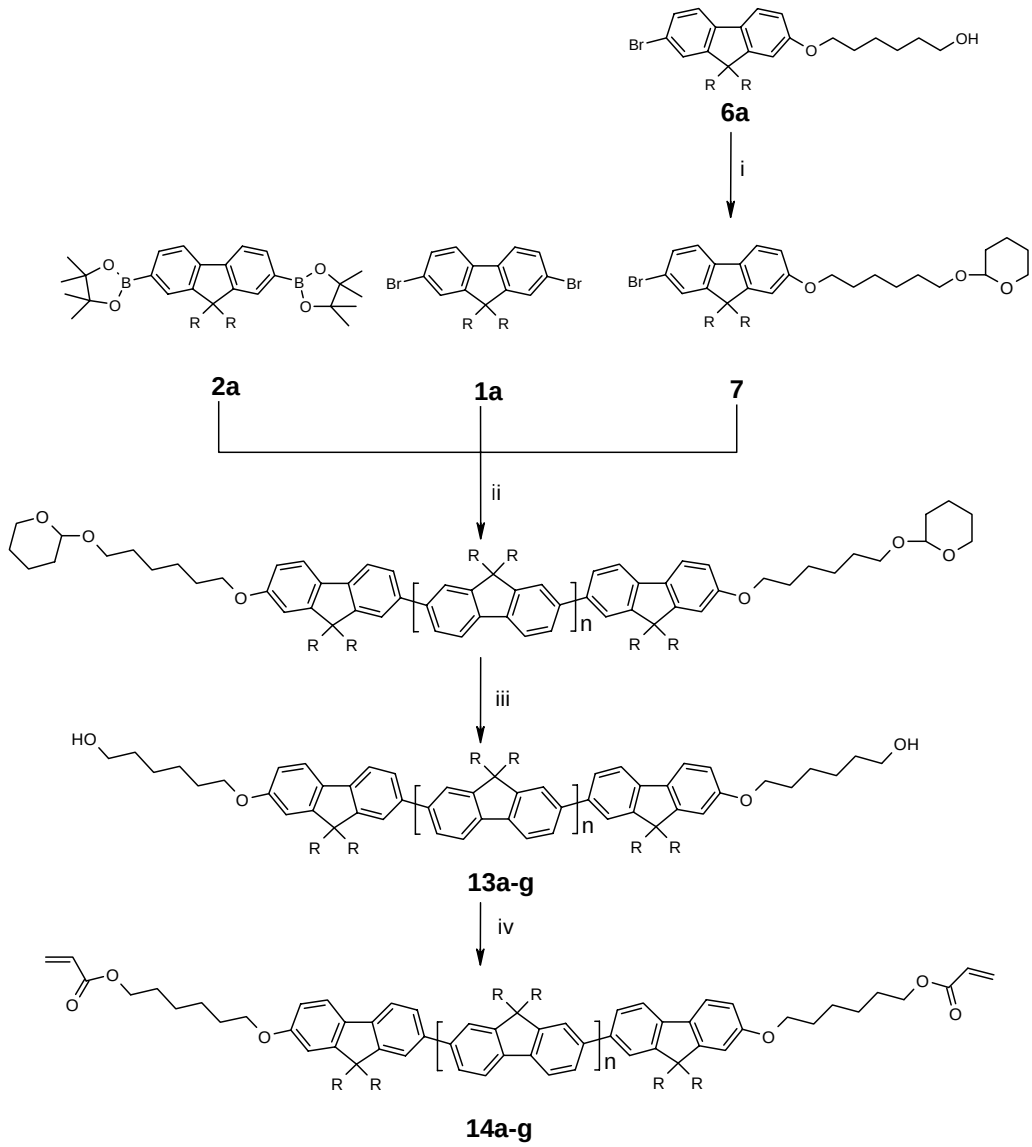

R = 2-ethylhexly

i) Et_2O, DHP, 0 °C; ii) $Pd(PPh_3)_4$, K_2CO_3 (2 M aq.), PTC, toluene, 50 °C; iii)ether,HCl,50 °C; iv) DMA, acryloyl chloride, toluene, 40 °C.

Scheme 5: Synthesis of photocrosslinkable fluorene containing oligomers **14a-g**.

From a mixture of two bifunctional monomers, the dibromofluorene **1a** and the diboronic ester **2a** with the monofunctional 2-bromofluorene derivative **7** the oligomeric mixtures **13a-g** are obtained. In this reaction the 2-monobromofluorene **7** acts as an end capper. It tunes the molecular weight of the oligomers and ensures that each oligomer has two acrylate end groups. In the course of our studies we found that the use of free hydroxy groups in suzuki cross coupling reactions leads to the formation of undesirable side products[24]. For that reason the OH-group of the 2-bromofluorene **6** was protected with tetrahydropyran (THP) [25]. After the suzuki cross coupling the THP group is cleaved quantitatively with a small amount of HCl. The esterfication with acryloyl chloride as the last step was performed in the same way as described for the trimer and pentamer reactive mesogens and delivers the reactive mesogens **14a-g**.

The different monomer ratios and resulting molecular weights of a number of runs are summarized in table 1.

Table 1: Molecular weights and transition temperatures of the fluoreneoligomers **14a-g**.

	molar ratio 1a/7	**M_n* [g/mol]**	**M_w* [g/mol]**	**$T_{n\text{-}iso}$ [°C]****
14a	3.00	5200	8800	-
14b	1.25	4200	6100	310
14c	1.00	4000	5900	243
14d	0.75	3300	4400	210
14e	0.33	2800	3700	176
14f	0.20	2500	3200	145
14g	0.10	2250	2600	100

*from GPC measurements, polystyrene calibration.
**detemined by polarized microscopy.

The molecular weight decreases with increasing amounts of the endcapper **7**. The main advantage of this synthetic strategy is that fluorene containing reactive mesogens can be easily made in a gram scale.

MALDI-TOF mass spectrometry and GPC measurements have been used to investigate the oligomeric mixtures **14a-g**. Figure 1 shows a MALDI-TOF spectrum and GPC scan of oligomer **14g**.

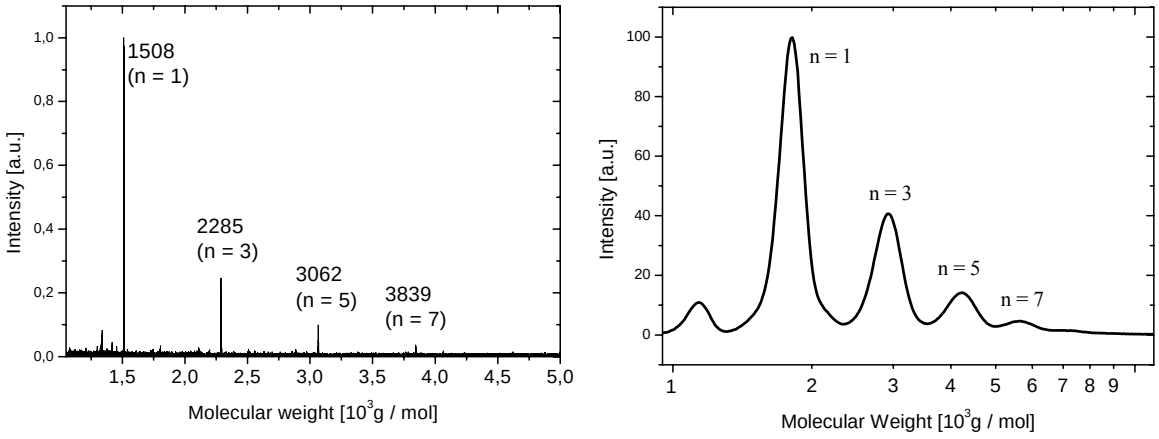

Figure 1: MALDI-TOF spectrum (left) and GPC scan (right) of Oligomer **14g**.

Due to the fact, that the oligomers form stable radical cations and have a strong absorption at the irradiation wavelength of 337 nm of the MALDI-TOF laser, the spectra could be recorded without any matrix and with a low laser intensity of 10 % of the maximum laser power. The peaks correspond to the trimer (n = 1), pentamer (n = 3), heptamer (n = 5) and nonamer (n = 7) of **14g**. From scheme 5 it becomes clear that only oligomers with an odd number of fluorene units can be formed using this synthetic strategy. Only twice end capped molecules are detected in the MALDI-TOF spectrum. There is no sign for mono or none endcapped molecules in the spectrum. The MALDI-TOF spectrum also demonstrates the high stability of the material. Most molecules tend to fracture if a MALDI-TOF experiment is carried out without a matrix. The stability of the radical cations and the strong absorption at 337 nm makes MALDI-TOF an ideal tool for the structure

determination of fluorene oligomers. In the GPC scan of **14g** the trimer (n = 1), pentamer (n = 3), heptamer (n = 5) and the nonamer (n = 7) can be clearly observed. Since the GPC equipment was calibrated with polystyrene standards, the molecular weight of the rigid, rodlike oligofluorenes is slightly overestimated.

The liquid crystalline properties of the fluorene bisacrylates were investigated by polarizing microscopy and DSC. All experiments were made in the presence of 3,5-di-tert.-butyl-4-hydroxytoluene (BHT) as inhibitor to prevent spontaneous polymerization of the acrylate end groups at higher temperatures. The trimers **10a-d** show only very small or no liquid crystalline phases. For example **10a** has a glass transition temperature of -25 °C and a nematic phase up to the clearing point at 38 °C. The phase behaviour of the other fluorene trimers is similar. For orientation experiments these phases are relatively small and at too low temperature. The phase behaviour of the pentamers makes these materials much more attractive for orientation experiments. **12c** with relatively short butyl side chains has a nematic phase between 133 °C and 170 °C. Pentamer **12a** with butyl groups in the center and 2-ethylhexyl groups on the outer fluorene units exhibits an ideal phase behaviour. This molecule has a glass transition at -10 °C and a nematic phase up to the clearing temperature of 123 °C and is well suited for the orientation experiments which will be described below.

The oligomeric mixtures **14a-g** show broad nematic phases, too. Due to the fact, that the sensitivity of the DSC was not sufficient to identify the transition temperatures of the oligomers they have been determined by polarizing microscopy (ref. Table 1). All oligomers show no sign of crystallization upon cooling and form supercooled nematic phases. The oligomer with the lowest molecular weight **14g** shows a transition from the nematic to the isotropic phase at 100 °C. The clearing temperature increases with the molecular weight of the oligomers. For example **14e** has a transition temperature of 176 °C and **14c** at 243 °C. The highest clearing temperature of 310 °C was detected for the

oligomer **14b** with a molecular weight M_n of 4200 g/mol. In **14a** with a slightly higher molecular weight it was not possible to determine the clearing point due to beginning decomposition of the material. So the variation of the molecular weight of nematic fluorene oligomers by endcapping allows to tailor the clearing temperature in a broad range from 100 °C to 310 °C.

Monodomain – Alignment and Photopolymerization

The broad nematic phases of the fluorene bisacrylate **12a** and of the oligomer **14c** have been used for orientation experiments on different orientation layers. In the following the orientation on rubbed polyimide layers is described.

After preparation of the polyimide alignment layer on quartz slides (ref. experimental part) films from the photocrosslinkable bisacrylates **12a** and **14c** with 1 weight % of photoinitiator (2,2-dimethoxy-2-phenyl-acetophenone, Irgacure 651, Ciba Geigy), were prepared from toluene solution. The alignment was achieved by a temperature program. First the samples were heated to 130 °C in the isotropic phase. Then they were cooled down slowly (5 K / min) to 100 °C in the nematic phase. This temperature was held for 30 min to achieve an optimal orientation. Photopolymerization was carried out by UV-irradiation with a Xenon short arc lamp (8 mW/cm^2 for 4 min), where the photoinitiator gives rise to the formation of free radicals. These radicals initiate the polymerization (crosslinking) of the acrylate endgroups in the fluorene bisacrylates. An oriented network is instantaneously formed (scheme 1) and prevents a thermal relaxation of the chromophore orientation. The degree of orientation is measured by polarised absorption and fluorescence spectroscopy. In figure 2 the polarized absorption and fluorescence spectra of a 30 nm thick crosslinked film of **12a** are shown.

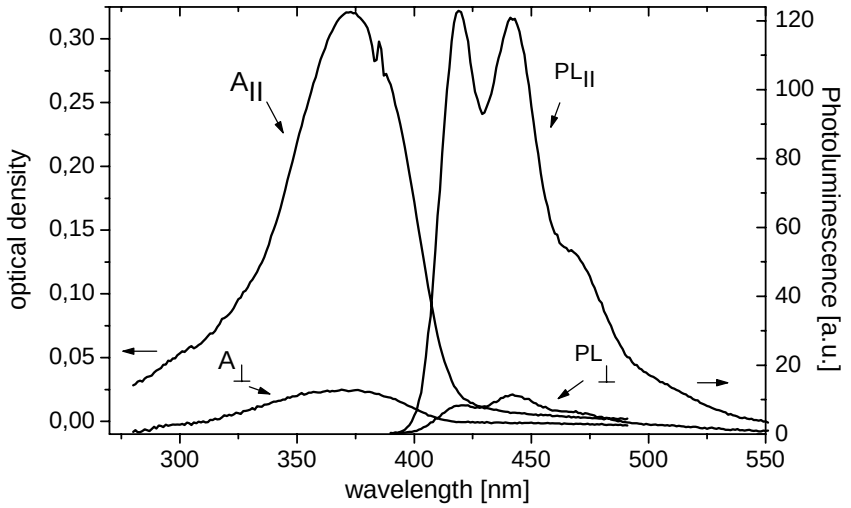

Figure 2: Absorption and photoluminescence of a 30 nm thick film of **12a** parallel (II) and perpendicular (⊥) to the rubbing direction of the polyimide alignment layer.

The spectra are measured with a linear sheet polarizer parallel and perpendicular to the rubbing direction of the polyimide layer. A maximum orientation ratio of 15:1 in fluorescence and 13:1 in absorption is obtained. The same orientation orientation ratio of 15:1 in photoluminescence was measured for the oligomeric mixture **14c**. These values are higher compared to poly(2,7-(9,9-bis-2-ethylhexyl)fluorene) where a polarization ratio of 12:1 was determined. We attribute this effect to the length of the molecules. It seems to be easier to orient shorter oligomers, because of the absence of entropic effects, which lead to coil formation in high molecular weight polymers.

These results make fluorene containing reactive mesogens like **12a** and **14c** attractive candidates for the use in polarized organic light emitting diodes (OLEDs)[18]. In another experiment we investigated if the orientation is homogenous throughout the whole film. To address this problem, a number of oriented samples with different thickness of the crosslinked reactive mesogen **12a** were prepared. Figure 3 shows the degree of orientation in films with different thickness. A decrease of orientation with higher film thickness is

detected. The highest orientation ratio of 15 is achieved with a 30 nm thick film and it goes down to 9 when the film thickness is increased to 90 nm.

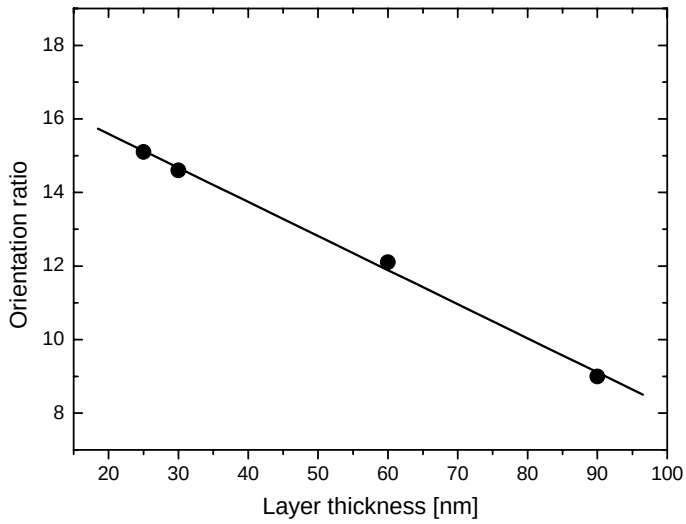

Figure 3: Photoluminescence orientation ratios (P_{II} / $P_{\perp}$)for crosslinked films of **12a** with different thickness.

This implies that the orientation of the fluorene pentamer is not homogeneous throughout the whole layer. The best orientation is obtained close to the polyimide orientation layer. With increasing distance to the polyimide layer the orientation decreases.

Conclusion

In this paper we describe the synthesis of new fluorene containing, photocrosslinkable reactive mesogens in detail. We have prepared both monodisperse trimers and pentamers and oligomeric mixtures with two photocrosslinkable acrylate endgroups. The synthesis of the building blocks has been optimized and gives an overall yield of 66 % over 6 steps leading to the endcapper **7**. Nevertheless the preparation of the trimers and particularly the pentamers involves a large number of steps and makes the synthesis of larger amounts of material rather difficult. For that purpose we have developed a method for the preparation of well defined fluorene oligomers with two acrylate endgroups by endcapping, which allows us to make such materials in a gram scale. MALDI-TOF spectrometry turned out to be an ideal tool to characterize the oligomers obtained by endcapping.

The reactive mesogen **12a** with five fluorene units shows a nematic phase between the glass transition at -10 °C and the clearing point at 123 °C. In the oligomeric mixtures **14a-g** the clearing temperature can be tuned between 100 °C and 310 °C by changing the molecular weight.

The orientation of two materials on rubbed polyimide layers was investigated. With an orientation ratio of 15:1 in photoluminescence the orientation is at a high level in both materials. Experiments with different film thicknesses of the fluorene pentamer **12a** show that the orientation is not homogeneous but decreases with increasing distance to the orientation layer. This is important for the layout of an OLED with linear polarized emission. If the recombination zone can be located close to the interface between orientation and emission layer, highly polarized OLEDs can be made.

Experimental section

Materials. All chemicals and reagents were used as received from commercial sources without further purification. All solvents for reactions and purification were once distilled, except tetrahydrofuran (THF) which was additionally distilled over potassium.

^{1}H-NMR and ^{13}C-NMR spectra were recorded with a Bruker AC 250 (250 MHz) apparatus and $CDCl_3$ as solvent. All data are given as chemical shifts δ [ppm] downfield from $Si(CH_3)_4$. The IR spectra were recorded using a Bio-Rad Digilab FTS-40. The UV-VIS spectra were recorded with a Hitachi U-3000 spectrometer. Emission spectra were obtained from a Shimadzu spectrofluorophotometer RF-5301PC. A Bruker Reflex III apparatus with highmass detector was used to record the high resolution MALDI-TOF mass spectra. For differential scanning calorimetry measurements (DSC) a Perkin Elmer DSC-7 apparatus was used (heating/cooling rate: 10 K/min). A Leitz Laborlux 12-pol, Nikon Diaphot 300 microscope with a Linkon hotstage under nitrogen atmosphere was used to determine the nematic phases of the oligomers. The purity of the target compounds was checked with a Waters gel permeation chromatography system (GPC) for oligomers (analytical columns: crosslinked polystyrene gel (Polymer Laboratories), length: 2 x 60 cm, width: 0.8 cm, particle size: 5 μm, pore size 100 Å, eluent THF (0.5 ml/min, 80 bar), polystyrene standards).

Samples for polarized photoluminescence were prepared on carefully cleaned quartz slides. For the preparation of polyimide alignment layers a solution of a polyamic acid precurser (PI-Kit ZLI 2650, MERCK) was spin-coated onto the substrate and subjected to thermal conversion in a nitrogen atmosphere (1 h at 100 °C, 1 h at 200 °C, 1 h at 300 °C). Finally the substrate was rubbed with a velvet drum using a commercial rubbing machine (1200 rpm, Optron Instruments).

The fluorene compounds were spin-coated from toluene solution in a concentration of 10 – 200 mg / ml at 2000 rpm. Additionally 1 mol % of a commercial photoinitiator (2,2-dimethoxy-2-phenylacetophenone DMPAP, Irgacure 651, Ciba Geigy) was added.

2,7-Dibromo-9,9-di-(2-ethylhexyl)-fluorene (1a). In a two phase system of 100 ml 50% NaOH, 300 ml DMSO and 1.5 g tetrabutylammonium chloride as phase transfer catalyst 2,7-dibromofluorene (25 g, 77.2 mmol) was dissolved. In argon atmosphere 2-ethylhexylbromide (115 g, 600 mmol) was added. After stirring for 12 h at 120 °C, diethyl ether was added to the cold solution. The organic phase was washed with water and distilled in high vacuum to remove the DMSO and 2-ethylhexylbromide. The residue was filtered with a short silicagel column with hexane as eluent to yield **1a** (41.2 g, 98%) as a light yellow oil. **1b** and **1c** were synthesized according to the same procedure with n-octylbromide and n-butylbromide as alkylating agents.

IR (KBr), (cm^{-1}): 3066, 2927, 2856, 1597, 1459, 1416, 1061, 879, 807.

^{1}H-NMR (250 MHz, $CDCl_3$), δ(ppm): 0.5 (t, 6H), 0.68-1.0 (m, 24H), 1.94 (d, 4H), 7.43 (dd, 2H), 7.50 (m, 2H), 7.52 (d, 2H).

^{13}C-NMR (66 MHz, $CDCl_3$), δ(ppm): 10.3, 14.0, 22.7, 27.1, 28.0, 33.5, 44.3, 55.3, 121.0, 127.3, 127.4, 130.0, 139.0, 153.8.

2,7-Bis-(4,4,5,5-tetramethyl-1,3,2-dioxaborolane-2-yl)-9,9-di-(2-ethylhexyl)-fluorene (2a). To a solution of **1a** (16.4 g, 30 mmol) in dry THF n-Butyllithium (1.6M in hexane) (39.2 ml, 63 mmol) was added in argon atmosphere at -78 °C. After stirring for 20 min 2-isopropoxy-4,4,5,5-tetramethyl-1,3,2-dioxaborolane (13.5 ml, 66 mmol) was added at the same temperature. The temperature was kept constant for 15 min and then the mixture was allowed to come to room temperature. After stirring for 12 h at room temperature, the crude product was poured in an excess of water and extracted with diethyl ether. The crude

product was purified by column chromatography with $CHCl_3$ as eluent to give **2a** as a slowly crystallizing oil (12.0 g, 63 %). **2b** and **2c** were synthesized according to the same procedure.

IR (KBr), (cm^{-1}): 2975, 1607, 1474, 1210, 1139, 1115, 1004, 959, 906, 882.

^{1}H NMR (250 MHz, $CDCl_3$), δ(ppm): 0.5 (t, 6H), 0.67-0.9 (m, 24H), 1.36 (s, 24H), 2.01 (d, 4H), 7.70 (d, 2H), 7.77 (s, 2H), 7.82 (dd, 2H).

^{13}C NMR (66 MHz, $CDCl_3$), δ(ppm): 10.3, 14.0, 22.7, 24.7, 27.1, 28.0, 33.9, 34.4, 44.3, 55.1, 83.6, 119.7, 127.1, 130.7, 133.8, 144.2, 152.5.

2-Bromo-9,9-di-(2-ethylhexyl)-fluorene (3a). The procedure for the alkylation of **1a** was followed to prepare **3a** from 2-bromofluorene and 2-ethylhexyl bromide as a pale yellow oil in 98% yield. **3b** and **3c** were synthesized analogously with n-octylbromide and n-butylbromide as alkylating agents.

IR (KBr), (cm^{-1}): 3062, 2960, 2870, 1716, 1599, 1464, 1406, 1377, 1004, 879.

^{1}H-NMR (250 MHz, $CDCl_3$), δ(ppm): 0.5 (t, 6H), 0.68-1.0 (m, 24H), 1.94 (d, 4H), 7.30 (m, 3H), 7.43 (dd, 1H), 7.50 (m, 1H), 7.54 (m, 1H), 7.64 (m, 1H).

^{13}C-NMR (66 MHz, $CDCl_3$), δ(ppm): 10.4, 14.1, 23.0, 27.2, 28.3, 33.8, 35.0, 44.5, 55.5, 119.5, 120.0, 120.6, 124.4, 127.0, 127.8, 130.5, 140.5, 140.7, 149.9, 152.9.

2-Bromo-7-acetyl-9,9-di-(2-ethylhexyl)-fluorene (4a). To a solution of $AlCl_3$ (10.2 g, 91 mmol) in 350 ml CH_2Cl_2, acetyl chloride (6.2 ml, 83 mmol) was added in argon atmosphere at 0 °C. Then 50 ml of **3a** (37.2 g, 79.5 mmol) in CH_2Cl_2 were added at the same temperature. After stirring at room temperature for 12 h the solution was poured into cold water. Precipitated $Al(OH)_3$ was redissolved by adding a small amount of HCl. The separated organic phase was dried with $NaSO_4$, before the product was purified by column

chromatography with hexane / ethylacetate as eluent and **4a** (32.6 g, 85 %) was obtained as light red oil. **4b** and **4c** were synthesized analogously.

IR (KBr), (cm^{-1}): 3070, 2960, 1683, 1607, 1566, 1404, 1356, 1257, 954, 813.

^{1}H-NMR (250 MHz, $CDCl_3$), δ(ppm): 0.5 (t, 6H), 0.68-1.0 (m, 24H), 1.94 (d, 4H), 2,63 (s, 3H), 7.50 (m, 1H), 7.54 (dd, 1H), 7.59 (d, 1H), 7.71 (d, 1H), 7.94 (dd, 1H), 8.00 (s, 1H).

^{13}C-NMR (66 MHz, $CDCl_3$), δ(ppm): 10.4, 14.1, 23.0, 27.0, 27.2, 27.5, 28.3, 34.0, 34.5, 35.0, 44.7, 55.7, 119.5, 120.0, 122.0, 127.5, 128.0, 130.5, 136.0, 139.2, 145.2, 150.5, 154.1, 197.8.

2-Bromo-7-hydroxy-9,9-di-(2-ethylhexyl)-fluorene (5a). HCOOH (10 ml, 30 mmol), aqueous 30% H_2O_2 (3.4 g, 30 mmol) and a few drops of trifluoroacetic acid were stirred for 1 h. The freshly prepared peroxo compound was added slowly to a solution of 5 g (9.9 mmol) **4a** in 200 ml HCOOH / ethyl acetate (1/1) at 0 °C. After stirring for 12 h the solvents were evaporated and the residue was washed two times with a $Na_2S_2O_3$ solution and with water. After evaporation of the solvents MeOH (100 ml) and KOH (2 g, 0.05 mmol) were added to the intermediate product. After refluxing for 12 h and cooling to room temperature, the mixture was acidified with HCl. After washing with water further purification was carried out by column chromatography with $CHCl_3$ as eluent and yields **5a** (3.6 g, 77%) as an orange oil. **5b** and **c** were synthesized analogously.

IR (KBr), (cm^{-1}): 3371, 2957, 2924, 1614, 1588, 1457, 1378, 1178, 808.

^{1}H-NMR (250 MHz, $CDCl_3$), δ(ppm): 0.5 (t, 6H), 0.68-1.0 (m, 24H), 1.94 (d, 4H), 4.60 (t, 1H), 6.82 (dd, 1H), 6.86 (d, 1H), 7.42 (dd, 1H), 7.40-7.55 (m, 3H).

^{13}C-NMR (66 MHz, $CDCl_3$), δ(ppm): 10.4, 14.3, 23.1, 27.0, 28.1, 33.8, 35.0, 44.7, 55.4, 110.1, 114.2, 119.9, 120.6, 120.0, 125.0, 129.7, 133.2, 140.2, 152.1, 152.3, 156.1.

2-Bromo-7-(6-hydroxyhexyloxy)-9,9-di-(2-ethylhexyl)-fluorene (6a). 6-chlorohexanole (8.3 ml, 61.8 mmol) was added to a solution of **5a** (10 g, 20.6 mmol) in 200 ml cyclohexanone with K_2CO_3 (8.5 g, 61.8 mmol) and KI (0.5 g, 3.0 mmol). After refluxing for 3 h the K_2CO_3 was removed by hot filtration. The crude product was purified by column chromatography with hexane / ethyl acetate (2/1) as eluent and yields **6a** (9.8 g, 80%) as a light yellow oil. **6b** and **6c** were synthesized according to the same procedure.

IR (KBr), (cm^{-1}): 3339, 2956, 1609, 1582, 1457, 1379, 1258, 1182, 1062, 876, 810.

^{1}H-NMR (250 MHz, $CDCl_3$), δ(ppm): 0.5 (t, 6H), 0.68-1.8 (m, 32H), 1.94 (d, 4H), 3.67 (t, 2H), 3.99 (t, 2H), 6.82 (dd, 1H), 6.86 (s, 1H), 7.40 (dd, 1H), 7.42-7.55 (m, 3H).

^{13}C-NMR (66 MHz, $CDCl_3$), δ(ppm): 10.5, 14.4, 23.2, 25.8, 26.0, 27.0, 28.2, 32.9, 33.8, 35.0, 44.7, 55.4, 62.9, 68.2, 110.1, 112.8, 119.5, 120.0, 120.4, 125.0, 129.5, 132.2, 140.2, 153.1, 153.3, 154.1.

2-Bromo-7-(2-tetrahydro-pyranyloxy)-9,9-di-(2-ethylhexyl)-fluorene (7). 6a (5.0 g, 8.5 mmol) and a catalytical amount of toluenesulfonic acid were dissolved in 50 ml diethyl ether. At 0 °C 3,4-dihydropyran (DHP) (1.1 ml, 8.7 mmol) was added dropwise to the solution. After 3 h the crude product was washed with water and then purified by column chromatography with hexane / ethyl acetate (2/1) as eluent and yields **7** (5.0 g, 88 %) as a colourless oil.

^{1}H-NMR (250 MHz, $CDCl_3$), δ(ppm): 0.5 (t, 6H), 0.68-1.8 (m, 38H), 1.94 (d, 4H), 3.67 (t, 2H), 3.80 (m, 2H), 3.99 (t, 2H), 4.50 (t, 1H), 6.82 (dd, 1H), 6.86 (s, 1H), 7.40 (dd, 1H), 7.42-7.55 (m, 3H).

^{13}C-NMR (66 MHz, $CDCl_3$), δ(ppm): 10.5, 14.4, 21,5, 23.2, 25.8, 26.0, 26.5, 27.0, 28.2, 29.5, 31.3, 32.9, 33.8, 35.0, 44.7, 55.4, 62.5, 62.9, 68.2, 96.5, 110.0, 112.9, 119.6, 120.1, 120.4, 125.1, 129.5, 132.2, 140.3, 153.0, 153.3, 154.2.

2,7-Bis-[7-(6-hydroxyhexyloxy)-9,9-di-(2-ethylhexyl)-fluoren-2yl]-9,9-di-(2-ethyl-hexyl)-fluorene (trimer 9a). To a degassed 2:1 mixture of toluene, 2 M aqueous K_2CO_3, 0.1 g tetrabutylammonium chloride as phase transfer catalyst, **2a** (1.0 g, 1.71 mmol) and **6a** (2.2 g, 3.42 mmol), $Pd(PPh_3)_4$ (2 mol %) was added. After degassing the solution again it was stirred for 12 h at 90 °C. After cooling and washing with water, saturated NaCl-solution and again with water the final purification was made via column chromatography with hexane / ethyl acetate (2/1) as eluent and yields **9a** (1.9 g, 80%) as a pale yellow powder. **9b** and **9c** were synthesized analogously.

IR (KBr), (cm^{-1}): 3339, 2956, 1609, 1581, 1460, 1379, 1258, 1210, 815.

^{1}H-NMR (250 MHz, $CDCl_3$), δ(ppm): 0.5 (t, 12H), 0.6-0.8 (m, 12H), 0.8-1.0 (m, 60H), 1.1-1.8 (m, 22H), 1.90-2.10 (m, 12H), 3.67 (t, 4H), 4.02 (t, 4H), 6.82 (dd, 2H), 6.92 (d, 2H), 7.60-7.80 (m, 14H).

^{13}C-NMR (66 MHz, $CDCl_3$), δ(ppm): 10.7, 14.5, 22.9, 25.8, 26.3, 27.0, 28.2, 29.5, 33.0, 33.9, 34.7, 44.7, 55.3, 62.9, 68.2, 110.2, 114.1, 118.5, 119.0, 120.2, 120.5, 122.1, 123.6, 125.8, 126.2, 134.4, 139.4, 140.4, 140.7, 143.8, 150.7, 151.3, 152.4, 154.0.

2,7-Bis-[7-(6-acryloyloxy-hexyloxy)-9,9-di-(2-ethylhexyl)-fluoren-2yl]-9,9-di-(2-ethylhexyl)-fluoren (trimer 10a). 9a (0.4 g, 0.29 mmol), N,N–dimethylaniline (0.08 ml, 0.63 mmol) and 1 mol % 2,6–di-tert.-butyl-p-kresol as stabilizer were dissolved in 30 ml toluene. After the addition of acryloyl chloride (0.08 ml, 0.95 mmol) the reaction mixture it is stirred at 40 °C for 12 h. The raw product is washed with dilute HCl and water before purification by column chromatography with $CHCl_3$ as eluent. Yield 0.34 g, 78 % of **10a** as a light yellow powder. **10b** and **10c** were synthesized analogously.

IR (KBr), (cm^{-1}): 2956, 2870, 1726, 1607, 1406, 1260, 1193, 811.

^{1}H-NMR (250 MHz, $CDCl_3$), δ(ppm): 0.5 (t, 12H), 0.6-0.8 (m, 12H), 0.8-1.0 (m, 60H), 1.1-1.8 (m, 22H), 1.90-2.10 (m, 12H), 4.03 (t, 4H), 4.19 (t, 4H), 5.80 (dd, 2H), 6.12 (dd, 2H), 6.41 (dd, 2H), 6.82 (dd, 2H), 6.92 (d, 2H), 7.60-7.80 (m, 14H).

^{13}C-NMR (66 MHz, $CDCl_3$), δ(ppm): 10.3, 13.9, 22.7, 25.7, 27.0 , 28.1, 28.5, 29.2, 30.3, 33.7, 33.9, 34.5, 37.5, 44.4, 54.8, 64.5, 68.0, 110.2, 113.6, 118.8, 119.6, 120.2, 122.7, 125.8, 128.5, 130.4, 134.10, 138.9, 139.9, 140.4, 150.4, 151.0, 152.5, 158.4, 166.2, 170.3.

2-[6-Hydroxyhexyloxy]-9,9-di-(2-etylhexyl)-fluorene-2yl]-7-[7-(4,4,5,5-tetramethyl-1,3,2-dioxaborolane-2yl)-9,9-di-(2-ethylhexyl)-fluorene (8a). **8a** was prepared by a suzuki cross coupling with equimolar amounts of **2a** (4.75 g, 8.12 mmol) and **6a** (5.15 g, 8.12 mmol) in the same way as described for the trimer **9a**. The final purification was made by column chromatography with hexane / ethyl acetate (2/1) as eluent and yields **8a** (1.76 g, 20%) as a pale red oil. **8b** and **8c** were synthesized analogously.

IR (KBr), (cm^{-1}): 3339, 2956, 2870, 1609, 1460, 1379, 1258, 1042, 815, 729.

^{1}H-NMR (250 MHz, $CDCl_3$), δ(ppm): 0.5 (t, 6H), 0.7 (t, 6H), 0.7-0.9 (m, 32H), 1.36 (s, 12H), 1.50-1.80 (m, 16H), 1.90-2.10 (m, 16H), 3.67 (t, 2H), 4.01 (t, 2H), 6.82 (dd, 1H), 6.92 (s, 1H), 7.60 (m, 6H), 7.70-7.80 (m, 4H).

^{13}C-NMR (66 MHz, $CDCl_3$), δ(ppm): 10.7, 14.5, 22.9, 25.2, 25.8, 26.3, 27.0, 28.2, 29.5, 32.1, 33.0, 33.7, 34.2, 34.7, 44.7, 55.9, 62.9, 68.2, 83.7, 110.2, 114.1, 119.0, 120.2, 120.5, 122.9, 123.9, 126.2, 126.8, 127.3, 128.8, 134.4, 139.4, 140.4, 140.7, 141.3, 142.2, 144.0, 150.1, 150.7, 151.3, 152.4, 152.7, 154.0.

2,7-Bis[7-{7-(6-hydroxyhexyloxy)-9,9-di-(2-ethylhexyl)-fluorene-2-yl}-9,9-di-(2-ethylhexyl)-fluorene-2-yl]-9,9-di-(2-butyl)-fluorene (pentamer 11a). A suzuki coupling with **1c** (0.43 g, 0.98 mmol) and **8a** (2.0 g, 1.96 mmol) was carried out in the same way as described for **9a**. Further purification via column chromatography in hexane / ethyl acetate

(2/1) as eluent yields **11a** (0.44 g, 21%) as a pale yellow powder. **11b** and **11c** were synthesized with the same proceeding.

IR (KBr), (cm^{-1}): 3347, 2956, 2857, 1608, 1459, 1377, 1257, 813.

^{1}H-NMR (250 MHz, $CDCl_3$), δ(ppm): 0.5-0.8 (m, 54 H), 0.6-0.7 (m, 20H), 0.8-1.05 (m, 36H), 1.15-1.82 (m, 36H), 1.95-2.1 (m, 4H), 2.05-2.2 (m, 20H), 3.68 (t, 4H), 4.03 (t, 4H), 6.88 (dd, 2H), 6.93 (s, 2H), 7.60-7.81 (m, 26H).

^{13}C-NMR (66 MHz, $CDCl_3$), δ(ppm): 10.3, 13.8, 14.0, 22.7, 23.1, 25.6, 25.9, 27.0, 28.2, 29.3, 32.7, 33.7, 33.9, 34.6, 34.7, 40.2, 44.4, 44.6, 54.9, 55.0, 62.9, 68.2, 110.2, 113.6, 118.9, 119.7, 120.3, 121.4, 122.8, 126.1, 134.0, 139.0, 139.9, 140.4, 140.7, 150.4, 151.1, 151.6, 152.6, 158.6.

2,7-Bis[7-{7-(6-acryloyloxy-hexyloxy)-9,9-di-(2-ethylhexyl)-fluorene-2-yl}-9,9-di-(2-ethylhexyl)-fluorene-2-yl]-9,9-di-(2-butyl)-fluorene (pentamer 12a). Esterfication with acryloyl chloride was carried out according to the same procedure as described for **10a** with **11a** (0.2 g, 0.1 mmol) in 30 ml toluene, N,N–dimethylaniline (0.0012 ml, 0.1 mmol) and acryloyl chloride (0.03 ml, 0.36 mmol) The purification was made by column chromatography with $CHCl_3$ as eluent and yields **12a** (0.15 g, 71 %) as a light yellow powder. **12b** and **12c** were synthesized analogously.

IR (KBr), (cm^{-1}): 2957, 2857, 1726, 1608, 1581, 1406, 1295, 1194, 813.

^{1}H NMR (250 MHz, $CDCl_3$), δ(ppm): 0.5-0.8 (m, 54 H), 0.6-0.7 (m, 20H), 0.8-1.05 (m, 36H), 1.15-1.82 (m, 36H), 1.95-2.1 (m, 4H), 2.05-2.2 (m, 20H), 4.05 (t, 4H), 4.19 (t, 4H), 5.82 (dd, 2H), 6.13 (dd, 2H,), 6.41 (dd, 2H), 6.88 (dd, 2H), 6.93 (s, 2H), 7.60-7.81 (m, 26H).

^{13}C NMR (66 MHz, $CDCl_3$), δ(ppm): 10.3, 13.7, 13.9, 22.7, 23.0, 25.8, 26.0, 27.0, 27.2, 28.2, 28.6, 29.3, 30.3, 33.7, 33.9, 34.5, 34.7, 40.2, 44.4, 44.6, 54.9, 55.0, 110.2, 113.6,

118.9, 119.7, 120.3, 121.3, 122.8, 125.5, 126.1, 126.6, 128.2, 128.6, 130.4, 135.7, 139.0, 139.9, 140.4, 140.8, 150.4, 151.6, 152.6, 158.5, 166.3.

α,ω-Bis(6-hydroxyhexyloxy)-oligo(9,9-di-(2-ethylhexyl)-fluoren-2,7-diyl) (oligomers 13a-g). The oligomers **13a-h** were prepared by suzuki cross coupling as described for **9a**. Different molar ratios of the dibromo compound **1a**, the diboronic ester **2a** and the endcapper **7** were used (ref. table 1). After the reaction the THP-protecting groups were cleaved by solving the substance in diethyl ether and adding dilute HCl. Further purification was made by filtration over silica gel with toluene as solvent and yields **13a-g** (80 %) as pale yellow powders.

IR (KBr), (cm^{-1}): 3350, 2958, 2860, 1609, 1460, 1377, 1259, 814.

^{1}H NMR (250 MHz, $CDCl_3$), δ(ppm): 0.5-1.1 (m, 172H), 1.2-2.1 (m, 47H), 3.70 (t, 4H), 4.03 (m, 4H), 6.90 (m, 4H),7.60-7.80 (m, 29H).

^{13}C NMR (66 MHz, $CDCl_3$), δ(ppm): 10.3, 14.0, 22.7, 25.6, 25.9, 26.9, 27.0, 28.1, 28.2, 29.4, 32.7, 34.0, 34.4, 34.6, 44.5, 55.0, 62.9, 68.2, 110.2, 113.5, 113.7, 118.9, 119.8, 120.2, 126.0, 126.1, 126.6, 127.1, 128.7, 134.1, 140.0, 140.1, 140.4, 150.5, 151.2, 151.4, 152.6, 158.6.

α,ω-Bis(6-acryloyloxy-hexyloxy)-oligo(9,9-di-(2-ethylhexyl)-fluoren-2,7-diyl) (oligomers 14a-g). The esterfication with acryloyl chloride was made analogously to the pentamer **12a** with **13a-g** (0.3 g, 0.14 mmol), acryloyl chloride (1.54 ml,19 mmol) and DMA (0.02 ml,0.17 mmol) in 40 ml toluene. After 12 h the same amounts of DMA and acryloyl chloride were added again to ensure full conversion. After washing the crude product with water it was precipitated from methanol and yields **14a-g** with over 70 % as white powders.

IR (KBr), (cm^{-1}): 2957, 2858, 1728, 1609, 1582, 1406, 1294, 1193, 814.

^{1}H-NMR (250 MHz, $CDCl_3$), δ(ppm): 0.50 (m, 30H), 0.67 (m, 30H), 0.88 (m, 80H), 1.26 (m, 10H), 1.4-1.6 (m, 8H), 1.7-2.0 (m, 8H), 2.11 (m, 20H), 3.68 (t, 4H), 4.03 (t, 4H), 5.80 (dd, 2H), 6.10 (dd, 2H,), 6.40 (dd, 2H), 6.88 (dd, 2H), 6.92 (s, 2H), 7.64-7.80 (m, 48 H).

^{13}C-NMR (66 MHz, $CDCl_3$), δ(ppm): 10.35, 14.01, 22.75, 25.60, 25.96, 27.11, 28.30, 29.39, 29.69, 32.72, 34.05, 34.73, 44.49, 55.04, 62.93, 68.21, 110.2, 113.66, 118.70, 119.79, 120.21, 122.94, 123.85, 125.22, 126.13, 126.61, 128.71, 140.17, 150.1, 151.18, 152.3, 158.58, 169.3.

---

[1] Lub, J.; Broer, D.J.; Hikmet, R.A.M.; Nierop, K.G.J. *Liquid Crystals* **1996**, *20*, 277.

[2] Bunning, T.J.; Kreuzer, F. *Trends Polym. Sci.* **1995**, *3*, 318.

[3] Broer, D.J.; Lub, J.; Mol, G.N. *Nature* **1995**, *378*, 467.

[4] O'Neill, M.; Kelly, S. M. *Adv. Mater.* **2003**, *14*, 1135.

[5] Sundar, V.C.; Zaumseil, J.; Podzorov, V.; Menard, E.; Willett, R.L.; Someya, T.; Gershenson, M.E.; Rogers, J.A. *Science* **2004**, *303*, 1644.

[6] Sirringhaus, H.; Wilson, R.J.; Friend, R.H.; Inbasekaran, M.; Wu, W.; Woo, E.P.; Grell, M.; Bradley D.D.C. *Appl. Phys. Lett*., **2000**, *77*, 406.

[7] Huisman, B.-H.; Valeton, J.J.P.; Nijssen, W.; Lub, J.; ten Hoeve, W. *Adv. Mater.* **2003**, *15*, 2002.

[8] McCulloch, I.; Zhang, W.; Heeney, M.; Bailey, C.; Giles, M.; Graham, D.; Shkunov, M.; Sparrowe, D.; Tierney, S. *J. Mater. Chem.* **2003**, *13*, 2436.

[9] Shkunov, M.; Zhang, W.; Graham, D.; Sparrowe, D.; Heeney, M.; Giles, M.; Tierney, S.; Bailey, C.; McCulloch, I.; Kreouzis, T. *SPIE-Int. Soc. Opt. Eng.* **2003**, *5217*,181.

[10] Grice, A.W.; Bradley, D.D.C.; Bernuis, M.T.; Inbasekaran, M.; Wu, W.W.; Woo, E.P. *Appl. Phys. Lett*. **1998**, *73*, 629.

[11] Grell, M.; Knoll, W.; Lupo, D.; Meisel, A.; Miteva, T.; Neher, D.; Nothofer, H.-G.; Scherf, U.; Yasuda, A. *Adv. Mater.* **1999**, *11*, 671.

[12] Sainova, D.; Zen, A.; Nothofer, H.-G.; Asawapirom, U.; Scherf, U.; Hagen, R.; Bieringer, T.; Kostromine, S.; Neher, D. *Adv. Funct. Mater.* **2002**, *12*, 50.

[13] Whitehead, K.S.; Grell, M.; Bradley, D.D.C.; Jandke, M.; Strohriegl, P. *Appl. Phys. Letters* **2000**, *76*, 2946.

[14] Klaerner, G.; Miller, R.D. *Macromolecules* **1998**, *31*, 2007.

[15] Jo, J.; Chi, C.; Höger, S.; Wegner, G.; Yoon, D.Y. *Chem. Eur. J.* **2004**, *10*, 2681.

[16] Geng, Y.; Chen, A.C.A.; Ou, J.J.; Chen, S.H.; Klubek, K.; Vaeth, K.; Tang, C.W. *Chem. Mater.* **2003**, *15*, 4352.

[17] Culligan, S.W.; Geng, Y.; Chen, S.H.; Klubek, K.; Vaeth, K.; Tang, C.W. *Adv. Mater.* **2003**, *14*, 1176.

[18] Aldred, M.P.; Eastwood, A.J.; Kelly, S.M.; Vlachos, P.; Contoret, A.E.A.; Farrar, S.R.; Mansoor, B.; O'Neill, M.; Tsoi,W.C. *Chem. Mater.* **2004**, *16*, 4928.

[19] Aldred, M.P.; Contoret, E.A.; Farrar, S.R., Kelly, S.M.; Mathieson, D.; O'Neill, M.; Tsoi, W.C.; Vlachos, P. *Adv. Mater.* **2005**, *17*, 1368.

[20] Jandke, M.; Hanft, D.; Strohriegl, P.; Whitehead, K.; Grell, M.; Bradley, D.D.C. *Proc. SPIE* **2001**, *4105*, 338.

[21] Woo, E.P.; Shiang, W.R.; Inbasekaran, M.; Roof, G.R. *US Patent* **1995**, US 5,708,130.

[22] Inbasekaran, M.; Weishi, W.; Woo, E.P. *US Patent* **1998**, US5777070.

[23] Fieser, L.F.; Fieser, M. *Reagents for organic synthesis I* **1973**, 457.

[24] Schlüter, A.D. *J. Polym. Sci. Part A: Polym. Chem.* **2001**, *39*, 1533.

[25] Jahromi, S.; Lub, J.; Mol, G.N. *Polymer* **1998**, *35*, 622.

Photopolymerization of reactive mesogens

Macromolecular Chemistry and Physics, 2005, *206*, 2153 – 2159.

Heiko Thiem, Peter Strohriegl*

*Makromolekulare Chemie I and Bayreuther Institut für Makromolekülforschung (BIMF), Universität Bayreuth, D-95440 Bayreuth, Germany

FAX: +49(0)921/553206

Phone: +40(0)921/553296

Email: peter.strohriegl@uni-bayreuth.de

Email: heiko.thiem@uni-bayreuth.de

Maxim Shkunov, Iain McCulloch

Merck Chemicals, Chilworth Science Park, Southampton, UK

Email: maxim.shkunov@merckchem.co.uk

Email: iain.mcculloch@merckchem.co.uk

Summary

The photopolymerization of two reactive mesogens with photopolymerizable acrylate endgroups, the methyl substituted 1,4-phenylene-bis[4-(6-(acryloyloxy)hexyloxy)benzoate] **1** and acrylic acid 6-{4-[6-(6-acryloyloxyhexyloxy)naphtalen-2-yl]-phenoxy}hexyl ester **2** has been investigated by Photo-DSC measurements. Photocrosslinking of **1** in the nematic phase at 100 °C proceeds faster than in the isotropic phase at 120 °C and leads to a final conversion of 87 % of the acrylate groups at both temperatures. It is possible to perform photopolymerization with very small amounts of photoinitiator. Even with 0.001 % (10 ppm) of photoinitiator 47 % of the acrylate groups polymerize within 15 minutes. The polymerization of the reactive mesogen **2** proceeds faster in the smectic A phase at 100 °C compared to the isotropic phase at 120 °C.and leads to a higher conversion of 75 %. This can be explained by an increased local concentration of the acrylate groups between the layers of the smectic cores.

Keywords:

acrylate, crosslinking, initiators, photopolymerization, reactive mesogens.

Introduction

Reactive mesogens are liquid crystalline materials with polymerizable end groups. Polymerization of reactive mesogens with two or more polymerizable groups leads to densely crosslinked networks in which the liquid crystalline order is permanently fixed.[1] The principle of this procedure is outlined in Scheme 1.

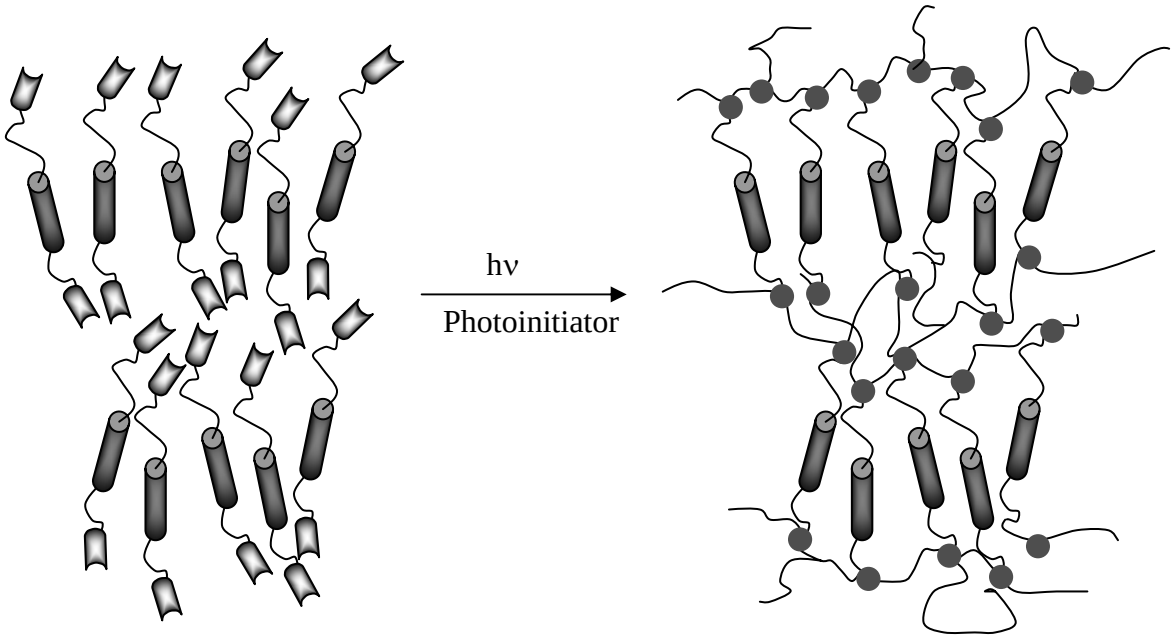

Scheme 1: Photopolymerization of reactive mesogens.

In situ photo-initiated polymerization of the end groups in the liquid crystal phase allows the attainment of the optimum mesophase morphology and alignment, followed by the "freezing in" of this structure on creation of the crosslinked network shown. The formation of large area, monodomain, aligned morphology on cooling from the clearing point is possible due to the relatively low viscosity of these small molecules (in comparison to the analogous polymer systems which are more viscous) in the liquid crystalline phases.

This class of materials is attractive for a number of applications. For example cholesteric polymer networks from reactive mesogens are used as colour flop pigments with a distinct viewing angle dependence of the colour.[2] A second application of crosslinked cholesteric

mesophases are broad band polarizers.[3] In such polarizers the reflected light is “recycled” and so transmissions up to 82 % have been reached. Another advantage of the use of reactive mesogens is that through the use of a shadow mask during the crosslinking process pattern formation like in a negative photoresist is possible. By the use of a sequence of photoisomerization and photopolymerization reactions Lub et al. produced a colour filter for all three fundamental colours with a pixel size of 100 μm, which can be used in liquid crystal displays.[4]

In the last years several groups utilised the benefit of ordered liquid crystalline states in the field of optoelectronic applications.[5] Two fields are of special interest, organic light emitting diodes (OLEDs) and organic field effect transistors (OFETs). In OLEDs ordered liquid crystalline molecules can be used for the emission of linear polarized light. For example Grell et al. reached a polarization ratio of 15 : 1 in electroluminescence by orienting poly(2,7-(9,9-bis(2-ethylhexyl)fluorene)) on a rubbed polyimide layer, doped with a commercial hole conductor.[6] We have reported the emission of polarized light with an orientation ratio of 25 : 1 with oriented poly(2,7-(9,9-bis(octyl)fluorene)) on a poly(1,4-phenylenevinylene) (PPV) orientation layer as well for a crosslinked fluorene based reactive mesogen on PPV.[7,8] Recent work of S. Kelly et al. showed the use of acrylate and diene photopolymerizeable end groups in the α,ω positions of mesogens containing fluorene and thiophene units.[9] They were able to orient them on photoorientation layers and achieve by the use of different mesogens a full colour OLED which emits linear polarized light. [10]

In 2000 Sirringhaus et al. reported the use of oriented liquid crystalline polymers as active materials in OFETs for the first time. The field effect mobility in a fluorene-bithiophene copolymer increases from 10^{-3} cm^2/Vs for an unoriented film up to $2 \cdot 10^{-2}$ cm^2/Vs for a film oriented on rubbed polyimide.[11] Recently Huisman et al. reported the synthesis and OFET-performance of reactive mesogens with a quaterthiophene core and two acrylate end

groups.[12] They achieved field effect mobilities of up to $6 \cdot 10^{-4}$ cm^2/Vs in the crosslinked liquid crystalline network. The field of low molar mass liquid crystals with high carrier mobilities has been pioneered by Hanna who investigated the liquid crystalline molecule 2-(4'-octylphenyl)-6-butyloxynaphthalene.[13] Upon cooling the molecule shows a transition from the isotropic to a smectic A phase at 129 °C followed by a transition to a smectic E phase at 125 °C. This phase is stable to 55 °C at which temperature the substance starts to crystallize. In the highly ordered smectic E phase, mobilities up to 10^{-2} cm^2/Vs have been measured by the TOF technique. In the less ordered smectic A phase the mobility drops to $4 \cdot 10^{-4}$ cm^2/Vs and in the isotropic phase again to 10^{-4} cm^2/Vs. Interestingly the material shows nearly the same mobilities for holes and electrons.

Recently we described the synthesis of similar reactive mesogens containing a 2-phenylnaphtalene core and photocrosslinkable acrylate and diene end groups.[14] One crucial step in the use of reactive mesogens is photopolymerization. We have carried out a detailed investigation of the polymerization of two different reactive mesogens containing acrylate groups with UV-light using the Photo-DSC method. In this paper we focus on some important aspects of photopolymerization. First we discuss the conversion of acrylate groups and its temperature dependence. The polymerization kinetics in different types of LC-phases will also be addressed. The performance of organic semiconductors is very sensitive towards impurities which typically leads to a decrease of the carrier mobility.[15] This makes it crucial to determine the minimum amount of initiator necessary to achieve photopolymerization.

Results and discussion

Photo-DSC experiments were carried out with the two reactive mesogens **1** and **2**. Both possess acrylate end groups, which ensure a fast polymerization like ionically curable vinyl ethers and oxetanes. Diacrylate **1** which was first described by Broer et al. has a nematic mesophase between 82 and 118 °C.[16] Upon cooling, recrystallisation takes place at. ca. 35 °C (Fig. 2). The moderate clearing temperature of **1** at 118 °C allows the monomer to be heated into the isotropic phase without spontaneous polymerization of the acrylate end groups. The structure and phase behaviour of the methyl substituted 1,4-phenylene-bis[4-(6-(acryloyloxy)hexyloxy)benzoate] **1**[16]**,** acrylic acid 6-{4-[6-(6-acryloyloxy-hexyloxy)naphthalen-2-yl]-phenoxy}hexyl ester **2** and the photoinitiator 2,2-dimethoxy-2-phenyl-acetophenone **3** (Irgacure 651; Ciba Geigy) are shown in Figure 1.

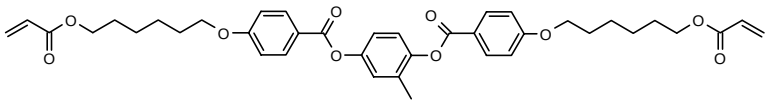

1

K 82 N 118 I (heating)

I 117 K 35 (cooling)

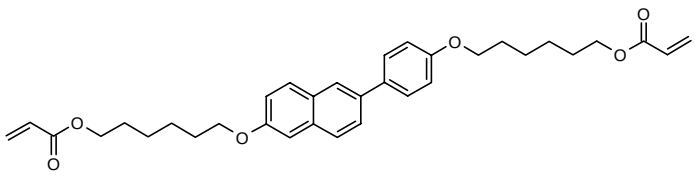

2

K 85 S_a 111 I (heating)

I 109 S_a 66 S_c 50 K (cooling)

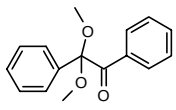

3

Figure 1: Structure and phase behaviour of the reactive mesogens **1** and **2** and the photoinitiator **3** (Irgacure 651, Ciba Geigy).

Recently we have reported the synthesis of the reactive mesogen **2** (acrylic acid 6-{4-[6-(6-acryloyloxyhexyloxy)naphthalen-2-yl]-phenoxy}hexyl) and its application as an organic

semiconductor in an OFET. [14] In contrast to **1**, monomer **2** exhibits two different smectic mesophases. The DSC scans of **1** and **2** are shown in Figure 2.

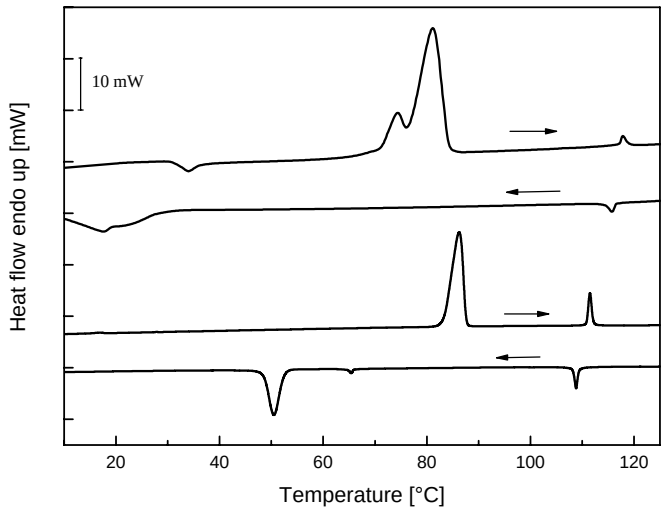

Figure 2: DSC scans of the reactive mesogens **1** (top) and **2** (bottom) (heating / cooling rate 10 K/min).

Upon heating a smectic A phase is observed between 85 °C and 111 °C. On cooling the molecule exhibits a smectic A phase between 109 °C and 66 °C and an additional monotropic smectic C phase between 66 °C and 50 °C.

For the photopolymerizations, the commercially available photoinitiator **3** (2,2-dimethoxy-2-phenyl-acetophenone; (Irgacure 651, Ciba Geigy) was used. Since thick samples are used in the Photo-DSC experiments it is important to irradiate at a wavelength where the reactive mesogen does not absorb light (Figure 3), thus ensuring that the photopolymerization proceeds homogenously through the whole sample. The use of the initiator **3** with an absorption at 365 nm (arrow in Figure 3) allows irradiation of the initiator outside the main absorption of the reactive mesogens.

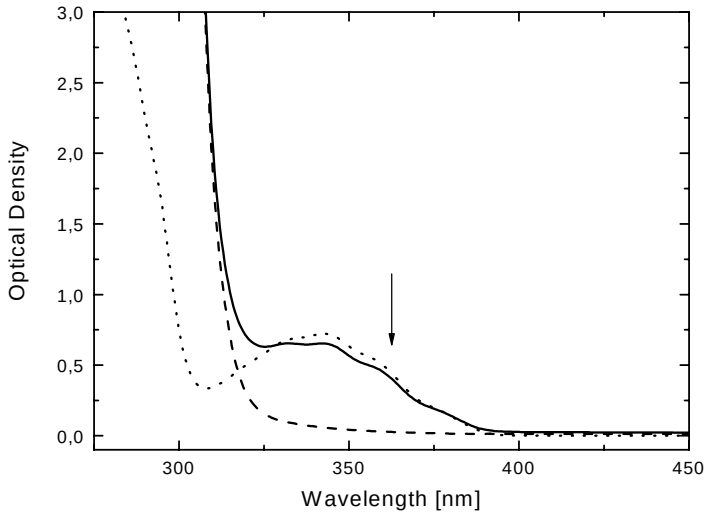

Figure 3: UV spectra of the reactive mesogen **1** (- - - - -), the photoinitiator **3** (·····) and a mixture of **1** and 1wt.-% of **3** (——). The spectra have been taken from THF solutions with concentrations of the monomer and photoinitiator that mimic the situation in a 50 μm thick film.

The principles of the Photo-DSC experiment are shown in Figure 4.

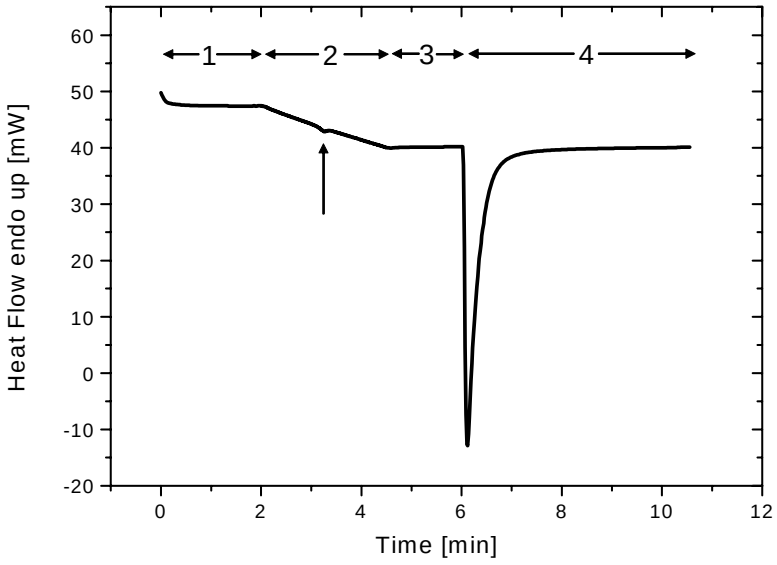

Figure 4: Photo-DSC experiment with the reactive mesogen **1** and 1 weight % of initiator **3**; excitation wavelength 365 nm.

The experiment can be divided in four phases. In phase 1 the mixture is heated to the isotropic phase (125 °C) and annealed for 2 minutes to ensure complete melting. In phase 2 the sample is slowly cooled to 100 °C where the reactive mesogen **1** is nematic. During cooling a small peak (illustrated by the arrow in Figure 4) for the transition from the isotropic to the nematic phase can be detected. In phase 3 the sample is kept at 100 °C for one minute. Then the shutter of the UV lamp is opened (phase 4) and photopolymerization starts immediately as can be seen by the strong exothermal peak. The irradiation is made with a very low light intensity of approx. 1 mW/cm^2 to ensure that the photopolymerization is slow enough to be followed by the DSC. From the integration of the peak the enthalpy of polymerization is obtained. With this value the conversion p of the acrylate groups can be calculated by Equation 1, where ΔH_{poly} is the enthalpy of polymerization [J/g], M the molecular weight [g/mol], z the number of acrylate groups per molecule and, $\Delta H_{acrylate}$ the enthalpy of polymerization per acrylate group [78.000 J/mol].[17]

$$p = \frac{\Delta H_{poly} \cdot M}{z \cdot \Delta H_{acrylate}} \qquad (1)$$

In the example shown in Figure 4, a final conversion of 87 % of the acrylate groups is achieved. During our experiments with monomer **1** we found that the polymerization enthalpies are difficult to reproduce in several runs, especially if the thermal pretreatment of the samples was varied. If a mixture of a pure diacrylate and photoinitiator is used, thermal polymerization cannot be fully prevented. It is advantageous therefore to use small amounts of inhibitor in addition to the photoinitiator. We have used the commercial inhibitor 3,5-di-tert.-butyl-4-hydroxytoluene (BHT) for that purpose. In all Photo-DSC

experiments reported in this paper BHT was added to the monomer. The amount of BHT is 50% by weight of the amount of initiator in all experiments.

One important issue in the photopolymerization of reactive mesogens is the dependence of the conversion on the polymerization temperature and mesophase. Photopolymerization of the reactive mesogen **1** at different temperatures was carried out as previously described. The results are summarized in Figure 5.

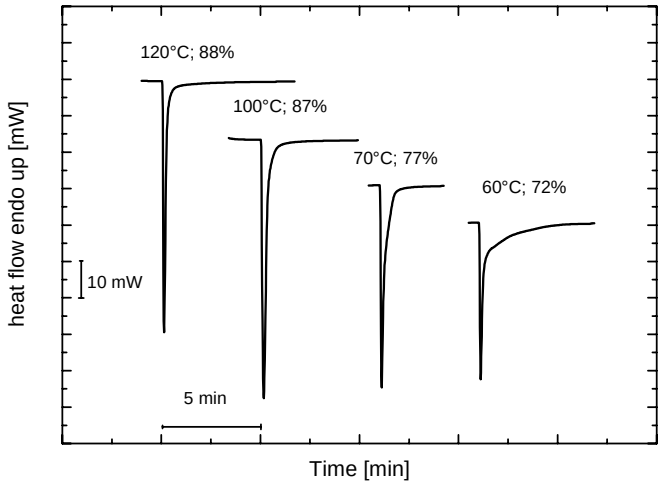

Figure 5: Photopolymerization of **1** (1% photoinitiator **3**, 0.5% BHT) at different temperatures and final conversion p of acrylate groups.

There is almost no difference in the final conversion of 88 % in the isotropic phase at 120 °C and of 87 % in the nematic phase at 100 °C. These values represent the lower limit of the conversion of acrylate groups during the crosslinking reaction or more precisely the conversion after a few minutes.[18] We cannot rule out that residual acrylate groups undergo very slow crosslinking over a period of hours which is below the detection limit of the DSC. Nevertheless a 100 % conversion of acrylate groups is unlikely in highly crosslinked polymer networks for topological reasons. Lowering the reaction temperature to 70 °C leads to a decrease to 77 % of converted acrylate groups. If the polymerization is carried out at 60 °C this behaviour becomes even more pronounced. Measurements at

lower temperatures were not possible since the mesogen starts to recrystallize when it is held at temperatures below 60 °C for a longer time. To examine the reaction time and kinetic details more clearly, the integration of the polymerization peak and therefore the calculated conversion versus time was plotted and is shown in Figure 6.

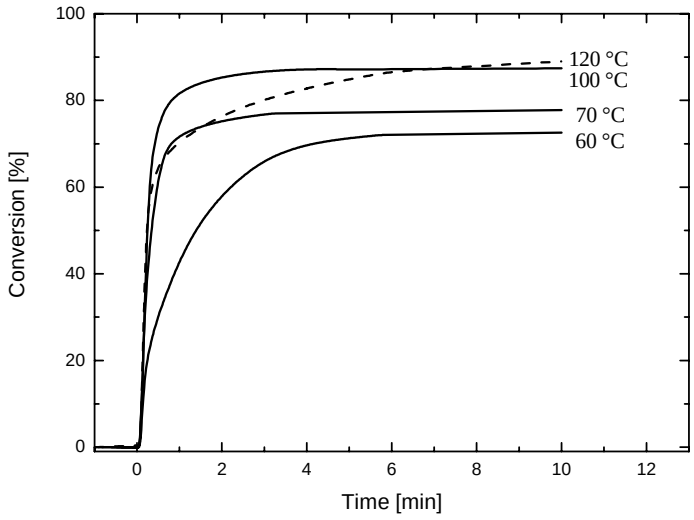

Figure 6: Time-conversion plot of photopolymerization of **1** (1% photoinitiator, 0.5% BHT) in the isotropic (120 °C) and in the nematic phase (100 °C, 70 °C, 60 °C).

Time-conversion plots in Figure 6 are obtained by numerical integration. Initially the reaction in the nematic phase at 100 °C is faster than in the isotropic phase at 120 °C (dashed curve). So a conversion of 80 % of the acrylate groups is reached after 50 s at 100 °C compared with 180 s at 120 °C. As we will demonstrate in the photopolymerization of **2**, this behaviour is even more pronounced in smectic mesophases. The final conversion of acrylate groups is almost the same if the polymerization is carried out at 120 °C or 100 °C. If the polymerization temperature is lowered to 70 °C and 60 °C, the polymerization proceeds much slower and as discussed before, the final conversion of acrylate groups reduces to 77 % and 72 %. We attribute this to the increasing viscosity and hence reduced mobility of the acrylate groups.

If reactive mesogens are used as organic semiconductors, minimising the impurity level is essential to achieve optimal electrical performance. Since the decomposition products of the photoinitiator will be present in the resulting polymer networks it is necessary to determine the minimum photoinitiator required for efficient crosslinking. The results of a series of experiments with different initiator concentrations are summarized in Figures 7 and 8.

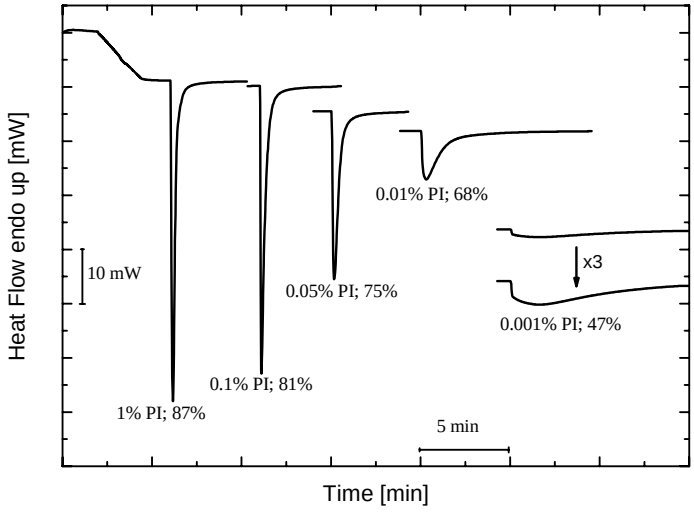

Figure 7: Photopolymerization of **1** at 100 °C with different amounts of photoinitiator and values for the final conversion p of acrylate groups.

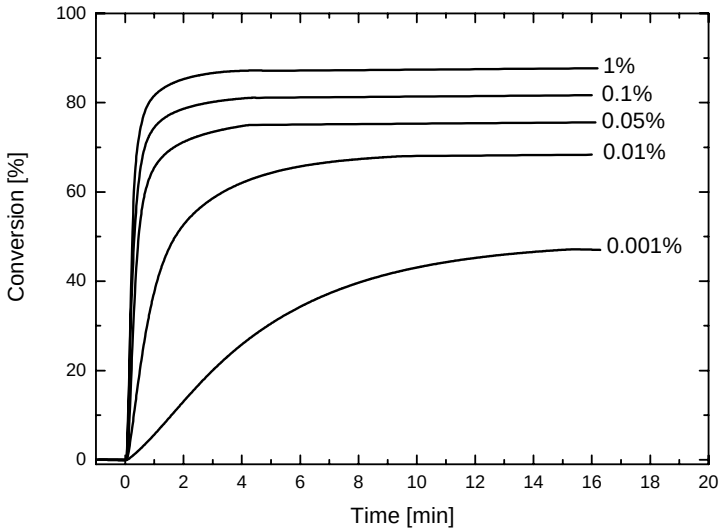

Figure 8: Time-conversion plot of the photopolymerization of **1** at 100 °C with different amounts of photoinitiator **3.**

With 1 % photoinitiator the final conversion is 87 % like in the previous experiments. If the initiator concentration is reduced to 0.1 %, the final conversion of acrylate groups is still 81 % and as can be seen from Figure 8 the reaction proceeds almost as fast as with 1 % initiator. A further reduction of the photoinitiator concentration to 0.05 % and 0.01 % leads to a decrease in both reaction rate and final conversion. Even with 0.001% (10 ppm) of photoinitiator 47 % of the acrylate groups polymerize within several minutes. In technical photopolymerization of acrylates the concentration of photoinitiator is usually in the range 1 % to 3 %.[19] These experiments have revealed that when the initiator concentration is a critical issue, much smaller amounts of photoinitiator are sufficient.

In contrast to the nematic monomer **1** the reactive mesogen **2** with a phenylnaphtalene core exhibits smectic mesophases. The photopolymerization of **2** at different temperatures is shown in Figures 9 and 10.

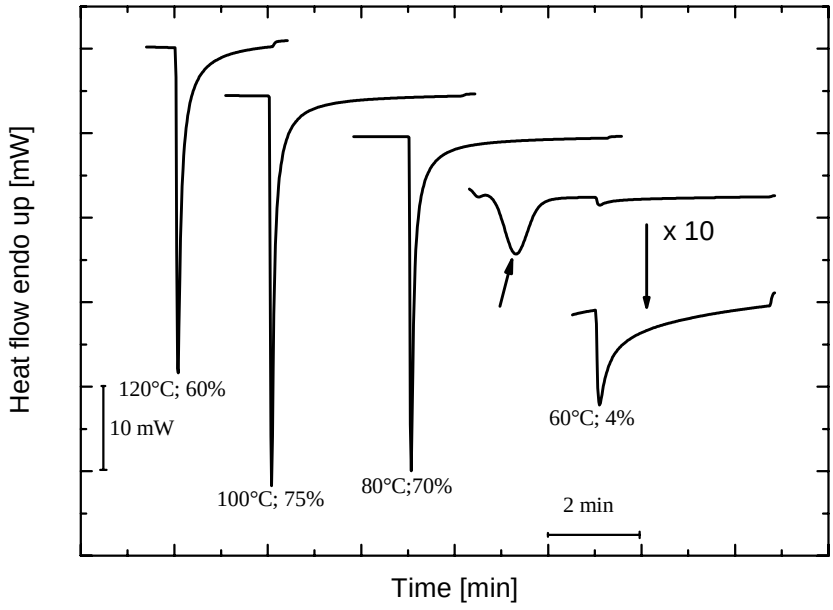

Figure 9: Photopolymerization of reactive mesogen **2** (1 % photoinitiator **3**, 0.5 % BHT) at different temperatures and final conversions.

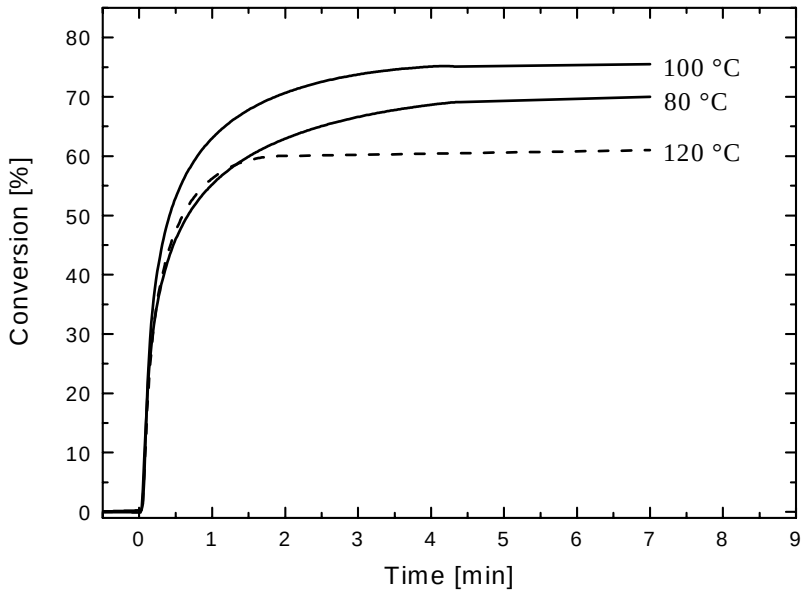

Figure 10: Time-conversion plot of photopolymerization of **2** (1 % photoinitiator **3**, 0.5 % BHT) in the isotropic (120 °C) and in the smectic A phase (100 °C, 80 °C).

The polymerization of **2** in the isotropic phase at 120 °C (dashed curve) leads to a conversion of only 60 %, as shown in Figure 9. In the smectic A phase at 100 °C the conversion increases to 75 %. From Figure 10 it becomes clear that after a few seconds the reaction in the smectic A phase proceeds faster and leads to a larger amount of crosslinking compared to the reaction carried out at a 20 °C higher temperature in the isotropic phase. We attribute this to the fact that the acrylate groups are situated between the layers of the mesogenic cores which leads to a more localised concentration of acrylate groups adjacent to each other within the aliphatic lamella, compared to the isotropic phase where the acrylate units are randomly distributed. Even at 80 °C the final conversion of acrylates is higher in the smectic A phase compared to the isotropic phase at 120 °C. Unfortunately we were not able to achieve photopolymerization in the monotropic smectic C phase since **2** recrystallizes upon slow cooling at ca. 65 °C (ref. Figure 9 arrow) within the timescale of the experiment. In the crystalline phase the conversion of acrylate groups reduces to 4 %.

Conclusion

We have addressed several issues in the photopolymerization of reactive mesogens. When the mesogen **1** is polymerized in the nematic phase at 100 °C a final conversion of 87 % of the acrylate groups is achieved, which is similar to the 88 % conversion in the isotropic phase at 120 °C. Although the temperature is 20 °C lower, polymerization proceeds faster in the nematic phase. Lowering the temperature to 60 °C leads to a decrease in both polymerization rate and final conversion of acrylate groups which we attribute to the increasing viscosity of the system.

We demonstrate that it is not necessary to use as much as 1 % initiator, a number commonly reported as the minimum required for technical systems. With 0.1 % of initiator 81 % of the acrylate groups are polymerized, and even with 0.001 % (10 ppm) of photoinitiator a conversion of 47 % is achieved.

The reactive mesogen **2** with a phenylnaphthalene core could be successfully polymerized in the smectic A phase. Remarkably the polymerization proceeds faster in this phase than in the isotropic phase and leads to higher final conversions. This can be explained by a more localised concentration of acrylate groups in the smectic A phase where the acrylate units are situated between the layers of the mesogenic cores in contrast to the isotropic phase with a random distribution of the acrylate groups.

Acknowledgement: We thank the German Federal Ministry of Education and Research (BMBF) for financial support in the POLITAG program, Weimin Zhang and Martin Heeney for material synthesis.

Experimental part

The synthesis of the reactive mesogens has been published elsewere.[14,16]

The Photo-DSC experiments were carried out with a commercial Perkin-Elmer setup which is schematically shown in Scheme 2.

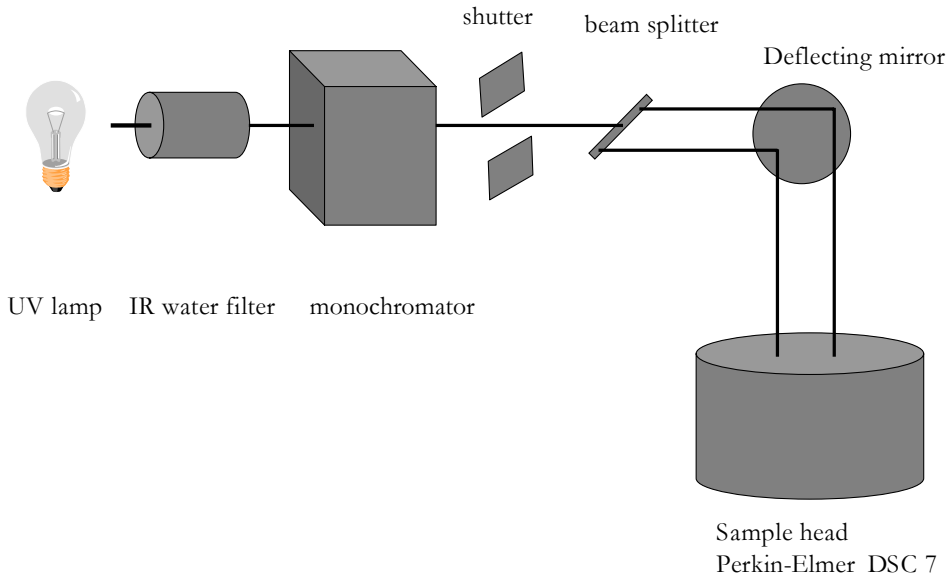

Scheme 2: Schematic representation of the PhotoDSC setup

The light from a 450 W Xenon short arc lamp is passed through an IR absorbing water filter and a monochromator and split into a sample and a reference beam which are focussed to the polymerizable sample and an empty reference pan in a Perkin-Elmer DSC 7 which monitors the heat of polymerization. The light intensity is ca. 1 mW/cm^2.

Sample preparation: Homogeneous mixtures of the reactive mesogen, the photoinitiator **3** and the inhibitor BHT were prepared by dissolving the compounds in CH_2Cl_2. After evaporation of the solvent about 6 mg of the mixtures were used in each photopolymerization experiment.

[1] D.J. Broer, J. Boven, G.N. Mol, G. Challa, *Makromol. Chem.* **1989,** *190*, 2255.

[2] T.J. Bunning, F. Kreuzer, *Trends Polym. Sci.* **1995**, *3*, 318.

[3] D.J. Broer, J. Lub, G.N. Mol, *Nature* **1995**, *378*, 467.

[4] J. Lub, P. van de Witte, C. Doornkamp, J.P.A. Vogels, R.T. Wegh, *Adv. Mater.* **2003**, *15*, 1420.

[5] M. O'Neill, S. Kelly, *Adv. Mater.* **2003**, *14*, 1135.

[6] M. Grell, W. Knoll, D. Lupo, A. Meisel, T. Miteva, D. Neher, H.-G. Nothofer, U. Scherf, A. Yasuda, *Adv. Mater.* **1999**, *11*, 671.

[7] K.S. Whitehead, M. Grell, D.D.C. Bradley, M. Jandke, P. Strohriegl, *Appl. Phys. Letters* **2000**, *76*, 2946.

[8] M. Jandke, D. Hanft, P. Strohriegl, K. Whitehead, M. Grell, D.D.C. Bradley, *Proc. SPIE* **2001**, *4105*, 338.

[9] M.P. Aldred, A.J. Eastwood, S.M. Kelly, P. Vlachos, A.E.A. Contoret, S.R. Farrar, B. Mansoor, M. O'Neill, W.C. Tsoi, *Chem. Mater.* **2004**, *16*, 4928.

[10] M.P. Aldred, A.E.A. Contoret, S.R. Farrar, S.M. Kelly, D. Mathieson, M. O'Neill, W.C. Tsoi, P. Vlachos, *Adv. Mater.* **2005**, *17*, 1368.

[11] H. Sirringhaus, R.J. Wilson, R.H. Friend, M. Inbasekaran, W. Wu, E.P. Woo, M. Grell, D.D.C. Bradley, *Appl. Phys. Lett.*, **2000**, *77*, 406.

[12] B.-H. Huisman, J.J.P. Valeton, W. Nijssen, J. Lub, W. ten Hoeve, *Adv. Mater.* **2003**, *15*, 2002.

[13] M. Funahashi, J. Hanna, *Appl. Phys. Lett.* **1998**, *73*, 3733.

[14] I. McCulloch, W. Zhang, M. Heeney, C. Bailey, M. Giles, D. Graham, M. Shkunov, D. Sparrowe, S. Tierney, *J. Mater. Chem.* **2003**, *13*, 2436.

[15] W. Warta, R. Stehle, N. Karl, *Appl. Phys.A* **1985**, *36*, 163.

[16] D. J. Broer, R.A.M. Hikmet, G.Challa, *Makromol. Chem.* **1989**, *190*, 3201.

[17] C.A. Guymon, E.N. Hoggan, D.M. Walaba, N.A. Clark, C.N. Bowman, *Liquid Crystals* **1995**, *19*, 719.

[18] D.J. Broer, G.N. Mol, G. Challa, *Macromol. Chem.* **1989**, *190*, 19.

[19] H.F. Mark, N.M. Bikales, C.C. Overberger, "*Encyclopedia of Polymer Science and Engineering*", 2nd edition, J.Wiley&Sons, New York, 1988; Vol. 11, p 186.

New fluorene-bithiophene based oligomers for the use in OFETs

Dedicated to Prof. Dr. Oskar Nuyken

Publication in a special issue of Designed Monomers & Polymers, in press.

*Heiko Thiem, Michael M. Rothmann, Peter Strohriegl**

Makromolekulare Chemie I and Bayreuther Institut für Makromolekülforschung (BIMF), Universität Bayreuth, D-95440 Bayreuth, Germany

Email: heiko.thiem@uni-bayreuth.de

Email: michael.rothmann@uni-bayreuth.de

Email: peter.strohriegl@uni-bayreuth.de

*Corresponding author:

Peter Strohriegl

Makromolekulare Chemie I and Bayreuther Institut für Makromolekülforschung (BIMF), Universität Bayreuth, D-95440 Bayreuth, Germany

Fax: + 49 / (0)921 / 55-3206

Abstract

We report the synthesis of oligo(9,9-dioctyl-2,7-diyl)-*alt*-bithiophenes **4a-e**. The molecular weight was tuned by an endcapping reaction with the monofunctional 2-bromo-9,9-di-(n-octyl)-fluorene **2**. All oligomers show nematic mesophases and no sign for crystallisation upon cooling. The clearing temperatures are in the range from 80 °C to 288 °C in oligomers with different molecular weight. A plot of $1/P_n$ versus the clearing temperature results in a clearing temperature of 366 °C for the ideal polymer. First orientation experiments on rubbed polyimide films give a maximum orientation of 8.2 to 1 parallel and perpendicular to the rubbing direction.

Keywords: bithiophene, F8T2, fluorene, nematic OFET, orientation

Introduction

Organic field effect transistors (OFETs) have undergone great progress in the last years since they were first described in 1986[1]. Some potential advantages over conventional silicon technology are the low cost fabrication, large area coverage and the use of flexible substrates[2,3,4]. Apart from single crystals of fused aromatic compounds like pentacene[5] materials which contain thiophene units are of great interest. Conjugated thiophenes like α-sexithiophene[6] are well described in literature and reach mobilities of $2 \cdot 10^{-2}$ cm^2/Vs in single crystal OFETs.[7]. Dimitrakopoulos et al. showed a further improvement of the mobility up to 0.13 cm^2/Vs in α,ω-dihexyl-sexithiophene[8] whith two termined hexyl substituents. Among the solution processable materials regioregular poly(3-hexylthiophene) (P3HT) is one of the most investigated materials. There a lamellar structure with two-dimensional conjugated sheets is formed by interchain stacking and leads to a field effect mobility of 10^{-1} cm^2/Vs for P3HT with a regioregularity of 96 %, which is in the same range as the mobility of amorphous silicon[9]. McCulloch et al. showed the synthesis of other polythiophenes with different substituent pattern and end up with mobilities up to 0.15 cm^2/Vs[10,11]. However, a significant drawback of oligo- or polythiophenes is their poor oxidative stability especially[12]. So the development of oxidative stable materials with high carrier mobilities is of great interest. One solution of this problem is the combination of thiophene with other conjugated systems to lower the HOMO level and increase the stability. Apart from the combination with one or two phenyl lrings[13,14], the introduction of fluorene units into the structure seems to be a promising way to improve the stability. H. Meng et al. demonstrated the use of trimers with one central bithiophene and two adjacent fluorene units in OFETs. They measured field effect mobilities up to 0.1 cm^2/Vs in evaporated polycrystalline films at the trimer 5,5'-bis-(7-hexyl-9H-fluoren-2-yl)-2,2'-bithiophene[15,16].

Among the solution processable materials with fluorene and bithiophene units poly[(9,9-dioctylfluorene-2,7-diyl)-*alt*-bithiophene] (F8T2) is of special interest. Due to the fact that the polymer has a nematic liquid crystalline phase, it can be aligned on orientation layers and this increase in molecular order in the material is accompanied by an increase of the carrier mobilities. The highest mobilities are reported by H. Sirringhaus et al.[17] who found an increase of the field effect mobility from 10^{-3} cm^2/Vs in a non oriented sample to $2 \cdot 10^{-2}$ cm^2/Vs if the polymer is oriented on a rubbed polyimide layer. Recent work showed, that F8T2 has a remarkably high electron mobility of $6 \cdot 10^{-3}$ cm^2/Vs[18], what makes the material also attractive for applications where both p- and n-type transport is needed (CMOS).

One major difficulty during the orientation of F8T2 is the high clearing temperature of the polymer. L. Kinder et al. determined a transition temperature from the nematic mesophase to the isotropic phase of 311 °C for a F8T2 with a molecular weight of 31000 g/mol[19]. This temperature makes it difficult to heat F8T2 to the isotropic phase what is beneficial to achieve an optimum orientation without degradation of the material.

To overcome this problem, we present in this paper the synthesis of F8T2 oligomers with lower molecular weight. These oligomers were prepared by end capping with a monofunctionalised fluorene. The molecular weight of the resulting (9,9-dioctylfluorene-2,7-diyl)-*alt*-bithiophene oligomers is tailored by the ratio of mono and difunctionalised monomers in the synthesis. We show that the clearing temperature of the oligomers can be varied from 80 °C to 288 °C with the molecular weight. In addition first orientation experiments of one oligomer on a rubbed polyimide layer are reported.

Results and discussion

The commercially available 2-bromo- and 2,7-dibromofluorene were alkylated with n-octylbromide in a phase transfer reaction[20] using aqueous NaOH and DMSO as solvents (scheme 1) to receive 2,7-dibromo-9,9-di-(n-octyl)-fluorene **1** and 2-bromo-9,9-di-(n-octyl)-fluorene **2**. The other building block 5,5'-bis(4,4,5,5-tetramethyl-1,3,2-dioxaborolane-2-yl)-2,2'-bithiophene **3** was obtained from the reaction of bithiophene with n-BuLi and N,N,N',N'-tetramethyl-1,2-ethanediamine (TMEDA) in hexane at -78 °C and subsequent addition of 2-isopropoxy-4,4,5,5-tetramethyl-1,3,2-dioxaborolane[21].

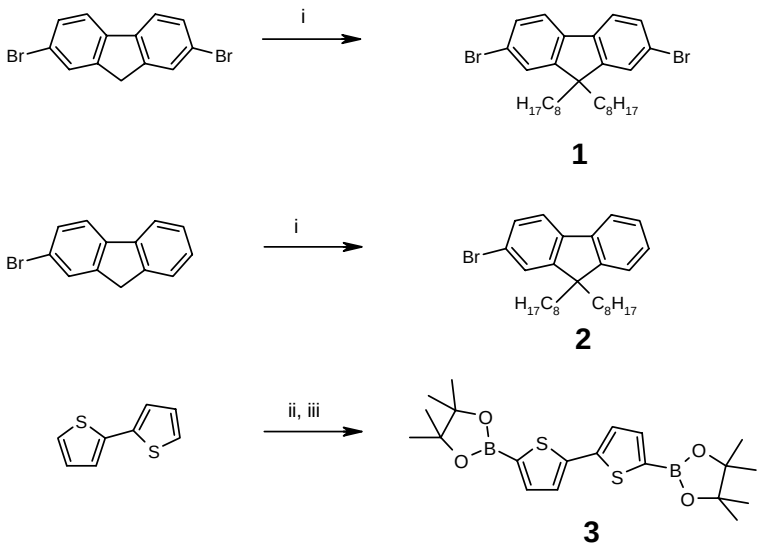

i) n-octylbromide, DMSO, NaOH, PTC, 90 °C; ii) n-BuLi, TMEDA, hexane, -78 °C, iii) 2-isopropoxy-4,4,5,5-tetramethyl-1,3,2-dioxaborolane, -78 °C.

Scheme 1: Synthesis of 2,7-dibromo-9,9-di-(n-octyl)-fluorene **1**, 2-bromo-9,9-di-(n-octyl)-fluorene **2** and 5,5'-bis(4,4,5,5-tetramethyl-1,3,2-dioxaborolane-2-yl)-2,2'-bithiophene **3**.

The synthesis of the liquid crystalline oligomers was made by Suzuki cross coupling which ensures a strictly alternating sequence of fluorene and bithiophene units. As catalytical system a mixture of palladium(II)-diacetat and tri-o-tolylphosphine was used. Due to the high reactivity of the catalyst, it was possible to run the reactions under mild conditions at 40 °C within two hours. The synthesis is outlined in scheme 2.

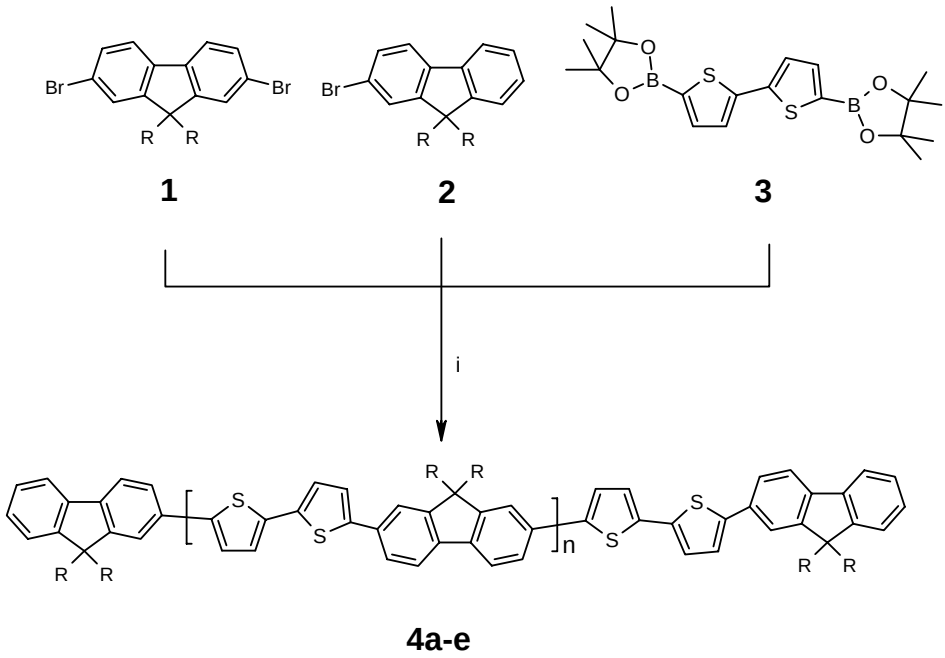

i) $Pd(OAc)_2$, tri-o-tolylphosphine, K_2CO_3 (2 M aq.), toluene, PTC, 40 °C.

Scheme 2: Synthesis of oligo(9,9-dioctylfluorene-2,7-diyl)-*alt*-bithiophene.

Polycondensation of equimolar amounts of the two bifunctional compounds **1** and **3** would yield the well known polymer F8T2. The addition of the monofunctional endcapper **2** leads to a reduction of the molecular weight and the F8T2 oligomers **4a-e** with terminal fluorene units are obtained. The molecular weight decreases with increasing amounts of the endcapper **2**. In Figure 1 the GPC scans of all oligomers **4a-e** are shown. The molecular weights are summarised in Table 1.

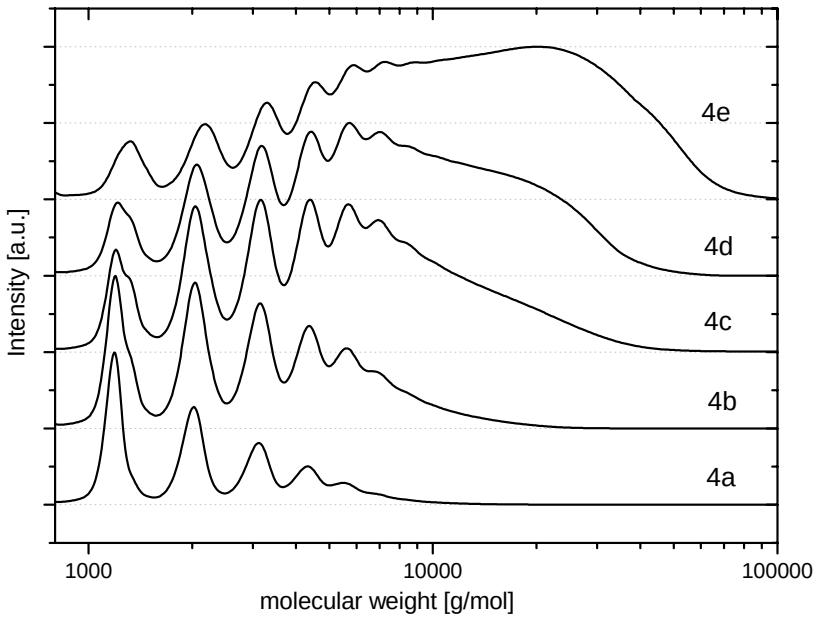

Figure 1: GPC scans of the oligomers **4a-e** (polystyrene calibration).

Table 1: Molecular weights, degree of polymerisation and clearing temperatures of oligomers **4a-e**.

	molar ratio 1 / 2	M_n [g/mol]*	M_w [g/mol]*	P_n	$T_{n\text{-}iso}$ [°C]**
4e	10	5030	12800	17.8	288
4d	3.0	3540	7050	12.4	245
4c	2.0	2900	5800	10.1	220
4b	1.0	2000	3350	6.8	155
4a	0.5	1500	2200	5.1	80

*From GPC measurements (polystyrene standards) and corrected by the factor 0.84.
**Determined by polarizing microscopy.

In the GPC scan of **4a** which was prepared with the largest amount of endcapper only low molecular weight oligomers can be seen. By comparison with an independently

synthesised trimer the first peak at a molecular weight of 1100 g/mol can be assigned to a trimer. The next peaks correspond to the pentamer (n = 1), the heptamer (n = 2), the nonamer (n = 3) and an undecamer (n = 4). With increasing molecular weight, the oligomers contain more and more longer chains with a molecular weight above 10000 g/mol. In the oligomer **4e** the polymeric part becomes dominant. Only one homologous series is observed in the low molecular weight oligomers like **4a**. This shows that the endcapping reaction works efficiently and each oligomer has two fluorene end groups.

Due to the fact, that the oligomers are rigid, rodlike molecules, the GPC which is calibrated with polystyrene standards always overestimates the molecular weights. The smallest possible oligomers are the trimer (n = 0) and the pentamer (n = 1) which can be seen in the GPC scan of **4a**. From molecular weight determined by GPC and the real molecular weight a correction factor of 0.84 was calculated and the average molecular weights from the integration of the GPC scans were corrected by that factor.

Due to the fact, that the sensitivity of the DSC was not sufficient to identify the phase transition temperatures of the oligomers, they were determined by polarizing microscopy. All oligomers exhibit nematic mesophases and the transition to the isotropic phase can be clearly seen. In addition they show no sign of crystallisation upon cooling. All oligomers form supercooled nematic phases. The transition temperatures from the nematic mesophase to the isotropic state are summarised in table 1. The oligomer with the lowest molecular weight (**4a**) shows the lowest transition temperature of 80 °C. With higher molecular weight an increase of this temperature can be observed till it reaches 288 °C at the oligomer **4e**. So the clearing temperature can be varied over a temperature range of 200 °C by the molecular weight of the oligomers. Figure 2 shows a picture taken from the polarising microscope with crossed polarizers at 140 °C from **4b**.

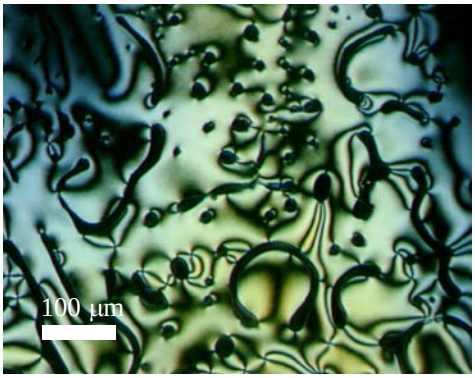

Figure 2: Nematic mesophase of **4b** at 140 °C from a polarizing microscope with crossed polarizers.

As it can be seen from Figure 2 a typical nematic Schlieren texture is obtained from the oligomers.

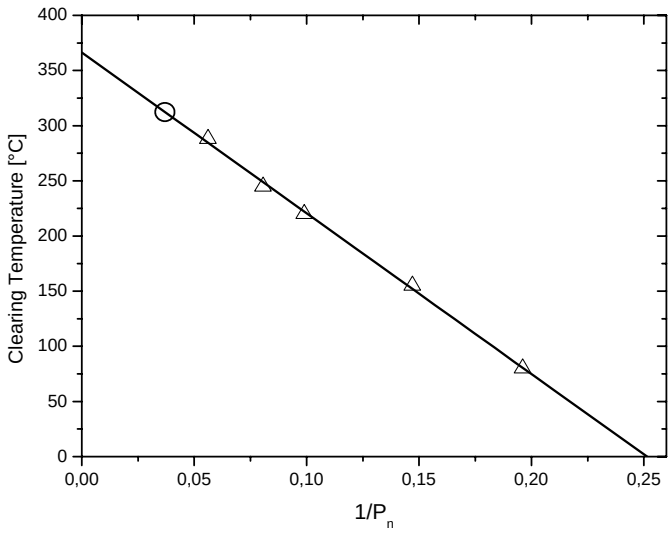

Figure 3: Plot 1/Pn versus clearing temperature of the oligomers **4a-e** (Δ) and the linear fit and literature value for F8T2 (O).

In Figure 3 a plot of $1/P_n$ versus the clearing temperature is shown. Such plots are usually made to extrapolate physical properties like the melting point or the absorption edge of a series of monodisperse oligomers to a polymer with infinite chain length like it is shown for fluorene oligomers[22]. As can be seen from Figure 3 the clearing temperature increases with the molecular weight of the oligomers. The quality of the fit in Figure 3 which was

obtained from oligomers with an average molecular weight and not from monodisperse model compounds is remarkable. To proof the linear regression of this plot the literature value for F8T2 (M_n = 14900 g/mol; M_w = 31300 g/mol) is also shown in Figure 3(O). The clearing temperature of this polymer fits very good to the measured temperatures of the oligomers. The extrapolation against zero results in a clearing temperature of 366 °C for the ideal polymer with an infinite degree of polymerisation.

Orientation experiments

These broad nematic mesophases and the low clearing temperatures make the oligomers 4a-e good candidates for orientation experiments. In this chapter we will describe the orientation of oligomer **4c** on rubbed polyimide layers. After the preparation of the orientation layer (see experimental part) **4c** was spin coated from a 1 weight % toluene solution at 2000 rpm. The resulting film thickness after drying was 50 nm. For the orientation experiment the sample was heated in argon to the isotropic phase (230 °C) and annealed there for five minutes. Then it was slowly cooled to 195 °C where the oligomer is in the nematic phase. This temperature was held for 30 minutes. After quenching to room temperature the orientation ratio was measured by polarized absorption spectroscopy. Figure 4 shows the polarized absorption spectra of an oriented film of **4c**.

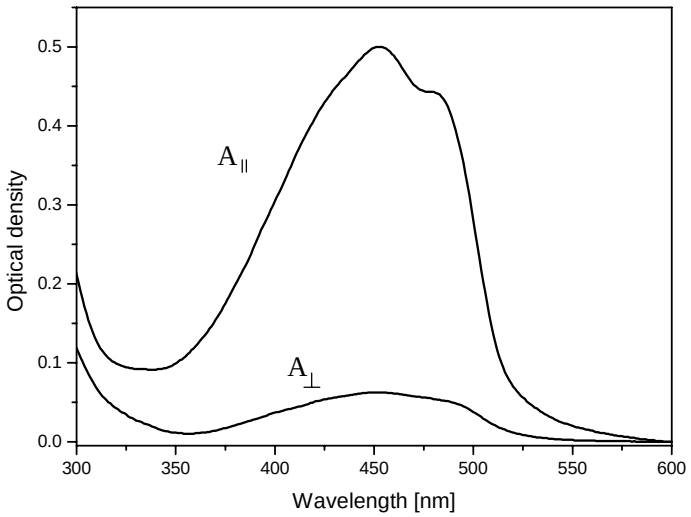

Figure 4: Absorption spectra of a 50 nm thick film of **4c** on rubbed polyimide measured parallel and perpendicular to the rubbing direction.

From the integral of the curves an orientation ratio of 8.2/1 was calculated. So the orientation of these oligomers is possible and provides promising results which are in the same range as for F8T2[17]. In the near future oriented materials will be tested in OFETs.

Conclusion

We describe an efficient method for the synthesis of fluorene and bithiophene containing F8T2 oligomers **4a-e** under mild conditions. GPC analysis showed that the endcapping process is efficient and the molecular weight can be tuned by the amount of monofunctionalised fluorene compound **2**. All oligomers exhibit broad nematic mesophases and form supercooled nematic phases upon cooling. The clearing temperatures vary from 80 °C for the oligomer with the lowest molecular weight (**4e**) to 288 °C for the one with the highest molecular weight (**4a**). The extrapolation to the clearing temperature of the F8T2 polymer with infinite chain length leads to a value of 366 °C.

The relatively low clearing temperatures of the oligomers facilitates orientation experiments at moderate temperatures. The oligomer **4c** was oriented on a rubbed polyimide layer and delivers an orientation ratio of 8.2/1 in absorption. In the future we will try to take benefit from the orientation of the F8T2 oligomers to increase the carrier mobility in OFETs.

Experimental part

Materials. All chemicals and reagents were used as received from commercial sources without further purification. All solvents for reactions and purification were once distilled, except tetrahydrofuran (THF) which was additionally distilled over potassium.

^{1}H-NMR and ^{13}C-NMR spectra were recorded with a Bruker AC 250 (250 MHz) apparatus and $CDCl_3$ as solvent. All data are given as chemical shifts δ [ppm] downfield from $Si(CH_3)_4$. The IR spectra were recorded using a Bio-Rad Digilab FTS-40. The UV-VIS spectra were recorded with a Hitachi U-3000 spectrophotometer. The LC phase transitions were determined with a Leitz Laborlux 12-pol, Nikon Diaphot 300 equipped with a Linkon hotstage. The molecular weight of the oligomers was determined with a Waters gel permeation chromatography system (GPC) for oligomers. The system includes a set of two 60 cm long and 0.8 cm thick columns (particle size: 5 μm; pore size: 1000 nm) and THF was used as eluent. It was calibrated with polystyrene standards.

Samples for polarized absorbance were prepared on carefully cleaned quartz slides. For the preparation of polyimide alignment layers a solution of a polyamic acid precursor (PI-Kit ZLI 2650, MERCK) was spin-coated onto the substrate and subjected to thermal conversion in a nitrogen atmosphere (1 h at 100 °C, 1 h at 200 °C, 1 h at 300 °C). Finally the substrates were rubbed with a velvet drum using a commercial rubbing machine (1200 rpm, Optron Instruments). The oligomeric compounds were spin-coated from toluene solution in a concentration of 1 weight % at 2000 rpm.

2,7-dibromo-9,9-di-(n-octyl)-fluorene (1). In a two phase system of 100 ml 50% NaOH, 300 ml DMSO and 1.5 g tetrabutylammonium chloride as phase transfer catalyst, 2,7-dibromofluorene (20 g, 62 mmol) was dissolved. In argon atmosphere n-octylbromide (59 ml, 340 mmol) was added. After stirring for 12 h at 120 °C, diethyl ether was added to the cold solution. The organic phase was washed with water and distilled in high vacuum to

remove the DMSO and n-octylbromide. The residue was filtered with a short silicagel column with hexane as eluent to yield **1** (33 g, 98%) as a white powder.

IR (KBr): 2955, 2851, 1579, 1398, 1060, 881, 722.

^{1}H-NMR (250 MHz, $CDCl_3$), δ(ppm): 0.5 (t, 6H), 0.68-1.0 (m, 24H), 1.94 (m, 4H), 7.43 (dd, 2H), 7.50 (m, 2H), 7.52 (d, 2H).

^{13}C-NMR (66 MHz, $CDCl_3$), δ(ppm): 14.1, 22.5, 23.6, 29.1, 29.8, 31.7, 40.1, 55.5, 121.0, 121.5, 126.1, 130.1, 138.9, 152.4.

2-bromo-9,9-di-(n-octyl)-fluorene (2). Following the same procedure as described for the synthesis of **1**, but with 2-bromofluorene (20 g, 81 mmol) as starting compound, **2** was obtained as a white powder in 95 % (27 g)yield.

IR (KBr): 2955, 2851, 1579, 1398, 1060, 881, 722.

^{1}H-NMR (250 MHz, $CDCl_3$), δ(ppm): 0.5 (t, 6H), 0.68-1.0 (m, 24H), 1.94 (m, 4H), 7.30 (m, 3H), 7.43 (dd, 1H), 7.50 (m, 1H), 7.54 (m, 1H), 7.64 (m, 1H).

^{13}C-NMR (66 MHz, $CDCl_3$), δ(ppm): 10.4, 14.1, 23.0, 27.2, 28.3, 33.8, 35.0, 44.5, 55.5, 119.5, 120.0, 120.6, 124.4, 127.0, 127.8, 130.5, 140.5, 140.7, 149.9, 152.9.

5,5'-bis(4,4,5,5-tetramethyl-1,3,2-dioxaborolane-2-yl)-2,2'-bithiophene(3). Bithiophene (4.9 g, 29 mmol) was dissolved in 100 ml dry hexane. After adding N,N,N',N'-tetramethyl-1,2-ethanediamine (TMEDA 10 ml, 68 mmol) to the solution, n-BuLi (1.6 M, 41 ml, 65 mmol) was added to the mixture under argon at -78 °C. The mixture was kept at -78 °C for 15 minutes and then refluxed for one hour and cooled to -78 °C again, where 2-isopropoxy-4,4,5,5-tetramethyl-1,3,2-dioxaborolane (16 ml, 77mmol) was added. The reaction mixture was allowed to come to room temperature and stirred for another 12 hours. After dilution with CH_2Cl_2 and washing with 10 % $NaHCO_3$ the solvents were

evaporated and the product recrystallized from hexane. Yield: 6.9 g (56 %) of **3** as a white powder.

IR (KBr), (cm^{-1}): 3064, 3038, 2999, 2926, 2875, 1608, 1456, 1418, 1356, 1141, 831.

^{1}H-NMR (250 MHz, $CDCl_3$), δ(ppm): 1.36 (s, 24H), 7.30 (d, 2H), 7.50 (d, 2H).

^{13}C-NMR (66 MHz, $CDCl_3$), δ(ppm): 25.2, 84.4, 126.0, 129.2, 138.4, 144.1.

Oligo(9,9-dioctylfluorene-2,7-diyl)-*alt*-bithiophene (4a-e). To a degassed 2:1 mixture of toluene and 2 M aqueous K_2CO_3, 0.1 g tetrabutylammonium chloride as phase transfer catalyst and different amounts of the dibromofluorene 1, the monobromofluorenes 2 and the diboronic ester 3 (see table 1) were added. After the addition of the catalyst($Pd(OAc)_2$ (2 mol %) and tri-o-tolylphosphine (6 mol %)) the reaction mixture was degassed again and stirred at 40 °C for 2 h. After cooling, it was washed with water, saturated NaCl-solution and again with water. The purification was completed by filtration over a short silica gel column and precipitation into MeOH. All oligomers are obtained with yields of more than 80 %.

IR (KBr), (cm^{-1}): 3060, 2965, 2926, 2860, 1455, 1378, 1258, 875, 790, 738.

^{1}H-NMR (250 MHz, $CDCl_3$), δ(ppm): 0.5 (m, 4H), 0.8 (t, 6H), 1.1 (m, 20 H), 2.0 (m, 4H), 7.20 (m, 4H), 7.68 (m, 7H).

[1] A. Tsumura, H. Koezuka,, T. Ando, *Appl. Phys. Lett.* **49**, 1210 (1986).

[2] C.D. Dimitrakopoloulos, P.R.L. Malenfant, *Adv. Mater.* **14**, 99 (2002).

[3] J. Veres, S. Ogier, G. Lloyd, D. deLeeuw, *Chem. Mater.* **16**, 4543 (2004).

[4] M.M. Ling, Z. Bao, *Chem. Mater.* **16**, 4824 (2004).

[5] O.D. Jurchescu, J. Baas, T.M. Palstra, *Appl. Phys. Lett.* **84**, 3061 (2004).

[6] F. Garnier, A. Yassar, R. Hajlaoui, G. Horowitz, F. Deloffre, B. Servet, S. Ries, P. Alnot, *J. Am. Chem. Soc.* **115**, 8716 (1993).

[7] A. Dodabalapur, L. Torsi, H.E. Katz, *Sience* **268**, 270 (1995).

[8] C.D. Dimitrakopoulos, B.K. Furman, T. Graham, S. Hegde, S. Purushothaman, *Synth. Met*. **92**, 47 (1998).

[9] H. Sirringhaus, P.J. Brown, R.H. Friend, M.M. Nielsen, K. Beechgard, B.M.W. Langeveld-Voss, A.J.H. Spiering, R.A.J. Jannsen, E.W. Meijer, D. deLeeuw, *Nature* **401**, 685 (1999).

[10] I. McCulloch, C. Bailey, M. Giles, M. Heeney, I. Love, M. Shkunov, D. Sparrowe, S. Tierney, *Chem. Mater.* **17** 1381 (2005).

[11] M. Heeney, C. Bailey, K. Genevicius, M. Shkunov, D. Sparrowe, S. Tierney, I. McCulloch, *J. Am. Chem. Soc.* **127**, 1078 (2005).

[12] W. Yu, H. Meng, J. Pei, W. Huang, *J. Am. Chem. Soc.* **120**, 11808 (1998).

[13] X.M. Hong, H.E. Katz, A.J. Lovinger, B.C. Wang, K. Raghavachari, *Chem. Mater.* **13**, 4686 (2001).

[14] M. Ichigawa, H. Yanagi, Y. Shimizu, S. Hotta, N. Suganuma, T. Koyama, Y. Taniguchi, *Adv. Mater.* **14**, 1272 (2002).

[15] H. Meng, Z. Bao, A.J. Lovinger, B.C. Wang, A.M. Mujsce, *J. Am. Chem. Soc.* **123**, 9214 (2001).

[16] H.Meng, J. Zheng, A.J. Lovinger, B.C. Wang, P. G. van Patten, Z. Bao, *Chem. Mater.* **15**, 1778 (2003).

[17] H. Sirringhaus, R.J. Wilson, R.H. Friend, M. Inbasekaran, W. Wu, E.P. Woo, M. Grell, D.D.C. Bradley *Appl. Phys. Lett.*, **77**, 406 (2000).

[18] L.-L. Chua, J. Zaumseil, J.-F. Chang, E.C.-W. Ou, P.K.-H. Ho, H. Sirringhaus, R.H. Friend, *Nature* **434,** 194 (2005).

[19] L. Kinder, J. Kanicki, P.Petroff, *Synthetic Metals* **146**, 181 (2004).

[20] E.P. Woo, M. Inbasekaran, W. Shiang, G.R. Roof, *US Patent* 5,708,130 (1998).

[21] J. Hellberg, T. Remonen, F. Allared, J. Slätt, M. Svensson, *Synthesis* **14**, 2199 (2003).

[22] J. Jo, C. Chi, S. Höger, G. Wegner, D.Y. Yoon, *Chem. Eur. J.* **10**, 2681 (2004).

New fluorene and bithiophene based trimers as p-type materials in OFETs

Synthetic Metals, in press.

*Heiko Thiem and Peter Strohriegl**

Makromolekulare Chemie I and Bayreuther Institut für Makromolekülforschung (BIMF), Universität Bayreuth, D-95440 Bayreuth, Germany

Email: heiko.thiem@uni-bayreuth.de

Email: peter.strohriegl@uni-bayreuth.de

Sepas Setayesh and Dago de Leeuw

Philips Research Laboratories, Prof. Holstlaan 4, 5656 AA Eindhoven, The Netherlands

Email: sepas.setayesh@philips.com

Email: dago.deleeuw@philips.com

Abstract

We report the synthesis of five new 5,5'-bis(9,9'-dialkylfluorene-2-yl)-2,2'-bithiophenes **4a-e** as active materials for the use in OFETs. Depending on the type of alkyl substituents crystalline or amorphous materials are obtained. Cyclovoltammetry shows that the materials are electrochemically stable and have a HOMO level at -5.3 eV. The different morphologies of thin films of **4a-e** have great influence on the performance of the materials in OFETs. The field effect mobilities are in the range of 10^{-5} cm^2/Vs in an amorphous film of **4c** to $3 \cdot 10^{-3}$ cm^2/Vs in a polycrystalline film of **4a**. This high mobility stays constant after three month at ambient conditions which proofs the high environmental stability of this class of materials.

Keywords: OFET, fluorene, bithiophene, Suzuki cross coupling, morphology

Introduction

Organic filed effect transistors (OFETs) have undergone great progress in the last several years since they were first described in 1986[1]. Potential advantages compared to conventional silicon technology are the low cost fabrication, large area coverage and the use of flexible substrates[2,3,4]. Apart from single crystals of fused aromatic compounds like pentacene[5] materials which contain thiophene units are of great interest. Among the solution processable polymers regioregular poly(3-hexylthiophene) (P3HT) is one of the best investigated materials. In P3HT a highly ordered lamellar structure with two-dimensional conjugated sheets is formed by interchain stacking. A field effect mobility of 10^{-1} cm^2/Vs, which is in the same range as amorphous silicon, can be obtained from regioregular P3HT [6].

Apart from polymers conjugated oligomers containing thiophene units are promising charge transport materials. The better control of purity compared to the polymers and the well defined structure make them attractive materials for the use in OFETs. One of the most investigated oligomers is α-sexithiophene[7], where a mobility of $2 \cdot 10^{-2}$ cm^2/Vs can be obtained[8]. Dimitrakopoulos et al. show an improve of the mobility up to 0.13 cm^2/Vs, when they introduce two hexylchains in the molecule to receive α,ω-dihexyl-sexithiophene[9]. However, a significant drawback of oligothiophenes is their poor stability and high sensitivity towards oxidation especially in the solid state[10]. A solution of this problem is the combination of thiophene with other conjugated systems to achieve a lower HOMO level and thus a better stability. Apart from the combination with one or two phenyl rings[11,12], the introduction of fluorene units seems to be a promising way to improve the stability. A well known polymer with both fluorene and bithiophene repeat units which shows additionally a nematic liquid crystalline mesophase, is poly[(9,9-dioctylfluorene-2,7-diyl)-*co*-bithiophene] (F8T2). Apart from hole mobilities up to $2 \cdot 10^{-2}$

cm^2/Vs[13] , recent work showed, that F8T2 has a remarkable high electron mobility of $6 \cdot 10^{-3}$ cm^2/Vs[14], if it is combined with a suitable dielectric. This makes the material attractive for applications where transport of both holes and electrons is needed (CMOS). H. Meng et al. demonstrated the use of trimers with one central bithiophene and two adjacent fluorene units in OFETs. They measured a field effect mobility of 0.02 cm^2/Vs in 5,5'-bis-(7-hexyl-9H-fluoren-2-yl)-2,2'-bithiophene using top gate devices[15]. Additionally they showed nicely the dependence of the morphology of the evaporated films on the OFET performance. The morphology of the film was tuned by varying the substrate temperature during evaporation from 25 °C to 180 °C[16]. The highest mobility was obtained at a substrate temperature of 180°C where homogeneous films with smooth surfaces are formed. These measurements show how important the morphology of an evaporated film is and how drastically it can influence the performance of an OFET.

In these trimers the 9 position in both fluorenes is not substituted by alkyl groups. As discussed in literature, this might lead to a degradation of the material and formation of fluorenone compounds[17]. In this paper we present the synthesis of new 5,5'-bis(9,9'-dialkylfluorene-2-yl)-2,2'-bithiophene trimers via the palladium catalyzed Suzuki coupling. We have tested these trimers in OFETs and show how the film morphology influences the performance.

Results and discussion

The synthesis of the basic building blocks for the novel fluorene-bithiophene trimers is outlined in scheme 1.

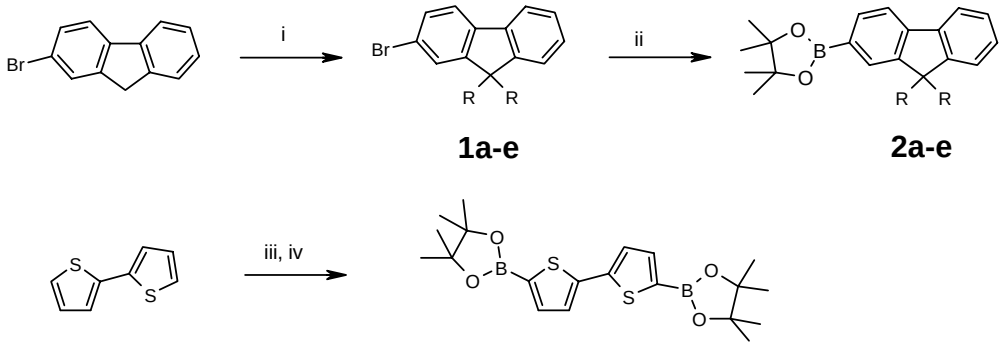

1a-e **2a-e**

3

	1a, 2a	**1b, 2b**	**1c, 2c**	**1d, 2d**	**1e, 2e**
R	ethyl	n-butyl	sec-butyl	2-ethylhexyl	n-octyl

i) alkylbromide, DMSO, NaOH, PTC, 90 °C; ii) n-BuLi, 2-isopropoxy-4,4,5,5-tetramethyl-1,3,2-dioxaborolane, THF; -78 °C iii) n-BuLi, TMEDA, hexane, iv) 2-isopropoxy-4,4,5,5-tetramethyl-1,3,2-dioxaborolane, -78 °C.

Scheme 1: Synthesis of the 2-bromo-9,9-dialkylfluorenes **1a-e**, 2-(4,4,5,5-tetramethyl-1,3,2-dioxaborolane-2-yl)-9,9-dialkylfluorenes **2a-e** and 5,5'-bis(4,4,5,5-tetramethyl-1,3,2-dioxaborolane-2-yl)-2,2'-bithiophene **3**.

1a-e and **2a-e** were synthesised using 2-bromofluorene as the starting material. The first step is the dialkylation of 2-bromofluorene with the different alkyl bromides in a phase transfer reaction using aqueous NaOH and DMSO as solvents[18,19]. The dialkylated 2-bromofluorenes **1a-e** are reacted with n-BuLi in THF at -78 °C, followed by the addition of 2-isopropoxy-4,4,5,5-tetramethyl-1,3,2-dioxaborolane, which leads to the formation of the boronic esters **2a-e**. The other building block 5,5'-bis(4,4,5,5-tetramethyl-1,3,2-dioxaborolane-2-yl)-2,2'-bithiophene **3** is obtained by the reaction of bithiophene with n-

BuLi and N,N,N',N'-tetramethyl-1,2-ethanediamine (TMEDA) and subsequent addition of 2-isopropoxy-4,4,5,5-tetramethyl-1,3,2-dioxaborolane[20].

From these building blocks the desired trimers are obtained by a suzuki cross coupling reaction. The different synthetic routes towards the mixed fluorene-bithiophene trimers are outlined in scheme 2.

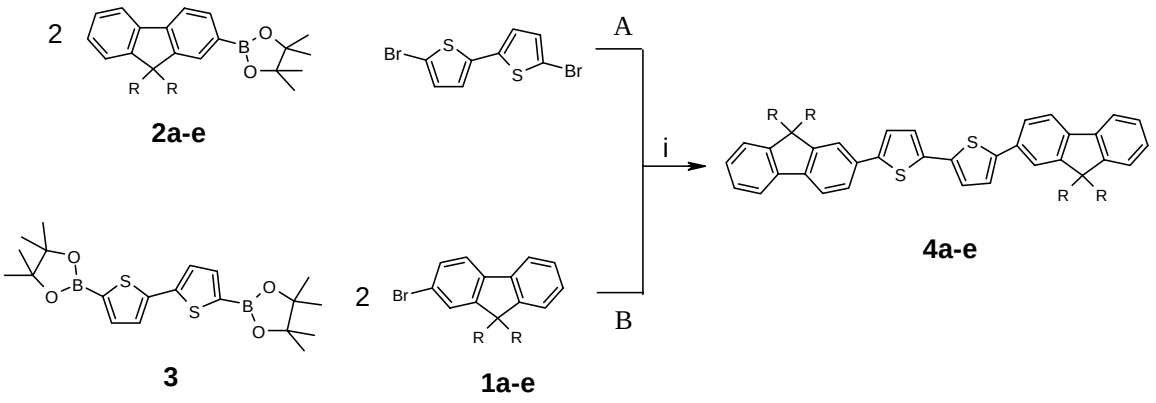

	4a	4b	4c	4d	4e
R	ethyl	n-butyl	sec-butyl	2-ethylhexyl	n-octyl

i) $Pd(OAc)_2$, tri-o-tolylphosphine, K_2CO_3 (2 M aq.), toluene, PTC, 40 °C.

Scheme 2: Different synthetic routes towards 5,5'-bis(9,9'-dialkylfluorene-2-yl)-2,2'-bithiophenes **4a-e**.

There are two possible ways to synthesise the trimeric molecules **4a-e**. The synthetic route A with the commercially available 5,5'-dibromo-2,2'-bithiophene can be carried out at 40 °C and is finished after 4 hours. During the reaction the formation of two byproducts is observed. One is a fluorene dimer, which is the coupling product of two boronic ester groups. Additional a fluorene-bithiophene dimer can be detected. These byproducts make the purification of the trimers difficult.

The use of the synthetic route B in scheme 2 ensures a faster reaction. Here the conversion is complete within two hours at 40 °C and **4a-e** are obtained in 75 % yield. Additionally the purification is much easier due to the lower amount of byproducts.

The thermal characterisation was carried out by TGA and DSC measurements. In the TGA all molecules show a thermal stability of approximately 350 °C. The results of the DSC measurements are summarised in table 1.

Table 1: Thermal properties of **4a-e**.

	R	**M [g/mol]**	**T_g [°C]***	**T_m [°C]***	**$T_{recryst}$ [°C]***
4a	ethyl	607	-	260	226
4b	n-butyl	718	-	207	136
4c	sec-butyl	718	95	-	-
4d	2-ethylhexyl	943	20	90	-
4e	n-octyl	943	-	120	40

* obtained from DSC measurements (heating / cooling rate 10 K/min).

The trimer with short ethyl side chains **4a** shows a melting point of 260 °C and recrystallisation starts at 226 °C upon cooling. Longer n-butyl alkyl chains in **4b** lead to a decrease of the melting point to 207 °C and 136 °C for the recrystallisation. Further decrease is obtained in **4e** with n-octyl side chains where the melting is detected at 120 °C and recrystallisation takes place at 40 °C. Branched sec-butyl side chains prevent **4c** from crystallisation and lead to a material which only shows a glass transition at 95 °C. Bulky 2-ethylhexyl side chains lead to a reduction of the glass transition to 20 °C in **4d**. Additionally this molecule shows melting at 90 °C only in the first heating run. So the thermal properties of the trimers can be tailored by the use of different alkyl side chains. Thus it is possible to synthesise crystalline and amorphous fluorene-bithiophene trimers by only changing the alkyl side chains.

To determine the purity of the fluorene-bithiophene trimers GPCs and MALDI-TOF spectra were taken from each trimer. Figure 1 shows both spectra of **4c**.

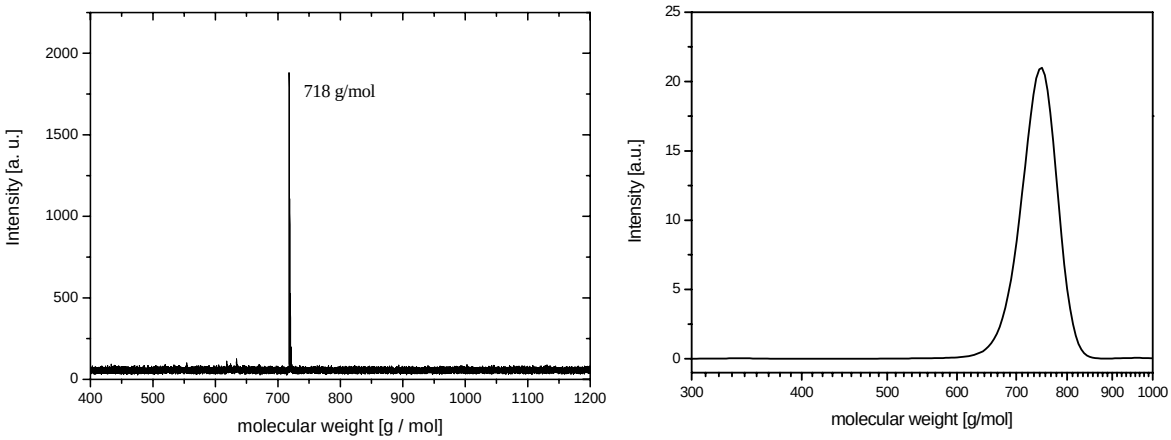

Figure 1: MALDI-TOF spectrum (left) and GPC trace (right) of **4c**.

Due to the fact, that the oligomers form stable radical cations and have an absorption at the irradiation wavelength of 337 nm of the MALDI-TOF laser, the spectrum could be recorded without a matrix and with a low laser intensity of 10 % of the maximum laser power. In both the GPC trace and the MALDI-TOF spectrum no byproducts are detected.

Furthermore the electrochemical properties were investigated. In Figure 2 the cyclic voltammetry measurement of **4c** is plotted and shows two fully reversible oxidation peaks. Repeated oxidation and reduction has no influence on the redox potential. This is a good proof for the electrochemical stability of the material. The oxidation potential was measured vs. $Ag/AgNO_3$ as reference electrode at 25 °C in CH_2Cl_2 as solvent. The calibration of the experiment was made with the standard ferrocene/ferrocenium redox system.

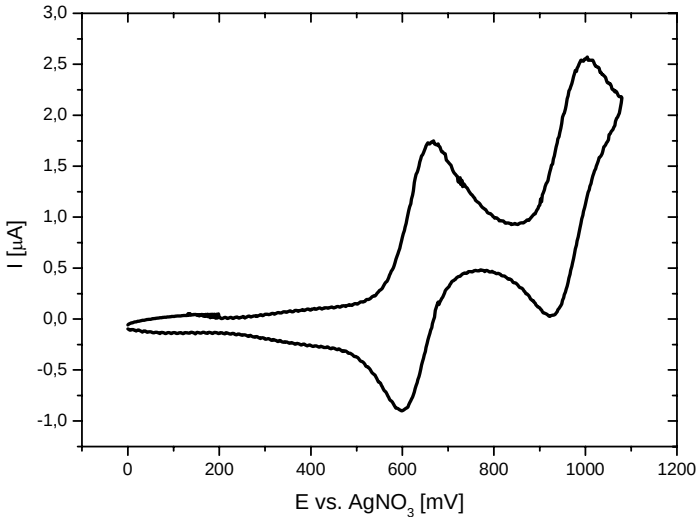

Figure 2: Cyclic voltammogram of **4c** in CH_2Cl_2 measured with $Ag/AgNO_3$ as reference electrode.

Taking -4.8 eV as the HOMO level of the ferrocene system[21], the HOMO level of **4c** is -5.3 eV. From the absorption edge at 470 nm (see Figure 3) an optical bandgap of 2.7 eV and a LUMO level of -2.6 eV can be calculated.

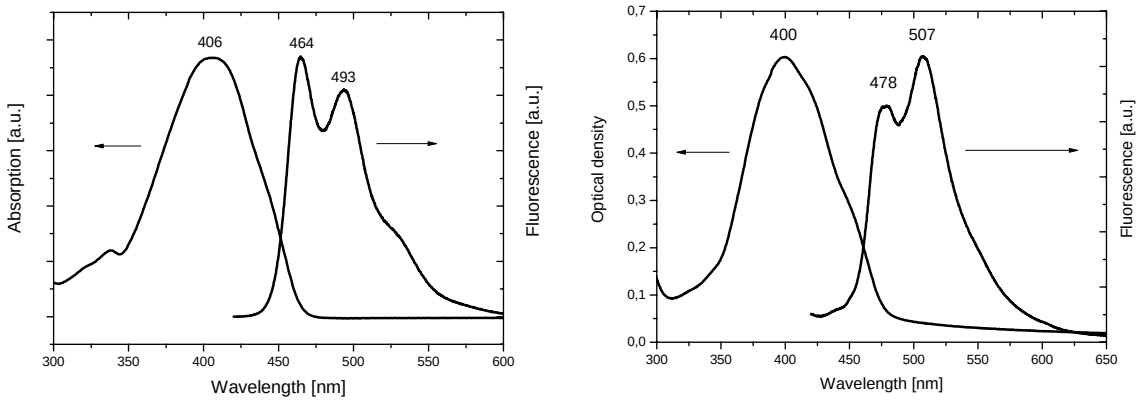

Figure 3: UV-VIS and photoluminescence spectra of **4b.** Left: measured in THF solution; Right: measured from an 80 nm thick evaporated film.

Figure 3 shows, that in solution **4b** has an absorption maximum at 406 nm and a greenish emission with two maxima at 464 nm and 493 nm. The absorption and fluorescence spectra for all fluorene-bithiophene trimers **4a-e** are identical what means that the

conjugated system is not affected by the alkyl substituent at the fluorene units. In a film of **4b** the maxima are slightly shifted to 400 nm for the absorption and 478 and 507 nm for the emission.

We have tested three of the materials **4a**, **4b** and **4c** as organic semiconductor in OFETs. Their HOMO level of -5.3 eV should lead to a good injection of charge carriers from the Au-electrodes. For the transistor measurements, thin films of **4a**, **4b** and **4c** have been prepared by thermal evaporation in a chamber with a pressure of 10^{-5} mbar, an evaporation temperature between 220 °C and 250 °C and a rate of 0.2 Å/s.

The evaporated films were investigated via polarized microscopy. Figure 4 shows pictures of the evaporated films under crossed polarizers.

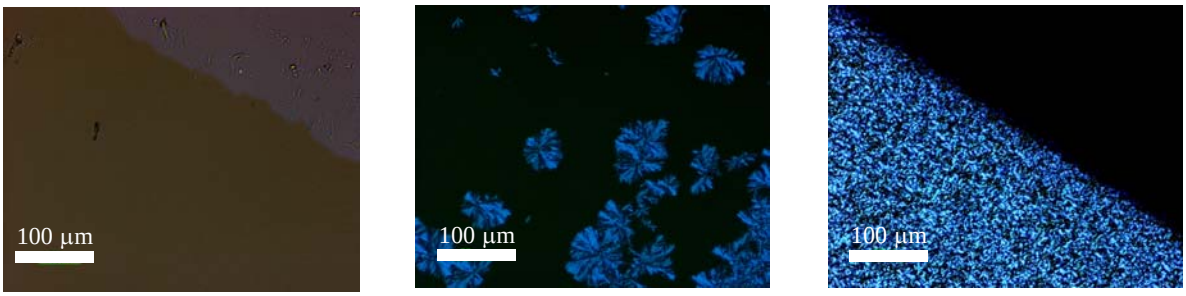

Figure 4: Pictures from polarized microscopy with crossed polarizers from 80 nm thick films of **4c** (left), **4b** (middle) and **4a** (right).

As expected from the DSC measurements (table 1) **4c** with branched sec-butyl substituents forms an amorphous film without any detectable crystalline structures. **4b** with n-butyl side chains forms a semicrystalline film morphology, in which both crystalline and amorphous areas are observed. **4a** with the short ethyl alkyl side chains forms a microcrystalline film without any detectable amorphous parts.

All three trimers were tested in OFETs. After evaporation on a preformed bottom-gate substrate[22] (see experimental section) the drain current was measured as a function of the gate bias (forward sweep from 0 V to –40 V / backward sweep from –40 V to 0 V). The

devices were tested with two fixed drain potentials of –2 V and –20 V, respectively (transfer characteristic). The mobility was calculated from the gate sweep according to equation[22]:

$$\mu_{FET} = (L/W\, C_i\, V_D)\, (\partial I_D/\partial V_G) \qquad (1)$$

Where L is the channel length, W is the channel width, C_i the capacitance of the insulator per unit area, V_D is the drain voltage, I_D is the drain current and V_G is the gate voltage. All measurements were performed in vacuum and after annealing the device for 20 minutes at 80 °C. The transfer characteristics of an OFET prepared from **4c** are shown in Figure 5.

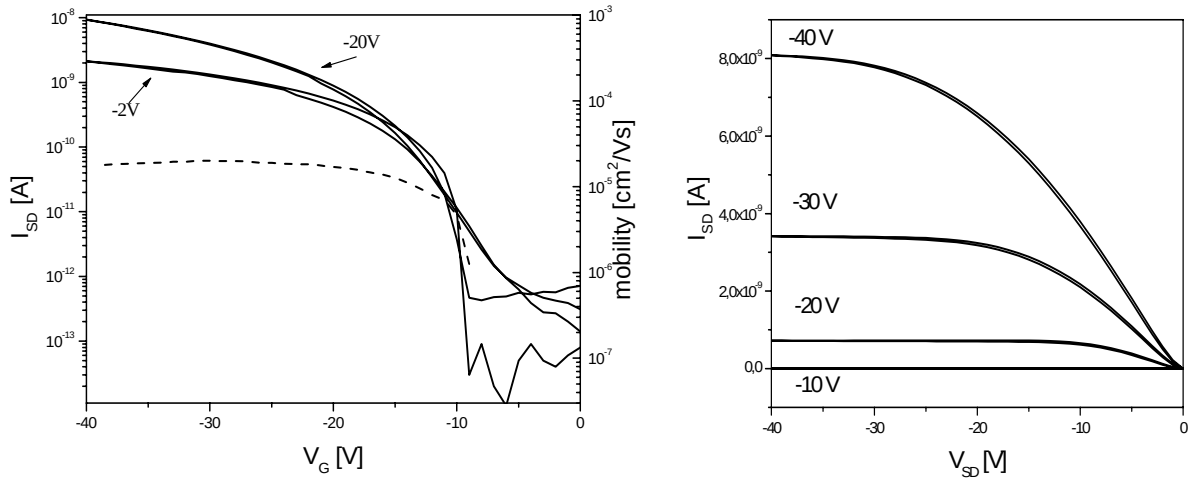

Figure 5: OFET characteristics of **4c**. Left: Transfer characteristics (solid lines, V_D = -2 V, -20 V). The dashed curve shows the mobility values (for V_D = -2 V). Right: Output characteristics of **4c** at different gate voltages.

The mobility of **4c** is 10^{-5} cm^2/Vs and an on/off ratio of 10^4 is measured. The turn-on voltage is at -10 V. Due to the fact, that **4c** is amorphous and has good film forming properties, it was possible to reach the same mobilities from solution processed devices. The output-characteristics (Figure 5 right) shows standard linear and saturation regions. In order to verify the purity and stability of the molecule in Figure 5 forward and backward

sweeps are plotted in Fig. 5 and almost no hysteresis effects are detectable. The semicrystalline molecule **4b** has a mobility of $2 \cdot 10^{-4}$ cm^2/Vs and on/off ratios of 10^4. The highest mobility is obtained in polycrystalline films of **4a** with short ethyl substituents. The characteristics of a freshly prepared OFET are shown in Figure 6.

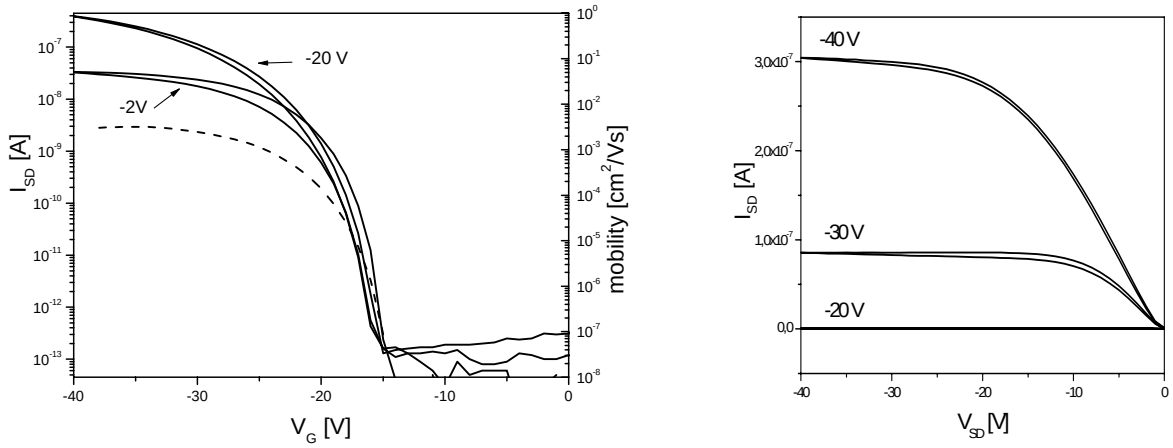

Figure 6: OFET characteristics of **4a**. Transfer characteristics (solid lines, V_D = -2 V, -20 V). The dashed curve shows the mobility values (for V_D = -2 V). Right: Output characteristics at different gate voltages.

From the transfer characteristics (Figure 6) a mobility of $3 \cdot 10^{-3}$ cm^2/Vs is obtained for **4a**. Additionally the on/off ratio of 10^6 is remarkably high. The turn-on voltage is at -15 V. This is the reasons why OFET behaviour is observed only for gate-voltages of more than -20 V in the output characteristics (Figure 6 right). Transistors from **4a** show almost no hysteresis effects in both measurements, which indicates the high purity of the material and its stability in OFETs.

To examine the stability of fluorene-bithiophene trimers the devices were stored at ambient conditions. A measurement after one month gave the same mobility and on/off ratio as shown in Figure 6. The only difference was the shift of the turn-on voltage from -15 V to -10 V. This effect becomes even more pronounced in measurements which were performed after three months which are shown in Figure 7.

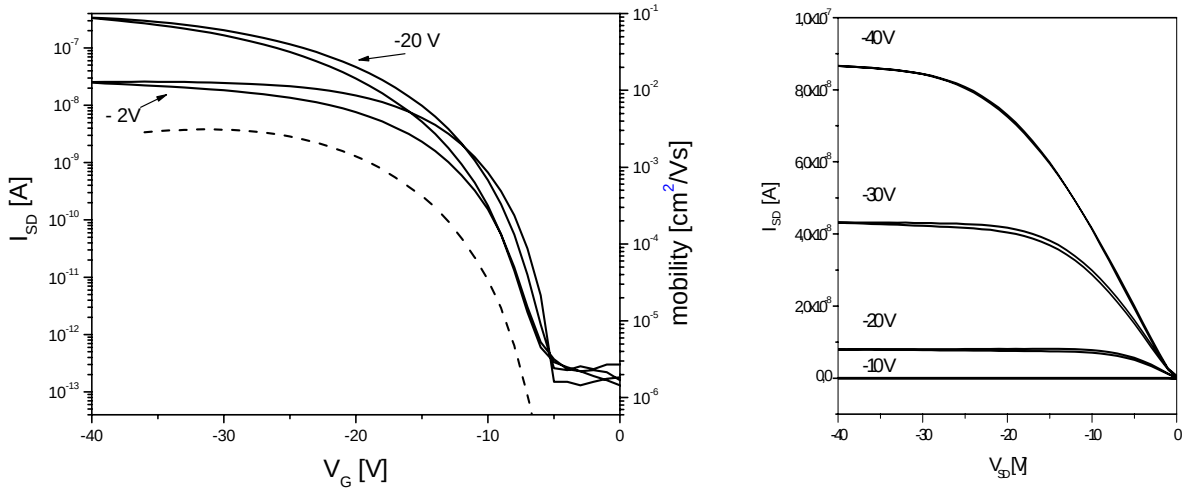

Figure 7: OFET characteristics of **4a** after three month storage under ambient conditions. Left: Transfer characteristics (solid lines, V_D = -2 V, -20 V). The dashed curve shows the mobility values (for V_D = -2 V). Right: Output characteristics at different gate voltages.

4a shows a high stability at ambient conditions. The measured mobility is still at the same level of $3 \cdot 10^{-3}$ cm^2/Vs like in the pristine OFET and the on/off ratio of 10^6 has not changed. The fast and nearly linear increase of the source-drain current (I_{SD}) with the source-drain voltage (V_{SD}) is an evidence, that the charge injection from the gold electrodes works well and the material has almost no specific resistance for the injection. After three months aging the onset voltage has been shifted from -15 V at the freshly prepared OFET to -5 V. Due to the shift of the turn on voltage OFET behaviour can now be detected at a gate voltage of -20 V at the output characteristics (Figure 7). Up to now the shift of the onset voltage is not fully understood. The excellent stability of the fluorene-bithiophene trimers under ambient conditions makes them an attractive material for OFETs. In the future we will try to further increase the mobility by optimising the evaporation process and the use of top gate devices.

Conclusion

We present the efficient synthesis of a series of five new trimeric 5,5'-bis(9,9'-dialkylfluorene-2-yl)-2,2'-bithiophenes **4a-e** via suzuki cross coupling. The coupling reactions were carried out with a very active catalyst consisting of $Pd(OAc)_2$ and tri-o-tolylphosphine and yields of 75 % were obtained. The thermal characterisation of the trimers shows that by different alkyl side chains the melting points of the molecules can be varied from 260 °C for **4a** (ethyl) to 120 °C for **4e** (n-octyl). The introduction of branched alkyl side chains in the molecules leads to the formation of amorphous materials. A HOMO level of -5.3 eV was determined by cyclic voltammetry and with this value and an optical band gap of 2.7 eV a LUMO level of -2.6 eV can be calculated. Three of the materials **4a**, **4b** and **4c** were tested in OFETs. The amorphous **4c** shows a mobility of 10^{-5} cm^2/Vs and an on/off ratio of 10^4. The semicrystalline **4b** has a slightly higher mobility of $3 \cdot 10^{-4}$ cm^2/Vs and on/off ratios in the same range as **4c**. Polycrystalline layers of 4c gave the best performance. A mobility of $3 \cdot 10^{-3}$ cm^2/Vs and an on/off ratio of 10^6 are obtained. In addition the molecules exhibit a high stability against water and oxygen. After three months storage at ambient conditions both the mobility of $3 \cdot 10^{-3}$ cm^2/Vs and the on/off ratio of 10^6 did not change. Future work will focus on top gate devices of these materials to further improve the mobility. Additionally the quality of the polycrystalline films and the mobility can probably be optimised by evaporation onto heated substrates.

Experimental part

General

All chemicals and reagents were used as received from commercial sources without further purification. All solvents for reactions and purification were distilled once, except tetrahydrofuran (THF) which was additionally distilled over potassium.

^{1}H-NMR and ^{13}C-NMR spectra were recorded with a Bruker AC 250 (250 MHz) apparatus and $CDCl_3$ as solvent. All data are given as chemical shifts δ [ppm] downfield from $Si(CH_3)_4$. The IR spectra were recorded using a Bio-Rad Digilab FTS-40. The UV-VIS spectra were made with a Hitachi U-3000 spectrometer. Emission spectra were obtained from a Shimadzu spectrofluorophotometer RF-5301PC. A Bruker Reflex III apparatus with highmass detector was used to record the high resolution MALDI-TOF mass spectra. Cyclic voltammetry was carried out with EG&G Potentiostat Model 263 A. For differential scanning calorimetry measurements (DSC) a Perkin Elmer DSC-7 apparatus was used (heating/cooling rate: 10 K/min). The purity of the target compounds was checked with a Waters gel permeation chromatography system (GPC) for oligomers (analytical columns: crosslinked polystyrene gel (Polymer Laboratories), length: 2 x 60 cm, width: 0.8 cm, particle size: 5 μm, pore size 100 Å, eluent THF (0.5 ml/min, 80 bar), polystyrene standard).

Material synthesis

2-Bromo-9,9-diethylfluorene (1a). In a two phase system of 100 ml 50% NaOH, 300 ml DMSO and 1.5 g tetrabutylammonium chloride as phase transfer catalyst 2-bromofluorene (20 g, 82 mmol) was dissolved. In an argon atmosphere ethyl bromide (33 ml, 560 mmol) was added. After stirring for 12 h at 120 °C, diethyl ether was added to the cold solution. The organic phase was washed with water and distilled in high vacuum to completely

remove the DMSO. The residue was filtered using a short silicagel column with hexane as eluent to yield **1a** (24 g, 97%) as white crystals.

IR (KBr), (cm^{-1}): 3059, 2960, 2910, 2847, 1440, 1375, 1256, 1130, 1003, 874, 731.

^{1}H-NMR (250 MHz, $CDCl_3$), δ(ppm): 0.5 (t, 6H), 2.1 (m, 4H), 7.30 (m, 3H), 7.43 (m, 2H), 7.50 (m, 1H), 7.64 (m, 1H).

^{13}C-NMR (66 MHz, $CDCl_3$), δ(ppm): 10.4, 32.4, 56.1, 119.5, 121.6, 122.7, 126.4, 127.2, 127.3, 120.0, 140.3, 140.5, 149.4, 152.0.

1b, **1c, 1d, 1e** were synthesised according to the same procedure with n-butylbromide, sec-butylbromide, 2-ethylhexylbromide and n-octylbromide as alkylating agents.

2-(4,4,5,5-tetramethyl-1,3,2-dioxaborolane-2-yl)-9,9-diethylfluorene (2a). To a solution of **1a** (8 g, 22.6 mmol) in dry THF n-Butyllithium (1.6M in hexane) (11.7 ml, 29.2 mmol) was added under argon at -78 °C. After stirring for 20 min 2-isopropoxy-4,4,5,5-tetramethyl-1,3,2-dioxaborolane (6.5 ml, 32 mmol) was added at the same temperature. The temperature was kept constant for 15 min and then the mixture was allowed to come to room temperature. After stirring for 12 h the crude product was poured into an excess of water and extracted with diethyl ether. The purification was carried out by column chromatography with $CHCl_3$ as eluent and yields **2a** as a white solid (7.3 g, 79 %).

IR (KBr), (cm^{-1}): 3059, 2960, 2910, 2847, 1440, 1375, 1256, 1130, 1003, 874, 731.

^{1}H-NMR (250 MHz, $CDCl_3$), δ(ppm): 0.5 (t, 6H), 1.38 (s, 12H), 2.1 (m, 4H), 7.30 (m, 3H), 7.68 (d, 1H), 7.76 (m, 3H)

^{13}C-NMR (66 MHz, $CDCl_3$), δ(ppm): 10.4, 24.9, 32.6, 56.2, 83.9, 118.9, 120.0, 122.9, 126.7, 127.5, 128.3, 129.2, 133.7, 141.3, 144.5, 149.0, 152.4.

2b, **2c**, **2d** and **2e** were synthesized according to the same procedure.

5,5'-bis(4,4,5,5-tetramethyl-1,3,2-dioxaborolane-2-yl)-2,2'-bithiophene (3). Bithiophene (4.9 g, 29 mmol) was dissolved in 100 ml dry hexane. After adding N,N,N',N'-tetramethyl-1,2-ethanediamine (TMEDA 10 ml, 68 mmol) to the solution, n-BuLi (1.6 M, 41 ml, 65 mmol) was added to the mixture under argon at -78 °C. The mixture was kept at -78 °C for 15 minutes and then refluxed for one hour and cooled to -78 °C again, where 2-isopropoxy-4,4,5,5-tetramethyl-1,3,2-dioxaborolane (16 ml, 77mmol) was added. Then the reaction was allowed to come to room temperature and stirred for another 12 hours. After dilution with CH_2Cl_2 and washing with 10 % $NaHCO_3$ the solvents were evaporated and the product recrystallized from hexane. Yields 6.9 g, 56 % of **3** as a white powder.

IR (KBr), (cm^{-1}): 3064, 3038, 2999, 2926, 2875, 1608, 1456, 1418, 1356, 1141, 831.

^{1}H-NMR (250 MHz, $CDCl_3$), δ(ppm): 1.36 (s, 24H), 7.30 (d, 2H), 7.50 (d, 2H).

^{13}C-NMR (66 MHz, $CDCl_3$), δ(ppm): 25.2, 84.4, 126.0, 129.2, 138.4, 144.1.

5,5'-bis(9,9'-diethylfluorene-2-yl)-2,2'-bithiophene (4a). To a degassed 2:1 mixture of toluene and 2 M aqueous K_2CO_3 **2a** (766 mg, 2.2 mmol), 5,5'-dibromo-2,2'-bithiophene (324 mg, 1.0 mmol), 0.1 g tetrabutylammonium chloride, $Pd(OAc)_2$ (2 mol%) and tri-o-tolylphosphine (6 mol%) were added. After degassing the solution again it was stirred at 40 °C for 4 h. After cooling down and washing with water, saturated NaCl-solution and again with water the final purification was made by column chromatography with hexane / THF (8/1) as eluent and yields **4a** (456 mg, 75%) as yellow crystals.

IR (KBr), (cm^{-1}): 3059, 2960, 2926, 2857, 1453, 1375, 1256, 874, 790, 737.

^{1}H-NMR (250 MHz, $CDCl_3$), δ(ppm): 0.5 (t, 12H), 2.1 (m, 8H), 7.20 (m, 2H), 7.34 (m, 8H), 7.54 (m, 4H), 7.68 (m, 4H).

^{13}C-NMR (66 MHz, $CDCl_3$), δ(ppm): 10.4, 24.9, 56.2, 118.9, 120.0, 122.9, 126.1, 126.7, 127.5, 128.3, 129.2, 133.7, 135.1, 141.3, 144.5, 149.0, 152.4.

Anal. Calcd for $C_{42}H_{38}S_2$: C, 83.12; H, 6.31; S, 10.57. Found: C, 83.08; H, 6.31; S, 10.5

4b, **4c**, **4d** and **4e** were synthesised analogously.

OFET device fabrication

The organic field effect transistor devices were prepared on heavily doped n^{++} silicon wafers as gate contact on top of which an insulating layer of silicon dioxide was thermally grown. Gold was evaporated and photolithographically patterned to form the source and drain contacts[22]. The devices were completed by evaporating the different fluorene-bithiophene trimers as the organic semiconducting material. The evaporation was performed with a Balzers PLS 500 at a pressure of 10^{-5} mbar, evaporation temperatures of 220 °C to 260 °C and a rate of 0.2 Å/s. The average film thickness of the semiconductor layer was 100 nm. The electrical measurements were carried out in vacuum (10^{-4} Torr) using a Hewlett-Packard semiconductor parameter analyzer Agilent 4155C. The reported transistors had a ring configuration with a channel length of 20 μm and a channel width of 1000 μm.

Acknowledgement

We thank the German Federal Ministry of Education and Research (BMBF) for financial support in the POLITAG program, D. Hanft for synthetic help, M. Bäte for the evaporation of the films and J. Ostrauskaite for CV measurements.

[1] A. Tsumura, H. Koezuka,, T. Ando, Appl. Phys. Lett. 49 (1986), 1210.

[2] C.D. Dimitrakopoloulos, P.R.L. Malenfant, Adv. Mater. 14 (2002), 99.

[3] J. Veres, S. Ogier, G. Lloyd, D. deLeeuw, Chem. Mater. 16 (2004), 4543.

[4] M.M. Ling, Z. Bao, Chem. Mater. 16 (2004), 4824.

[5] O.D. Jurchescu, J. Baas, T.M. Palstra, Appl. Phys. Lett. 84 (2004) 3061.

[6] H. Sirringhaus, P.J. Brown, R.H. Friend, M.M. Nielsen, K. Beechgard, B.M.W. Langeveld-Voss, A.J.H. Spiering, R.A.J. Jannsen, E.W. Meijer, D. deLeeuw, Nature 401 (1999) 685.

[7] F. Garnier, A. Yassar, R. Hajlaoui, G. Horowitz, F. Deloffre, B. Servet, S. Ries, P. Alnot, J. Am. Chem. Soc. 115 (1993) 8716.

[8] A. Dodabalapur, L. Torsi, H.E. Katz, Sience 268 (1995) 270.

[9] C.D. Dimitrakopoulos, B.K. Furman, T. Graham, S. Hegde, S. Purushothaman, Synth. Met. 92 (1998) 47.

[10] W. Yu, H. Meng, J. Pei, W. Huang, J. Am. Chem. Soc. 120 (1998) 11808.

[11] X.M. Hong, H.E. Katz, A.J. Lovinger, B.C. Wang, K. Raghavachari, Chem. Mater. 13 (2001) 4686.

[12] M. Ichigawa, H. Yanagi, Y. Shimizu, S. Hotta, N. Suganuma, T. Koyama, Y. Taniguchi, Adv. Mater. 14 (2002) 1272.

[13] H. Sirringhaus, R.J. Wilson, R.H. Friend, M. Inbasekaran, W. Wu, E.P. Woo, M. Grell, D.D.C. Bradley Appl. Phys. Lett., 77 (2000) 406.

[14] L.-L. Chua, J. Zaumseil, J.-F. Chang, E.C.-W. Ou, P.K.-H. Ho, H. Sirringhaus, R.H. Friend, Nature 434 (2005) 194.

[15] H. Meng, Z. Bao, A.J. Lovinger, B.C. Wang, A.M. Mujsce, J. Am. Chem. Soc. 123 (2001) 9214.

[16] H.Meng, J. Zheng, A.J. Lovinger, B.C. Wang, P. G. van Patten, Z. Bao, Chem. Mater. 15 (2003) 1778.

[17] E.J.W. List, R. Guentner, P. Scanducci de Freitas, U. Scherf, Adv. Mater. 14 (2002), 374.

[18] Woo, E.P.; Shiang, W.R.; Inbasekaran, M.; Roof, G.R. US Patent 1995, US 5,708,130.

[19] Inbasekaran, M.; Weishi, W.; Woo, E.P. US Patent 1998, US5777070.

[20] J. Hellberg, T. Remonen, F. Allared, J. Slätt, M. Svensson, Synthesis 14 (2003), 2199.

[21] J. Pommerehne, H. Vestweber, W. Guss, R. F. Mark, H. Bässler, M. Porsch, J. Daub, Adv. Mater. 7, 55 (1995).

[22] A. R. Brown, C. P. Jarrett, D. M. de Leeuw, M. Matters, Synth. Met. 88, 37 (1997).

6. Summary

The major topic of this PhD thesis is the synthesis of a number of conjugated polymers and low mass model compounds from fluorene and bithiophene building blocks. Such materials are attractive candidates for application in organic light emitting diodes (OLEDs) and organic field effect transistors (OFETs).

The first part of my thesis deals with the synthesis of reactive mesogens with conjugated fluorene units and acrylate end groups as photopolymeriseable species. The structure is shown in Figure 44. They were prepared by Suzuki cross coupling reactions with the use of a monofunctional endcapper. Careful MALDI-TOF and GPC analysis show that this procedure leads to fluorene oligomers which are terminated with two acrylate units.

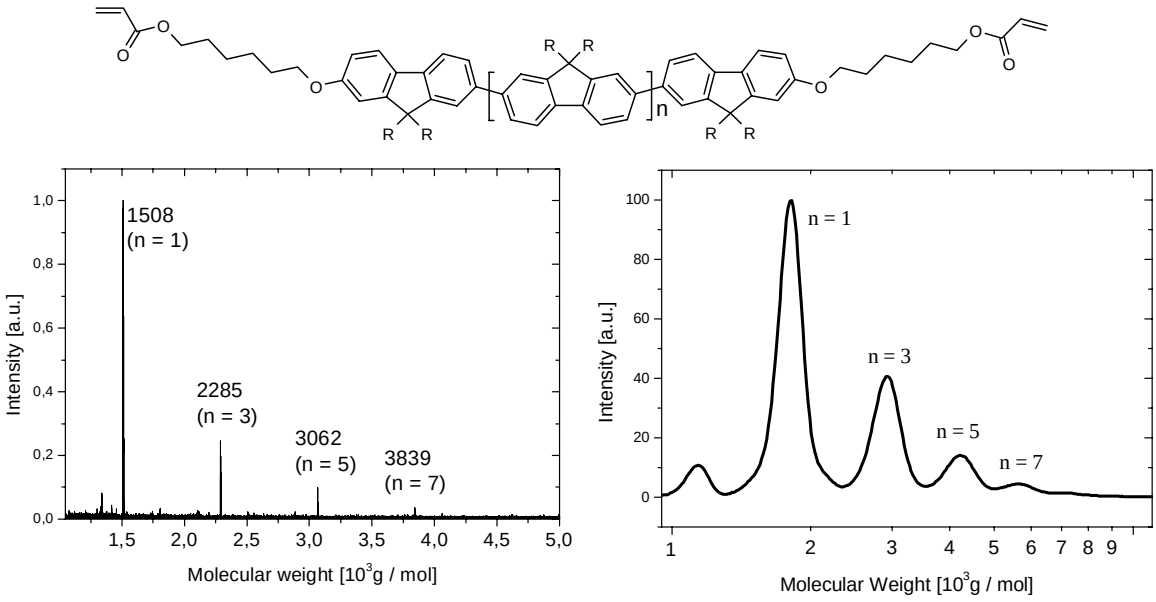

Figure 44: Structure, MALDI-TOF (left) and GPC scan (right) of the fluorene reactive mesogen (M_n = 2250 g/mol).

This synthetic route drastically reduces the number of steps compared to the synthesis of monodisperse fluorene trimers or pentamers and makes fluorene reactive mesogens available in a gram scale.

The materials show broad nematic mesophases. The clearing temperatures can be shifted from 100 °C to 310 °C by changing the molecular weight of the oligomers. The orientation of the crosslinked reactive mesogens on top of rubbed polyimide layers results in a maximum orientation ratio of 15/1 parallel and perpendicular to the rubbing direction.

A major advantage of reactive mesogens as materials for OLEDs and OFETs is their ability to be photocrosslinked. By this procedure the liquid crystalline orientation is permanently fixed by a densely crosslinked network. In order to apply reactive mesogens it is necessary to understand the process of photocrosslinking in detail. This process was investigated by PhotoDSC measurements on two different mesogens, one with a nematic and one with a smectic mesophase.

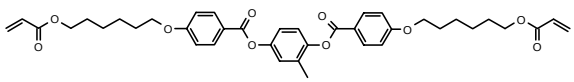

Reactive mesogen **1**

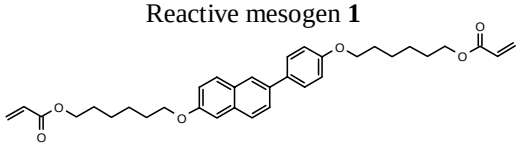

Reactive mesogen **2**

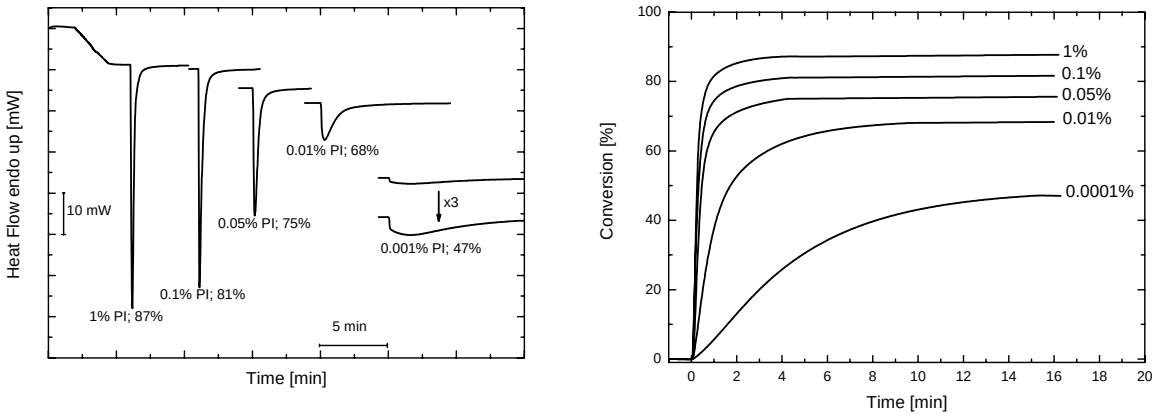

Figure 45: Above: Structures of the reactive mesogens; below: PhotoDSC traces of the photopolymerisation at 100 °C of the reactive mesogen **1** with different amounts of photoinitiator (Irgacure 651), irradiation wavelength 365 nm (left); time conversion plots of these measurements (right)

The kinetics of the photopolymerisation reactions and the total conversion in dependence from initiator concentration of the reactive mesogen **1** are shown in Figure 45. It becomes

clear that the reaction rate and the total conversion decrease with smaller amounts of photoinitiator. Nevertheless a conversion of 75 % can be realised with only 0.01 weight % of initiator, which is much less than is usually used in photopolymerisations.

We were able to polymerise the reactive mesogen **2** in the smectic mesophase. Nevertheless this phase is at lower temperatures compared to the isotropic phase, the polymerisation kinetics is faster and a maximum conversion of 75 % is reached.

Apart from the work on reactive mesogens new materials for the use in OFETs are part of this thesis. Since the HOMO levels of pure fluorene compounds are too low for an efficient charge carrier injection in OFETs fluorene and bithiophene building blocks have been combined. For the use in OFETs the alternating polymer containing 9,9-dioctylfluorene and bithiophene monomers (F8T2) is one of the best investigated polymers. To overcome the problem of the very high transition temperature from the nematic in the isotropic phase which hinders an efficient orientation a synthesis of oligomers based on the F8T2 structure but with a lower molecular weight was developed, to obtain a new class of stable and solution processable materials for OFET applications. The synthesis was again carried out by the Suzuki cross coupling as shown in Figure 46.

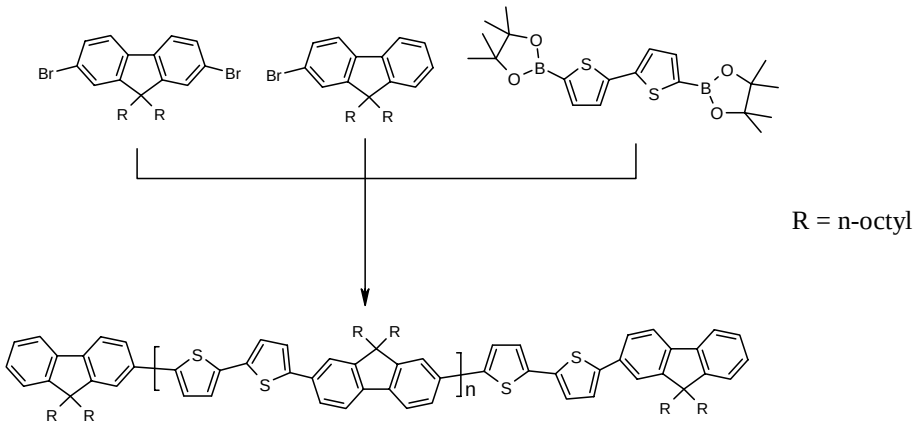

Figure 46: Synthesis of fluorene – bithiophene based oligomers.

The molecular weight can be tuned by the amount of the monofunctionalised 2-bromofluorene which acts as an endcapper. Like F8T2, all oligomers show broad nematic phases. The clearing temperature can be tailored by varying the molecular weight of the oligomers between 80 °C and 288 °C. A plot of $1/P_n$ versus the clearing temperature of these oligomers with different degree of polymerisation results in a clearing temperature of 366 °C for the ideal polymer.

The better control of purity compared with polymers or oligomers and the well defined structure renders small molecules attractive candidates for the use in OFETs. A number of mixed fluorene-bithiophene trimers with different alkyl side chains in the 9 position have been synthesised and one example is shown in Figure 47.

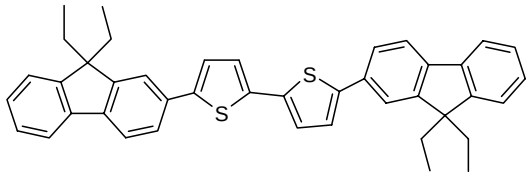

Figure 47: Structure of 5,5'-bis(9,9'-diethyllfluorene-2-yl)-2,2'-bithiophene.

The characterisation by cyclic voltammetry results in a HOMO level of – 5.3 eV. This is exactly the desired level for efficient hole injection from the gold or conducting polymer electrodes in an OFET. We have tested three of the trimers in OFETs and found that the mobility varied from 10^{-5} cm^2/Vs in an amorphous film to $3 \cdot 10^{-3}$ cm^2/Vs in a polycrystalline material. To demonstrate the stability of this material, measurements were performed after three months storage under ambient conditions. The mobility was the same as in a freshly prepared device. The characteristics are shown in Figure 48. As it can be seen, almost no hysteresis can be detected even after a few months at ambient conditions. The preserved high mobility is another hint, that the molecules are much more stable than pure thiophene materials.

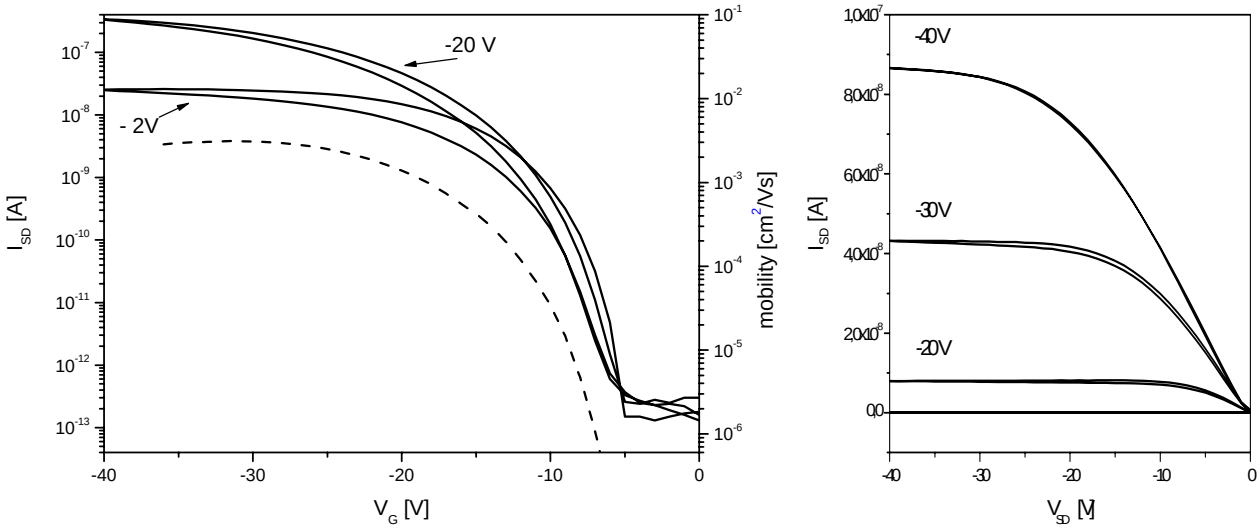

Figure 48: OFET characteristics of the fluorene – bithiophene trimer with ethyl side chains (see Figure 47) after three months of storage under ambient conditions. Left: Transfer characteristics (solid lines, V_D = -2 V, -20 V). The dashed curve shows the mobility values (for V_D = -2 V). Right: Output characteristics at different gate voltages.

7. Zusammenfassung

Meine Dissertation beschäftigte sich mit der Synthese von konjugierten Polymeren und niedermolekularen Verbindungen, die auf Fluoren- und Bithiopheneinheiten basieren. Diese Materialklassen eignen sich sehr gut für die Verwendung in organischen Leuchtdioden (OLEDs) und organischen Feldeffekttransistoren (OFETs).

Der erste Teil meiner Arbeit bestand in der Synthese von so genannten Reaktivmesogenen, die aus einem Fluorengrundgerüst bestehen und photovernetzbare Acrylatgruppen enthalten. Diese Verbindungen wurden mittels Suzuki Kupplung synthetisiert, wobei ein monofunktioneller Endcapper als Molekulargewichtsregler fungierte. Detaillierte MALDI-TOF und GPC Analysen zeigen, dass diese Synthesestrategie Fluorenoligomere liefert, die jeweils zwei Acrylatgruppen am Ende besitzen.

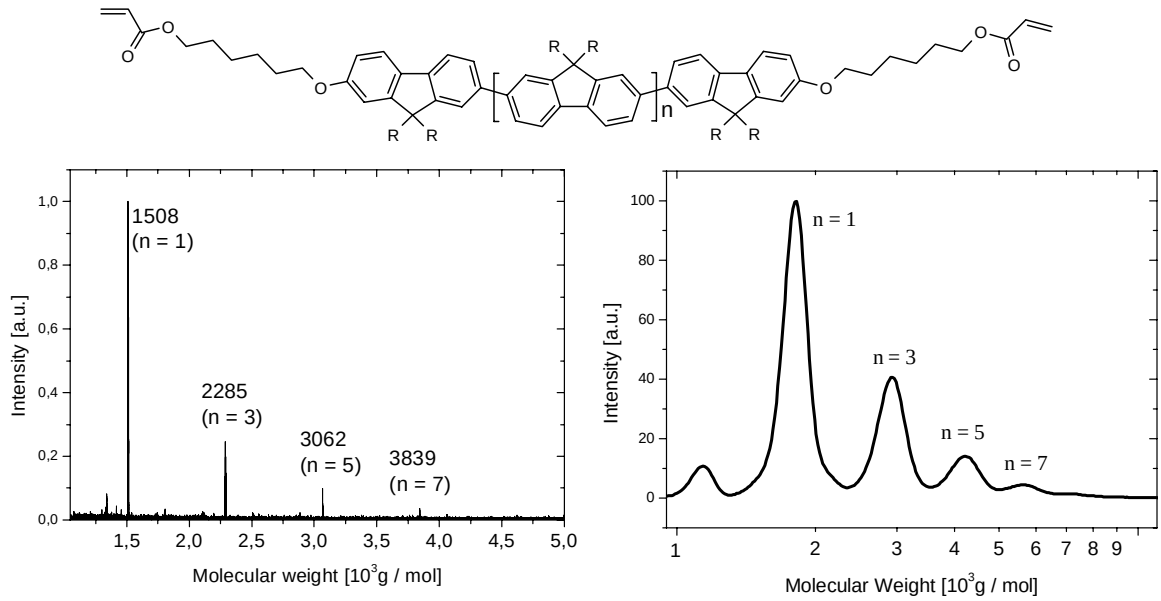

Abb. 44: Struktur, MALDI-TOF (links) und GPC (rechts) Analysen eines Reaktivmesogens (Mn = 2250 g/mol).

Durch diese Syntheseroute wurden die Stufen, verglichen mit der Herstellung von monodispersen Verbindungen der gleichen Klasse, drastisch reduziert. Reaktivmesogene dieser Art sind dadurch im Grammaßstab zugänglich.

Die Materialien besitzen breite nematische Mesophasen. Insbesondere die Klärtemperatur kann bei den Oligomeren von 100 °C bis 310 °C durch eine Änderung des Molekulargewichtes variiert werden. Orientierungsexperimente der photoverentzten Reaktivmesogene auf geriebenen Polyimidschichten lieferten maximale Orientierungsverhältnisse von 15/1.

Ein großer Vorteil von Reaktivmesogenen bei der Verwendung in OLEDs oder OFETs ist ihre Photovernetzbarkeit. Dadurch kann die flüssigkristalline Orientierung permanent durch die Ausbildung eines Netzwerkes fixiert werden. Um den Prozess der Photovernetzung genauer zu beleuchten, wurden an zwei verschiedenen Reaktivmesogenen PhotoDSC Messungen durchgeführt.

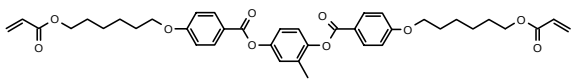

Reaktivmesogen **1**

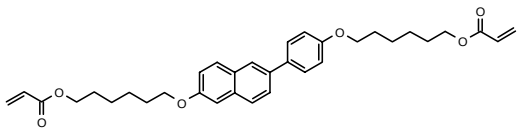

Reaktivmesogen **2**

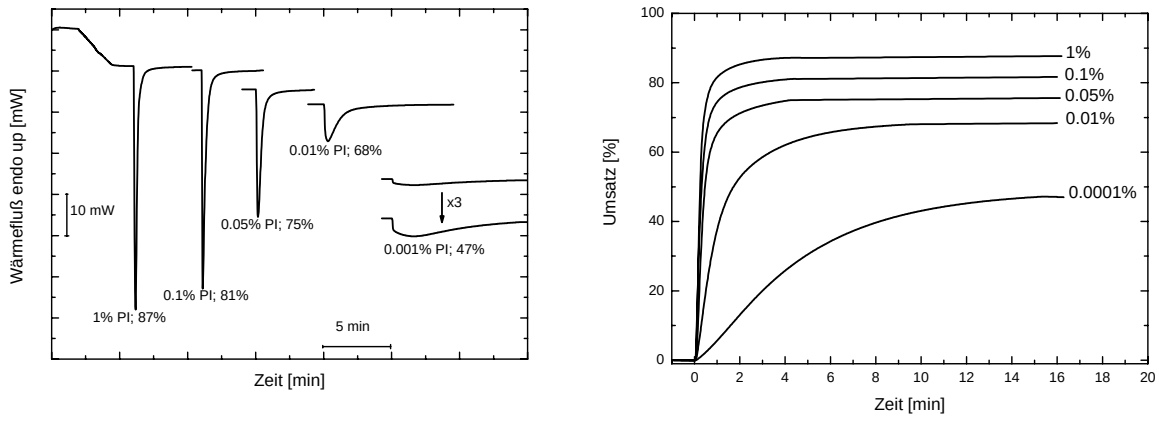

Abb. 45: Oben: Strukturen der verwendeten Reaktivmesogene; unten: PhotoDSC Kurven der Photopolymerisationen bei 100 °C des Reaktivmesogens **1** mit verschiedenen Initiatorkonzentrationen (Irgacure 651), Anregungswellenlänge: 365 nm (links); Zeit – Umsatzkurven der gleichen Experimente (rechts).

Die Abhängigkeit der Polymerisationskinetik und des Umsatzes von der Initiatorkonzentration des Reaktivmesogens **1** ist in Abb. 45 dargestellt. Es wird deutlich, dass die Reaktionsgeschwindigkeit und der Umsatz mit sinkender Initiatorkonzentration zurückgehen. Trotzdem wird bei 0,01 Gew.%, was erheblich weniger ist als üblicherweise bei Photopolymerisationen verwendet wird, immer noch ein Umsatz von 75 % erreicht.

Wir konnten das Reaktivmesogen **2** in der smektischen Phase photovernetzen. Obwohl sich diese Mesophase bei niedrigeren Temperaturen befindet als die Isotrope, ist trotzdem die Polymerisationsgeschwindigkeit und der Umsatz höher.

Der zweite Teil meiner Dissertation beschäftigte sich mit der Synthese von neuen Materialien für OFETs. Aufgrund des zu niedrigen HOMO Niveaus eignen sich Moleküle, die nur Fluoreneinheiten enthalten, nicht für den Einsatz in OFETs, da eine effiziente Ladungsträgerinjektion nicht gewährleistet ist. Daher wurden Fluorenbausteine mit Bithiophen kombiniert, um damit Materialien zu erhalten deren Energieniveaus zu denen des Elektrodenmaterials passen. Das alternierende Copolymer aus 9,9-Dioktylfluoren und Bithiophen (F8T2) wird von vielen Forschungsgruppen als Halbleiter in OFETs verwendet. Der Nachteil dieses Polymers ist die hohe Übergangstemperatur von der nematischen in die isotrope Phase von über 300 °C, wodurch eine optimale Orientierung nicht möglich ist. Diese kritische Größe wurde durch die Synthese von Oligomeren beseitigt, die ein geringeres Molekulargewicht als F8T2 besitzen. Dadurch wurde eine neue aus Lösung verarbeitbare Materialklasse für den Einsatz in OFETs erschlossen. Die Synthese wurde wiederum mittels Suzuki Kupplung durchgeführt und ist in Abb. 46 dargestellt.

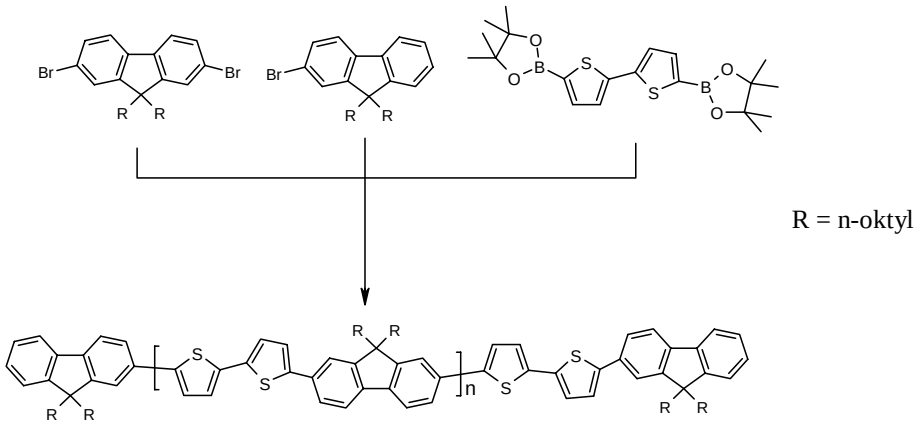

Abb. 46: Synthese von Oligomeren basierend auf Fluoren- und Bithiopheneinheiten.

Das Molekulargewicht kann durch die Menge an monofunktionellem Endcapper 2-Bromfluoren geregelt werden. Genau wie F8T2 besitzen die hergestellten Oligomere breite nematische Phasen. Die Klärtemperatur kann durch das unterschiedliche Molekulargewicht der Oligomeren zwischen 80 °C und 288 °C variiert werden. Eine Auftragung des reziproken Polymerisationsgrades gegen die Klärtemperatur der Oligomere liefert eine Klärtemperatur von 366 °C für ein ideales Polymer.

Die bessere Kontrolle über die Reinheit im Vergleich zu polymeren Systemen macht auch kleinere Moleküle zu potentiellen Kanditaten für den Einsatz in OFETs. Eine Reihe von Trimeren mit einer Bithiophen- und zwei endständigen Fluoreneinheiten wurde mittels Suzuki Kupplung hergestellt. Ein Beispiel ist in Abb. 47 dargestellt.

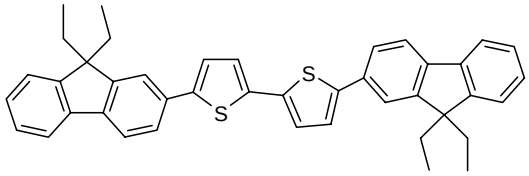

Abb. 47: Struktur von 5,5'-bis(9,9'-Diethyllfluoren-2-yl)-2,2'-bithiophen.

Cyclovoltammertriemessungen lieferten ein HOMO Niveau von -5,3 eV, welches eine sehr gute Ladungsträgerinjektion von den verwendeten Goldelektroden gewährleisten sollte. Drei der hergestellten Trimere wurden in OFETs getestet. Die Mobilität konnte von 10^{-5} cm^2/Vs in

einem amorphen Film auf $3 \cdot 10^{-3}$ cm^2/Vs in einem polykristallinen Film gesteigert werden. Um die Stabilität dieser Verbindungsklasse zu demonstrieren, wurden diese Messungen nach dreimonatiger Lagerung an Luft und Licht wiederholt. Die Mobilitäten waren auf dem gleichen Niveau wie bei den ursprünglichen Messungen. Die verschiedenen Charakteristiken sind in Abb. 48 dargestellt. Auch nach dieser langen Lagerung kann immer noch nahezu keine Hysterese detektiert werden. Dieses ungewöhnlich konstante Verhalten ist ein weiterer Hinweis darauf, dass diese Verbindungsklasse viel stabiler ist als reine Thiophenmaterialen.

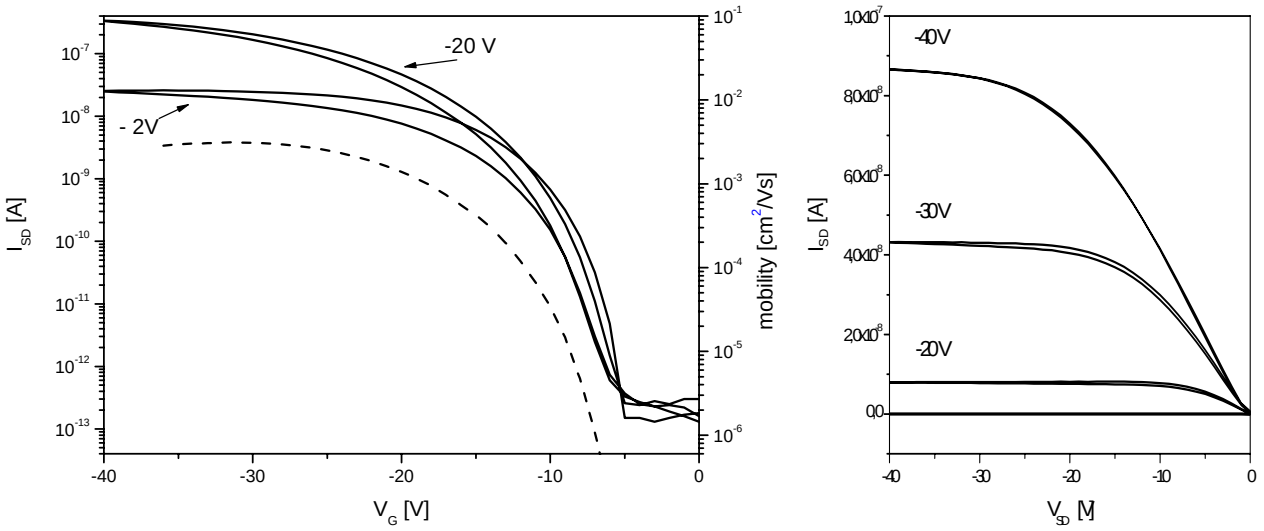

Abb. 48: OFET Daten des Fluoren – Bithiophene Trimeren mit Ethylseitenketten (Siehe Abb. 47)) nach dreimonatiger Lagerung an Licht und Luft. Links: Transfer Charakteristiken (V_D = -2 V, -20 V). Die gestrichelte Linie zeigt die Mobilität für V_D = -2 V. Rechts: Output Charakteristiken bei verschiedenen Gatespannungen.

Contributions to conferences

Apart from the papers which are part of the thesis I gave contributions to the following conferences.

Oral presentations:

H. Thiem

“Fluorene based reactive mesogens for optoelectronic applications”

Sixth int. symposium on functional π-electron systems (Fπ 6), Cornell University

(Ithaca, USA), 2004

Since my work was sponsored by the BMBF in the POLITAG program and the EU in the EUROFET/TMR network, I gave several talks on the different project meetings all over Europe in the last years.

Posters:

H. Thiem, K. Kreger, P. Strohriegl

„Fluorene model compounds for optoelectronic applications“

Bayreuther Polymer & Materials Research Symposium (BPS), Bayreuth 2001

K. Kreger, H. Thiem, P. Strohriegl

„New starburst model compounds for OLEDs“

European Conference on organic electronics and related phenomena (ECOER ’01), Potsdam 2001

H. Thiem, K. Kreger, M. Jandke, P. Strohriegl

„Fluorene containing materials for optoelectronic applications“

Makromolekulares Kolloquium, Freiburg 2002

H. Thiem, K. Kreger, M. Jandke, P. Strohriegl

„Fluorene containing materials for optoelectronic applications

Fifth int. symposium on functional π-electron systems (Fπ 5), Ulm 2002

H. Thiem, M. Jandke, P. Strohriegl

„Fluorene containing reactive mesogens for optoelectronic applications“

Molecular Organization for Nanosystems (MLO), Kloster Banz 2003

H. Thiem, D. Hanft, P. Strohriegl

„Fluorene – bithiophene based materials for optoelectronic applications“

Fachgruppentagung makromolekulare Chemie der GdCh, Düsseldorf 2004

H. Thiem, P. Strohriegl

„New fluorene – bithiophene based molecules for OFET applications”

Winterschool on organic electronics (OEWS ’04), Planneralm (Austria), 2004

H. Thiem, D. Hanft, P. Strohriegl

„Fluorene – bithiophene based molecules for the use in OFETs

EUROFET mid term meeting, Strasbourg, 2004

“Wir können alles schaffen…..

……wir müssen nur wollen!”

(Wir sind Helden, 2003)

Erklärung

Die vorliegende Arbeit habe ich selbst verfasst und keine anderen als die von mir angegebenen Quellen und Hilfsmittel verwendet.

Ferner erkläre ich, dass ich nicht versucht habe, anderweitig mit oder ohne Erfolg eine Dissertation einzureichen oder mich der Doktorprüfung zu unterziehen.

Bayreuth, Juni 2005

(Heiko Thiem)